This is to certify that the

dissertation entitled

Interpreting Crystal Growth
Kinetics of Ancient Dolomites

presented by

Lisa Ann Kessels

has been accepted towards fulfillment
of the requirements for

Ph.D. degree in Geological Sciences

Duncan F. Sibley
Major professor

Date 8/8/01

INTERP

INTERPRETING CRYSTAL GROWTH KINETICS OF ANCIENT DOLOMITES

By

Lisa Ann Kessels

A DISSERTATION

Submitted to
Michigan State University
in partial fulfillment of the requirements
for the degree of

DOCTOR OF PHILOSOPHY

Department of Geological Sciences

2001

INTERPRETING CRYSTAL GROWTH KINETICS OF ANCIENT DOLOMITES

By

Lisa Ann Kessels

AN ABSTRACT OF A DISSERTATION

Submitted to
Michigan State University
in partial fulfillment of the requirements
for the degree of

DOCTOR OF PHILOSOPHY

Department of Geological Sciences

2001

Professor Duncan F. Sibley

ABSTRACT

INTERPRETING CRYSTAL GROWTH KINETICS OF ANCIENT DOLOMITES

By

Lisa Ann Kessels

Crystal growth has been described by the following models; 1) mononuclear growth model, 2) birth and spread growth model, 3) polynuclear growth model, and 4) spiral growth model (Christian 1972, Nielson 1964, Ohara and Reid 1959, Burton *et al.* 1951). In order to apply these growth models to ancient dolomite reservoirs, an estimate of the growth rate is necessary. The zone width in concentrically-zoned, luminescent dolomites can be used to estimate growth rate (Nordeng and Sibley 1996, Carlson 1989, Kretz 1974, 1973). By rearranging the equations for the known growth models, crystal population trends on a zone-width vs. crystal-size plot can be constructed to distinguish between groups of crystals growing by mononuclear growth versus the following mechanisms: 1) polynuclear growth, 2) birth and spread growth, 3) diffusion-limited and 4) spiral growth mechanisms. To determine the extent that any group of crystals within a dolomite unit grew by the same crystal growth mechanism, samples were examined at regular intervals from three luminescent dolomites: 1) Saluda and Whitewater Formations (Ordovician), Indiana, U.S., 2) Burlington-Keokuk Formation (Mississippian) Missouri, U.S., and 3) Seroe Domi

Formation (Miocene), Curacao, Netherland Antilles. Plots of zone-width vs. crystal-size for crystals in an individual sample were constructed. Crystal growth equations fitted to each sample's zone-width vs. crystal-size plot were compared among samples from: 1) the same lithology and formation, 2) different lithologies and the same formation, 3) the same lithology and different formations and 4) different lithologies and different formations. Analysis of crystal growth equations from all three dolomites indicate a linear relationship, $dr/dt = k'r$, where growth rate increases with crystal size (r) indicating crystal growth mechanism does not vary on the outcrop scale with lithology, $\delta^{13}C$, $\delta^{18}O$, or age of formation. The average slope (k') of all three dolomites was 0.181. Correlation coefficients for the equation $dr/dt = kr$ ranged from 23% to 81%. Zone-width vs. crystal-size plots constructed for pairs of crystals adjacent to each other in the Saluda and Burlington-Keokuk formations revealed the same growth mechanism $dr/dt = k'r$, indicating growth was controlled by a crystal surface process instead of solution variability.

ACKNOWLEDGMENTS

I would like to thank and acknowledge Duncan Sibley or his guidance and patience over the years. I would also ike to thank the members of my committee, Mike Velbel, ave Long and Tom Vogel. Their insights and comments have roved invaluable. I am also deeply indebted to Bruce ouke for thin section samples and locations for the Seroe omi Formation samples. Last, but not least, I would like o thank Eldon who saw me through to the end.

TABLE OF CONTENTS

LIST OF TABLES

List of Figures

Figure

Figure

Figure

Figure

Figure

Figure

Figure

Figure

Figure

Figure

Figure

Figure

Figure

Figure 2

Figure 2

Figure 2

Figure

Figure

Figure

Figure

Figure

Figure

Figure

Figure

INTRODUCTION

Carbonate reservoirs are conservatively estimated to contain approximately 60 percent of recoverable oil globally (Roehl and Choquette 1985). Carbonate rocks also cover approximately 10% of the continents (Ehlers and Blatt 1982) and serve as productive aquifers in the subsurface (Domenico and Schwartz 1990). As a result, much effort has been devoted to the study of carbonate precipitation (Berner 1982, Lasaga 1981, Land 1980, Berner and Morse 1974). Carbonate precipitation and dissolution have been studied in every environment ranging from the surface to deep subsurface (Lucia and Major 1994, Negra *at al.* 1994, Purser *et al.* 1994, Feazel and Schatzinger 1985, Harris *et al.* 1985, Sandberg 1985, Walter 1985, Choquette and Steinen 1980, Mattes and Mountjoy 1980). In particular, much attention has been paid to dolomitization because of 1) the abundance of dolomite in the rock record compared to the modern day and 2) the reservoir potential of dolomite (Nordeng and Sibley 1996, Sibley *et al.* 1994, Sibley 1980).

The dolomitization reaction has been investigated extensively both from a microscopic and a macroscopic viewpoint resulting in identification of kinetic catalysts and inhibitors as well as formation-scale dolomitization models (Morrow and Abercrombie 1994, Nordeng and Sibley 1994, Sibley *et al.* 1994, Simo *et al.* 1994, Usdowski 1994,

Vahrenkamp and Swart 1994, Whitaker *et al.* 1994, Fouke and Reeder 1992, Middleburg *et al.* 1990, Sibley 1990, Sibley *et al.* 1987, Sibley and Bartlett 1987, Bullen and Sibley 1984, Gregg and Sibley 1984, Saller 1984, Sibley 1982, Baker and Kastner 1981, McKenzie 1981, Carpenter 1980, Choquette and Steinen 1980, Gaines 1980, Land 1980, Lumsden and Chimahusky 1980, Muir *et al.* 1980, Zenger and Dunham 1980, Katz and Matthews 1977, Badiozamani 1973). However, very little is known about the mechanism of dolomite crystal growth because of two factors: 1) the lack of a modern analog for massive ancient dolomites, and 2) the inability to precipitate dolomite at standard temperature and pressures in the laboratory. The latter obstacle has been overcome by extrapolating high-temperature, laboratory crystal growth experiments to lower temperatures. From these experiments in dolomitization, researchers have found: 1) an induction period for dolomite precipitating on a calcite, aragonite or dolomite substrate (Sibley *et al.* 1994, Gaines 1980, Katz and Matthews 1977), 2) an increase in the rate of dolomitization with increasing temperature, surface area of substrate, and Mg/Ca ratio of solution (Sibley 1990, Sibley and Bartlett 1987, Katz and Matthews 1977), 3) a faster rate of reaction when aragonite is used as the substrate as opposed to calcite (Katz and Matthews 1977), and 4) a decrease in the rate of dolomitization with the addition of sulfate to solution (Baker and Kastner 1981). However,

these experiments have not demonstrated whether the growth mechanism is a diffusion-limited or surface reaction-limited process. Diffusion of CO_3^{2-} ions or diffusion of dehydrated Mg^{2+} are possibilities for a rate-limiting step. A surface reaction-limited process is also feasible.

The progression from a less than 50% molar Mg dolomite to a stoichiometric (50% molar Mg dolomite) allows for a change in surface free energy and a possible change in available nucleation sites. SEM images of partially dolomitized calcite show dolomite preferentially grows at substrate edges and corners (Kessels 1995 Figure 6, Sibley *et al.* 1987) suggesting either: 1) a higher concentration of CO_3^{2-} ions as a result of faster dissolution of calcite corners or 2) the development of favorable kink sites for nucleation and/or layer growth at the dissolving calcite edges. Thus, the question of diffusion-limited versus surface reaction-limited growth cannot be answered by *ex situ* observations. Kessels (1995) also indicates surface topographies consistent with a two-dimensional nucleation and layer growth mechanism. However, two-dimensional nucleation and layer growth can occur in both the diffusion-limited and surface reaction-limited growth cases since the method of attachment in diffusion-limited growth is independent of the rate-limiting step.

Recent methods of dolomite crystal growth mechanism determination include dolomite crystal size distributions and ca

Experi

Exp

succe

then

standa

distri

model

determ

There a

crystal

certai

at any

nucleat

Group

crysta

is a p

valid

A

estima

Kretz

Growth

Kretz

Bridge

Batist

normal

and cathodoluminscent zone-width vs. crystal-radius plots (Eberl *et al.* 1998, Nordeng and Sibley 1996, Sibley 1980). Eberl *et al.* (1998) generated crystal size distributions by successive iterations of known crystal growth models and then uses the crystal size distributions generated as a standard for each model. Thus, the crystal size distributions of actual crystal data can be compared to the model distributions and used as an indirect means to determine crystal growth mechanism of natural crystals. There are three assumptions that are necessary to use crystal size distributions to determine crystal growth mechanism: 1) the crystal growth mechanism does not change at any time during precipitation, 2) crystals do not nucleate at different times, and 3) no one crystal precipitates for a longer period of time than any other crystal. The extent to which any crystal size distribution is a determinant of crystal growth mechanism depends on the validity of these three assumptions.

A second approach is the measurement of zones as an estimate of growth rate (Carlson 1989, Kretz 1974, 1973). Kretz (1974, 1973) and Carlson (1989) investigated the growth of garnet crystals by examining compositional zones. Kretz (1974) considered growth rate as a change in radius, $dR/dt=k$, volume, $dV/dt=k$, and surface area, $dA/dt=k$. Carlson (1989) plotted the normalized radius versus the normalized rate for garnet crystal measurements. The measure

the rad

lines a

crysta

contou

both f

crystal

Figure

changin

models.

trend t

in temp

and Sib

cathod

section

growth

fit any

1996

thin se

Cr

for dol

solute-

Sibley

dolomit

same do

changes

measurement technique outlined in Kretz (1973, 1974) uses the radial distance between any two compositional contour lines as the rate and the distance from the center of the crystal to the midway-point between the compositional contours as the radius. Kretz (1974) and Carlson (1989) both found actual measurements of garnet zones versus garnet crystal radius did not fit any of the three models (see Figure 3, Carlson 1989). Kretz (1974, 1973) identifies changing rates of nucleation as a possible problem for the models. Like Kretz (1974), Carlson (1989) attributes the trend to changes in nucleation rate caused by the increase in temperature (thermally-accelerated nucleation). Nordeng and Sibley (1996) followed a similar procedure using cathodoluminescence zones. Data for individual thin sections could be fit with a straight line, dr/dt=kr, where growth rate increased with crystal size, that also did not fit any of the known growth models. Nordeng and Sibley (1996) interpreted the size dependency of growth rate to thin section-scale, solute flux-limited growth.

Crystal zone data and crystal size distribution data for dolomite have been interpreted as an indicator of a solute-flux limited reaction (Eberl *et al.* 1998, Nordeng and Sibley 1996). This interpretation would suggest the dolomite growth rate of adjacent lithofacies exposed to the same dolomitizing fluid will vary with lithofacies type, or changes in porosity and permeability, that affect solute

flux. Thus, a lithofacies with an initially high permeability would undergo a faster rate of dolomite growth than adjacent lithofacies with initially low permeability. Consequently, in open and closed systems, porous lithofacies would grow faster than adjacent less porous lithofacies until the porosity of the adjacent, initially less-porous lithofacies, was reached. This evolution toward "porosity equilibrium" is one possible explanation for the consistency of dolomite rock textures.

In order to determine the variation in crystal growth mechanism spatially, cathodoluminscent zones widths and crystal radii are determined for samples from a regularly spaced grid. A body of rock that does not have a variable crystal growth rate mechanism can be described as a unit of rock in which: 1) the *net* rock-water interaction is precipitation and 2) the rate-limiting step in precipitation is the same throughout the unit of rock. Net rock-water interactions that add to a crystal are based on the amount of influence exerted by two processes in crystal growth; solute flux and solute uptake. Solute flux to a growing crystal surface in a formation is influenced by the amount of interface between crystal surface and solution (pore size) and transportation of solute to the crystal surface (hydraulic potential, pore geometry and interconnectivity). The latter affects the concentration of solute in the bulk solution that in turn affects the concentration and ould

solut

where

stron

temper

crysta

betwe

energ

repea

T

conta

solute

limit

would

know

the gr

the or

itself

limite

result

change

two el

entire

solute

rate-l

proced

thickness of the interfacial solution. The interfacial solution is the fluid that is bound to the crystal surface where dangling ions and surface charge attract H_2O more strongly than surrounding molecules of H_2O in solution. The tendency for ions to attach and detach from the surface of a crystal is a result of the drive to maintain equilibrium between the interfacial solution and crystal surface. Precipitation results when the net ion surface exchange represents solute uptake.

The rate-limiting step in crystal growth can be dominated by either of the two processes, solute flux or solute uptake. For solute-flux limited growth, the rate-limiting step is delivery of ions to the surface. For an individual crystal in a stagnant solvent, this process is known as the diffusion limited growth model (Table 1) and the gradient in solute concentration projecting outward from the crystal surface results from the growth of the crystal itself. For a population of crystals growing by solute-flux limited growth, variation of the solute concentration may result from: 1) interaction of crystals with solution or 2) changes in the external source of the solution. Mixing of two fluids, meteoric and marine, or introduction of an entirely new fluid would represent an external source for solute variation. On the scale of a crystal, when the rate-limiting step is attachment of ions to the surface, the process is referred to as surface-reaction limited growth.

Table 1. Radial Growth Rate Equations for Crystal Growth

Rate Limiting Step for Crystal Growth Model	Crystal Growth	Reaction order

Table 1. Radial Growth Rate Equations for Crystal Growth

Rate Limiting Step for Modeling Zone Widths	*Crystal Growth Model*	*Crystal Growth Equation*	*Reaction order in r*
ion delivery to surface	Diffusion Limited Growth	$dr/dt = k/r$	-1
ion uptake on surface	Mononuclear Growth	$dr/dt = kr^2$	2
ion uptake on surface	Polynuclear Growth	$dr/dt = k$	0
ion uptake on surface	Spiral Growth	$dr/dt = k$	0
ion uptake on surface	Birth and Spread Growth	$dr/dt = k/r$ or $dr/dt = k$	-1 0

k is a constant representing solution concentration, solute diffusion and crystal form
r is crystal radius

For a p

to as s

Bo

been p

styles

includ

a pl

there a

crystal

growth

where g

K, depe

section

and cl

growth

by the

In

scale

growth

specie

in oil

are t

exerti

variat

same d

For a population of crystals, the process will be referred to as solute-uptake limited growth.

Previous surface-reaction limited mechanisms which have been proposed and mathematically modeled for the different styles of ion attachment to theoretical crystal surfaces include: 1) mononuclear growth, 2) birth and spread growth, 3) polynuclear growth and 4) spiral growth (Christian 1975, Ohara and Reid 1973, Nielsen 1964, Burton *et al.* 1951). A crystal growing by any one mechanism will fit the crystal growth rate equation:

$$dr/dt = f(x) = k_n r^n$$

where f(x) is a function of crystal size, r, or a constant, k, depending on the model type (Table 1, see Reaction Rate section for a detailed description of each model). Thus, a unit of rock could be described by one mechanism if the growth of the crystals in that unit of rock can be described by the same crystal growth rate equation.

The intention of this study is to determine: 1) the scale of rock units that can be described by one crystal growth mechanism and 2) if rock units characterized by a specific crystal growth mechanism coincide with lithofacies in dolomites. If a single lithofacies can be represented by more than one crystal growth mechanism, then the fluid is exerting a greater control on the rate of precipitation than variation in lithofacies. If different lithologies from the same dolomite share the same crystal growth mechanism, again the fu

represe

limits

growth

control

differ

than th

variat

Hetero

by the

Reactio

Th

Demand

and sp

growth

it wil

increa

rate.

indepe

al. 19

for a

based

gradie

of the

the fluid exerts a greater control than the variation represented by the different lithologies. If only similar lithofacies from different dolomites share the same crystal growth mechanism then the lithology is exerting a greater control on the rate of precipitation than variation in the dolomitizing fluids. If different lithologies from different dolomites have the same crystal growth mechanism then the mechanism is: 1) independent of the lithology variation represented by the rock types compared and 2) operating over a range of fluid compositions as represented by the variation in dolomitizing fluids.

Reaction Rate

The rate of crystal growth is related to crystal growth mechanism (Sunagawa 1982). Mononuclear ($dr/dt = kr^2$), birth and spread ($dr/dt=k/r$ or $dr/dt=k$), and polynuclear ($dr/dt=k$) growth mechanisms represent a spectrum of growth mechanisms in which nucleation rate is increasing (Figure 1). The increase in nucleation rate leads to an increase in growth rate. Spiral growth, which is represented by $dr/dt=k$ is independent of crystal size and nucleation rate (Burton *et al.* 1951). Nielson (1964) proposed the equation $dr/dt=k/r$ for a combination of mononuclear and polynuclear growth based on the results of a probabilistic model. The equation $dr/dt = k/r$ is a result of polynuclear growth occurring 60% of the time and mononuclear growth occurring 40% of the time

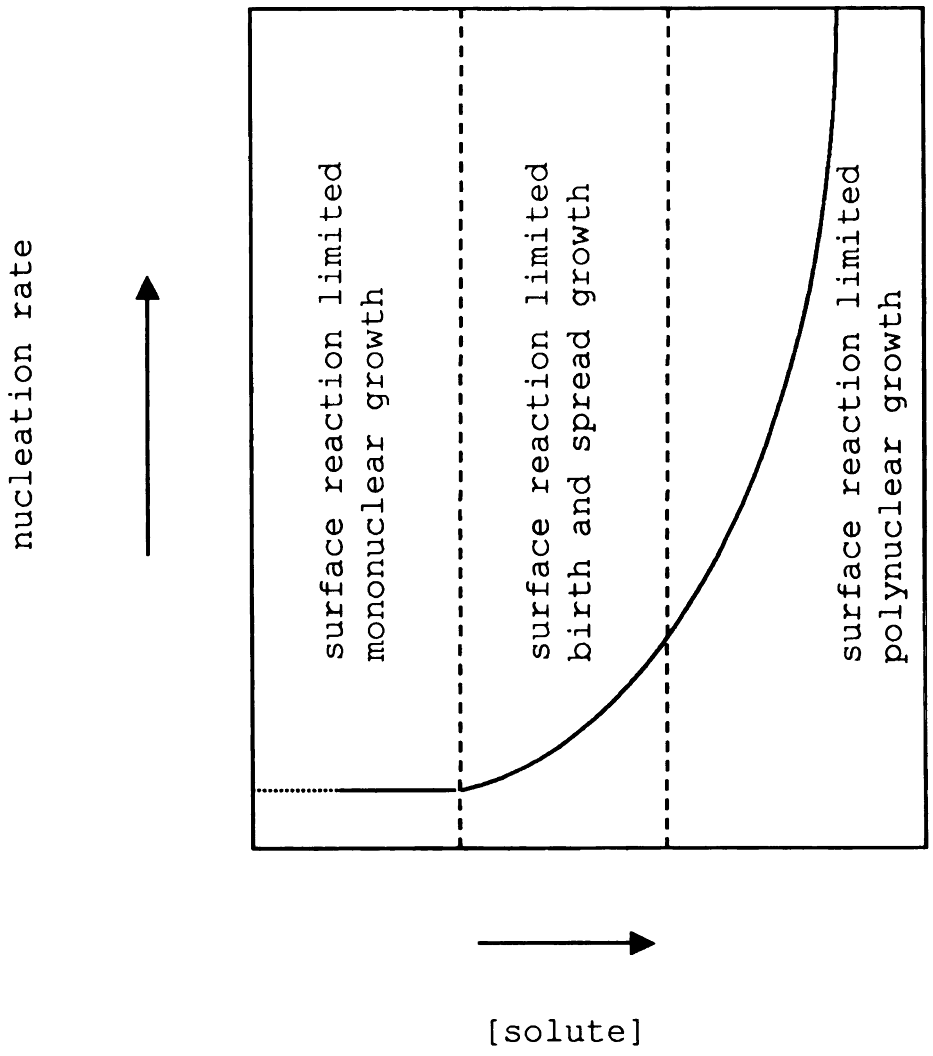

Figure 1. Qualitative Comparisons of Growth Rate
(after Sunagawa 1984)

during
contin-
growth
the lat
by mor-
occurs
This
shoulc
assump-
The tw
the gr
assump-
that t
crystal
in fact
form a
nuclei
size.
where
result
crystal
I
separa-
surface
the cr
growth

during any time period of growth. Ohara and Reid (1973) combined the physical models of mononuclear and polynuclear growth to define the birth and spread model, dr/dt = k. In the latter version of the model, a layer is always generated by more than one nucleus and layer growth between the nuclei occurs at a finite rate. In review of the models, Nyvlt (1985) also indicates the equation for birth and spread should be independent of radius based on the physical assumptions behind the birth and spread growth mechanism. The two assumptions are: 1) nuclei can form anywhere and 2) the growth rate of faces is constant (Nyvlt 1985). If the assumption of a constant nucleation rate per unit area per unit time is true, then the rate of radial growth of a crystal growing by birth and spread growth is only dependent on factors affecting nucleation rate. By allowing nuclei to form anywhere on the surface and allowing more than one nucleus to form at a time, growth is independent of crystal size. This is in contrast to the mononuclear growth model where each layer grows laterally away from only one nucleus resulting in growth dependent on the surface area of the crystal.

Diffusion-limited growth (dr/dt=k/r) is treated separately since the way in which the ions attach to the surface is not the rate-limiting step. Fewer ions approach the crystal surface per unit time in diffusion-limited growth than necessary for any of the surface reaction

[illegible]

[illegible]

growth

The gr

is [illegible]

[illegible]

F

[illegible]

[illegible]

will [illegible]

growth

populat

populat

populat

growth,

populat

latter

[illegible]

growth

[illegible]

surface

[illegible]

the [illegible]

[illegible]

[illegible]

limited growth models under the same conditions. Consequently, diffusion-limited growth has the slowest growth rate when comparing growth rates of any one mineral. The growth rate in the spiral growth ($dr/dt = k$) model, which is independent of nucleation rate, cannot be compared qualitatively to the other growth models.

For each of the different crystal growth mechanisms, relationships between growth rate and crystal size can be derived from the crystal growth equations and assumptions about ion attachment. By integrating the three crystal growth equations over one increment of growth, three crystal population trends emerge: 1) $zw=[kTr_1^2/(1-kTr_1)]$, the population trend for mononuclear growth, 2) $zw=kT$, the population trend for polynuclear growth, birth and spread growth, and spiral growth, and 3) $(zw)^2+2(zw)r_1 = 2kT$, population trend for diffusion-limited growth (Table 2) (the latter growth model trend will be rejected in favor of $zw=kT$, see discussion in Population Trends for Crystal Growth Mechanisms section). In the population trend equations, zw is the increment of precipitate added to the surface (or r_2-r_1), r_1 is the crystal size before the increment began precipitating, r_2 is the crystal size after the increment finished precipitating, T is the time interval over which precipitation occurred, and k represents solution and growth conditions. The increment of precipitation or

Table [illegible]

[illegible]

Table 2. Summary of relationship between crystal size and increment of new precipitate

Mononuclear Growth	Spiral Growth and Polynuclear Growth	Any mechanism of ion attachment
surface-reaction-limited growth	surface-reaction-limited growth	diffusion-limited growth
$dr/dt=kr^2$ $dr(1/r^2)=kdt$ $r^{-2}dr=kdt$ $\int_{r1}^{r2} r^{-2}dr = k\int_{t1}^{t2} dt$ $(1/r_1)-(1/r_2)=k(t_2-t_1)$ let $T=t_2-t_1$ $(1/r_1)-(1/r_2)=kT$	$dr/dt=k$ $dr=kdt$ $\int_{r1}^{r2} dr = k\int_{t1}^{t2} dt$ $r_2-r_1=k(t_2-t_1)$ let $T=t_2-t_1$ $r_2-r_1=kT$	$dr/dt=k/r$ $rdr= kdt$ $\int_{r1}^{r2} rdr = k\int_{t1}^{t2} dt$ $1/2\ (r_2^2-r_1^2)=k(t_2-t_1)$ let $T=t_2-t_1$ $r_2^2-r_1^2 = 2kT$
$zw=[kTr_1^2/(1-kTr_1)]$ *	$zw=kT$ *	$(zw)^2+2(zw)r_1=2kT$ *

* zw is the width of the next increment of precipitate added, or r_2-r_1.
k is a constant representing solution concentration, solute diffusion and crystal form.
r_1 is the crystal radius before precipitation of the zone.
r_2 is the crystal radius after precipitation of the zone.

cone

[illegible]

[illegible]

[illegible]

[illegible]

[illegible]

[illegible]

[illegible]

surfa

ment,

surfa

[illegible]

[illegible]

nucle

[illegible]

laying

surfa

energy

surfa

nucle

across

growth

[illegible]

relat

diffu

and la

zone width (zw) can represent luminescent zones or other nonluminescent compositional zones.

As ions approach the crystal surface, each event can be described as: 1) ions contact the crystal surface and "bounce back" away from the surface, 2) ions contact the crystal surface and "stick", 3) ions contact the surface and then migrate laterally across the surface, or 4) an ion collides with another ion in solution or another ion migrating along the surface of the crystal. In the latter event, the ions may adhere to each other and the crystal surface or "bounce" away from each other and disperse either into the solution or across the surface. If the collision results in the ions adhering to the crystal surface, a nucleus is formed. A nucleus is a unit of the new precipitate inferred to have the shape of a half sphere laying on the crystal surface. The shape is deduced from surface area to volume ratios. A half sphere is the most energetically stable configuration ions could form on the surface. Ions that contact and adhere to the exposed nucleus form a layer of precipitate, which spreads laterally across the surface. This process is referred to as layer growth.

Crystal growth mechanisms have been modeled with relative rates of nucleation and lateral growth. In diffusion-limited growth, the relative rates of nucleation and layer growth across the crystal face vary as a result of

variable solute concentrations. Since the diffusion of ions to the surface is the rate-limiting step and the size of the diffusive layer surrounding the crystal increases as the crystal grows, the overall rate of crystal growth is inversely proportional to crystal size. As the crystal grows larger, it will grow more slowly since it has grown by diffusion-limited growth longer and has created a larger diffusion-depleted "halo". Thus, as an individual crystal grows, the rate of nucleation and layer growth decreases proportionately to its size. Mononuclear crystal growth is dominated by lateral growth in each growth layer. The rate of lateral layer growth is much greater than the rate of nucleation. Thus, an individual nucleus spreads laterally across the surface before another nucleus forms. The formation of a nucleus is the rate-limiting step. Polynuclear crystal growth is the other end member of the spectrum between mononuclear and polynuclear growth. In the polynuclear case, the rate of nuclei formation greatly exceeds the rate of lateral growth. In Nielson's version (1964) of polynuclear growth, there is minimal lateral growth occurring as nuclei intergrow at a finite rate. In Ohara and Reid's version (1973) there is zero lateral growth occurring between nuclei. Using either version, individual monolayers form almost entirely by accretion of nuclei rather than lateral growth. Both versions of polynuclear growth lead to $dr/dt = k$. Thus, the boundary between

I [illegible]

In [illegible]

in [illegible]

cur [illegible]

In [illegible]

n [illegible]

sur [illegible]

pro [illegible]

defe [illegible]

spre [illegible]

layer [illegible]

prem [illegible]

repre [illegible]

corr [illegible]

In or [illegible]

used [illegible]

layer [illegible]

Where [illegible]

T is [illegible]

Order [illegible]

Subst [illegible]

Subst [illegible]

In or [illegible]

Yields [illegible]

mononuclear and polynuclear growth is defined by the number of nuclei. In mononuclear growth, one nucleus gives rise to one growth layer (one d-spacing high or greater) and the time between individual nucleation events may be very long. In polynuclear growth, a single growth layer (one d-spacing high or greater) forms by accretion of nuclei on the surface. The intermediate case between mononuclear and polynuclear growth is described by a separate growth model referred to as birth and spread growth. In the birth and spread growth model, more than one nucleus forms per growth layer but lateral growth still occurs. As discussed previously, birth and spread growth has been tentatively represented by $dr/dt = k/r$ and $dr/dt = k$. Nielson's model (1964) combining mononuclear and polynuclear growth resulted in $dr/dt = k/r$. In that study, a probabilistic model was used in which the average time for completion of a growth layer was defined as:

$$\tau = \tau_1 + 0.6\,\tau_2 \qquad \text{(page 50, Nielson 1964)}$$

where τ_1 is the time between successive nucleation events and τ_2 is the time required to form a complete growth layer. In order to express the equation in terms of growth, τ_1 is substituted with the mononuclear growth equation and τ_2 is substituted with the polynuclear growth equation to result in $dr/dt = k/r$. While the analysis is straightforward, Nielson warns "such detailed conclusions are not justified

because
above
Haig
polymer
Again,
Each
unstr
model
due to
These
and sp
Ruth
approx
= K.
rate p
equati
1964
sugges
polym
declin
crysta
nucle
area p
crysta
Descri

because so many approximations have been made in order to arrive at this point." (page 52, Nielson, 1964). Ohara and Reid (1973) combined the ideas of mononuclear and polynuclear growth to arrive at birth and spread growth. Again, in this model there is no intergrowth between nuclei. Each nucleus is modeled as if it will grow to the edge unobstructed. The other two critical assumptions of this model are: 1) lateral growth is constant regardless of the size of the layer growing and 2) nuclei can form anywhere. These assumptions result in the equation $dr/dt = k$ for birth and spread growth. While no definitive equation exists for birth and spread growth, the analysis in this study will approximate birth and spread growth with the equation $dr/dt = k$. This choice is based on the argument the nucleation rate per unit area per unit time is constant. Another equation has been tentatively proposed by Nordeng and Sibley (1996) from empirical evidence. Nordeng and Sibley (1996) suggest $dr/dt = kr$ may represent a hybrid mononuclear-polynuclear crystal growth mechanism. This equation is also declined in favor of $dr/dt = k$. If each square unit of crystal surface has the same random chance of forming a nucleus on the surface, then the nucleation rate per unit area per unit time will not vary with crystal size. Thus, crystal size, given the model's assumptions is best described by $dr/dt = k$.

A growth model, which is not constrained by relative nucleation rates, is the Spiral Growth Model (Burton *et al.* 1951). The spiral growth model describes layer growth away from the crystal face expression of a slip plane. Since portions of the slip plane rise to different heights above the crystal face, adding ions to the leading edge (created by a slip plane) perpetuates the edge of the growth layer through time. This eliminates the need for nucleation, implying spiral growth can occur at saturations below the saturation state necessary for the formation of stable nuclei.

Factors such as solution composition, solute diffusion and crystal form affect nucleation and layer growth by changing surface free energy and free energy of formation of the new precipitate (Steefel and Van Cappellen 1990, Nielson 1964). The radial growth rate, $dr/dt = k$, for polynuclear growth is independent of the radius which intuitively follows from the fact layer growth is an absent to minor component in polynuclear growth. Spiral growth, like polynuclear growth, is also independent of radius. The spiral growth and polynuclear growth rates are both approximated by k (Nielsen 1964). In polynuclear and spiral growth the number of available sites to add an ion to the crystal surface are not constrained by the radius of the crystal when evaluating an individual crystal. Polynuclear growth involves multiple layers precipitating at one time.

Crys

Spiral growth involves addition of ions along turns of a spiral defect. Thus, the growth rate of polynuclear and spiral growth are controlled respectively by the factors influencing the nucleation of simultaneous layers on a growth surface and the distance between adjacent turns of a spiral or collectively by k. Unlike spiral and polynuclear growth, mononuclear growth is a function of radius as well as k for an individual crystal. In mononuclear growth, the number of available sites is proportional to crystal size since only one layer grows across the surface at any point in time and the overall radial growth is limited by nucleation of the next layer. Thus, the larger the crystal, the greater the likelihood of a successful collision resulting in the formation of a nucleus. In birth and spread growth, nuclei may form on any size layer. Thus, there is more than one available nucleation site utilized per growth layer similar to the polynuclear case. Likewise, birth and spread growth is also independent of crystal size since the number of layers formed per unit area per unit time will not vary with crystal size.

Crystal Growth Mechanisms in Natural Systems

The determination of the mechanism and rate of crystal growth has included the use of many different techniques with unique approaches. Previous studies of carbonates used methods including but not limited to petrography, bulk previo[illegible]

subtra[illegible]

fluid [illegible]

tempera[illegible]

Ideal [illegible]

Sible, [illegible]

Sible, [illegible]

1984, [illegible]

Carlso[illegible]

1991, [illegible]

approa[illegible]

column[illegible]

1986, [illegible]

sharp [illegible]

interp[illegible]

the do[illegible]

recur[illegible]

colum[illegible]

solut[illegible]

would [illegible]

Deter[illegible]

With [illegible]

Subst[illegible]

Prop[illegible]

et a[illegible]

chemical analysis, weight of precipitate, crystal size distributions, cathodoluminscence zone data and crystal and fluid composition from crystals grown at different temperatures and solution compositions in the laboratory (Eberl *et al.* 1998, Nordeng and Sibley 1996, Nordeng and Sibley 1994, Sibley *et al.* 1994, Sibley and Bartlett 1987, Sibley *et al.* 1987, Bullen and Sibley 1984, Gregg and Sibley 1984, Saller 1984 , Carlson 1983, Morse 1983, Sibley 1982, Carlson and Rosenfeld 1981, McKenzie 1981, Reddy *et al.* 1981, Choquette and Steinen 1980, Gaines 1980). Field approaches included measuring the extent and abundance of dolomite from outcrop and thin sections (Wilkinson *et al.* 1996, Sibley 1980). Sibley (1980) found dolomite often has sharp boundaries between dolomite and limestone. He interprets the sharp contact as representing the extent that the dolomitizing solution was in contact with the limestone precursor for a time longer than the induction period of dolomite. Limestone in contact with the dolomitizing solution for any period shorter than the induction period would not begin dolomitization.

A more recent method applied to crystal growth determination is the *in situ* analysis of growing crystals with scanning force microscopy. This tool has provided substantial evidence for the growth models originally proposed by Nielsen (1964), Ohara and Reid (1973) and Burton *et al.* (1951). However, this particular method is best used

[illegible]

betwe[illegible]

[illegible]

[illegible]

soil [illegible]

[illegible]

suffer[illegible]

satura[illegible]

et al. [illegible]

experi[illegible]

[illegible]

event [illegible]

surface[illegible]

[illegible]

natural[illegible]

given [illegible]

C[illegible]

Precip[illegible]

[illegible]

[illegible]

Determ[illegible]

[illegible]

Metho[illegible]

Determ[illegible]

Metho[illegible]

for *in situ* analysis or *ex situ* analysis for differentiation between different surface reaction-limited crystal growth models and not as an *ex situ* tool to distinguish diffusion-limited growth from surface reaction-limited growth. *In situ* growth of calcite and gypsum under a controlled fluid composition gives insight into the transition between the different surface reaction-limited mechanisms at different saturations (Stipp *et al.* 1994, Gratz *et al.* 1993, Hillner *et al.* 1992, Rachlin *et al.* 1992). However, these experiments determine the crystal growth mechanism for laboratory-grown crystals and only the last precipitation event in crystals from naturally occurring rocks. Sample surface alteration in natural rocks can etch this surface, altering growth features. In addition, surface analysis of natural crystals does not indicate if all crystals in a given lithofacies had contact with the last fluid.

Cathodoluminescence indicates extent and timing of precipitation from fluids of different Mn and/or Fe compositions. Zonal stratigraphy of an individual luminescent zone appearing in each crystal is used to determine the extent of the rock-water interaction for a particular cathodoluminscent zone. The concentric cathodoluminescent zoning in dolomites can be used to determine the crystal growth mechanism for each internal cathodoluminescent zone (Nordeng and Sibley 1996).

Fe [illegible]
of [illegible]
the [illegible]
Fe [illegible]
the [illegible]
a s [illegible]
pre [illegible]
and [illegible]
Fe [illegible]
deta [illegible]
Fe re [illegible]
betwe [illegible]
three [illegible]
shou [illegible]
in th [illegible]

I [illegible]
of co [illegible]
and co [illegible]
with [illegible]
part [illegible]
the [illegible]
chang [illegible]
requ [illegible]
cryst [illegible]

In carbonate rocks, cathodoluminescence is caused by Mn (Mn^{2+}, Mn^{4+}), which is incorporated into the mineral. Ferrous and ferric iron has the opposite effect. Zoned crystals reflect variations in Mn and Fe concentrations in the precipitating solution through time (Machel 1989, 1983, Fairchild 1983, Pierson 1978). When Mn is incorporated into the Mg or Ca sites of dolomite, spectral analysis indicates a shift to longer wavelengths giving a range of colors from green to yellow to dark red depending on the valence state and concentration of the Mn incorporated (Pierson 1981). Pierson (1981) also found Mn concentration of only 100 ppm necessary to induce luminescence and a minimum of 10,000 ppm Fe needed to suppress luminescence. Sharp boundaries found between individual cathodoluminescent zones may result from threshold values for the substitution of Mg by Mn that induces jumps in the spectral shift as a result of changes in bond length (Pierson 1978, 1981).

The sharp boundaries and variable luminescent intensity of zonation in carbonates allows measurement of zone widths and correlation of zones within formations. To use a zone width as a measure of the rate of precipitation from a particular solution and the three-dimensional variation in zone width from crystal to crystal as a spatial indicator of changes in the rate of precipitation, the following is required: 1) concentric zones can be correlated from crystal to crystal and 2) individual zones are isochronous.

The f
of cry
same p
ones,
corre
assump
onal
crysta
have p
is su
lithi
can be
spaced
Change
simul
ultim
The s
In th
compo
Table
ultim
spec
In so
ultim
to da
Resul

The first requirement can be visually checked by inspection of crystals over the sampling interval. Crystals with the same zonal stratigraphy should have: 1) the same number of zones, 2) the same ordering of zones by intensity, and 3) correlated zones with similar intensities. The second assumption of isochronous zones is based on groupings by zonal stratigraphy and nucleation arguments. A group of crystals with the same zonal stratigraphy are assumed to have precipitated from similar solutions. This assumption is similar to assigning the same age to correlated lithofacies. In both cases, the assumption of isochronity can be stated with greater confidence for more closely spaced samples and only inferred for samples further apart. Changes in solution are assumed to have occurred nearly simultaneously (faster than the induction period for dolomite growth on dolomite) over the range of crystals with the same zonal stratigraphy. The latter assumption is based on the idea that an induction period should exist for compositional changes in dolomite. Experiments conducted by Sibley and Bartlet (1987) indicate an induction period for dolomite precipitating on dolomite when dolomite seeds are added as a reactant in the dolomitization process. Changes in solution that change the composition (% Mg) of the dolomite may be one cause for an induction period. However, to date, exact experiments investigating dolomite precipitation on dolomite have not been performed due to the difficulty of assaying the composition of initial, small quantities of precipitate.

Combination of Crystal Growth and Solute Flux

If a crystal growth unit is defined as a unit of rock that shares the same crystal growth equation, then a crystal growth unit can be defined theoretically by combining reaction rate with solute flux. Solute flux can be divided into high and low solute flux based on the rate of solute flux compared to the rate of solute uptake by crystal growth. High solute flux is when the rate of solute delivered to the surface is greater than the rate of solute uptake by crystal growth (Surface-Reaction-Limited Crystal Growth). Low solute flux is when the rate of solute delivered to the surface is less than the rate of uptake by crystal growth (Diffusion-Limited Crystal Growth). Since k is a function of solution composition, solute diffusion and crystal form; k will be assumed constant for any one crystal. K will also have a constant value for any lithofacies or portions therein containing a homogeneous solution. Since lithological heterogeneity is a function of scale, any heterogeneous rock unit can be described in terms of its homogeneous parts. Each growth model; diffusion-limited growth, mononuclear growth, birth and spread growth, spiral growth, and polynuclear growth represent their own spectrum of conditions under which that style of growth takes place with threshold values at either end of the spectrum. Thus, a range of k values exist for each growth model (Sunagawa 1984). When k is considered to be roughly approximate to solute concentration, the threshold values become threshold saturation states between the different growth models as represented by vertical lines between growth models in Figure 1. Spiral growth can occur over the entire range of saturation represented in Figure 1 because it is independent of nucleation. Defects on the surface of the crystal provide an edge for attachment of ions. As ions attach to this edge, the defect (screw dislocation) propagates through time. The spiral growth rate will also increase with increasing solute concentration but its rate relative to other models is unknown.

By integrating the growth rate equations for diffusion-limited crystal growth and the end members of surface-reaction-limited crystal growth from r_1 to r_2 and rearranging the equations in terms of r_1 and the width of the next increment of precipitate (zone width) yields a function that relates the rate of precipitation to crystal size (Table 2). As stated earlier, in the integrated equations, r_1 is the crystal size at the onset of precipitation and r_2 is the crystal size at the end of precipitation. Thus r_2-r_1 is equal to zone width or the increment of new precipitate added to the crystal surface.

[illegible]

[illegible]
[illegible]
[illegible]
[illegible]
[illegible]
[illegible]
[illegible]
[illegible]
[illegible]
[illegible]
[illegible]
[illegible]
[illegible]

A plot [illegible]
linear [illegible]
well a [illegible]
[illegible]
[illegible]
betwe [illegible]
added [illegible]
the [illegible]
for t [illegible]
a pro [illegible]

Population Trends for Crystal Growth Mechanisms

In order to determine crystal growth mechanism, plots of r_2-r_1 (new precipitate added or zone width) versus r_1 (crystal size) for crystal populations can be used (Nordeng and Sibley 1996, Carlson 1989, Kretz 1974). The population trend will reflect the crystal growth equation of the rate-limiting process. The expected trend of zone width vs. crystal size for each of the possible growth mechanisms (Table 2) can be represented by a different family of functions. Mononuclear growth is a complex quadratic equation similar to a parabola except the distance from the vertex increases as distance along the x-axis increases (Figure 2). Rearrangement of the zone width-crystal size population equation for mononuclear growth yields the following equation:

$$r_1 = (1/k) - (r_1^2/zw)$$

A plot of (r_1^2/zw) vs. r1 will yield a slope of -1. Thus, a linear fit to the modified mononuclear plot describes how well a data set fits mononuclear growth. Diffusion-limited growth is an inverted hyperbolic function that asymptotically approaches zero (Figure 3). The relationship between zone width, or the thickness of new precipitate added to the surface, and r_1, crystal size, is a function of time and increasing boundary layer thickness per unit time for that particular crystal. The equation does not describe a population of crystals because it does not describe any

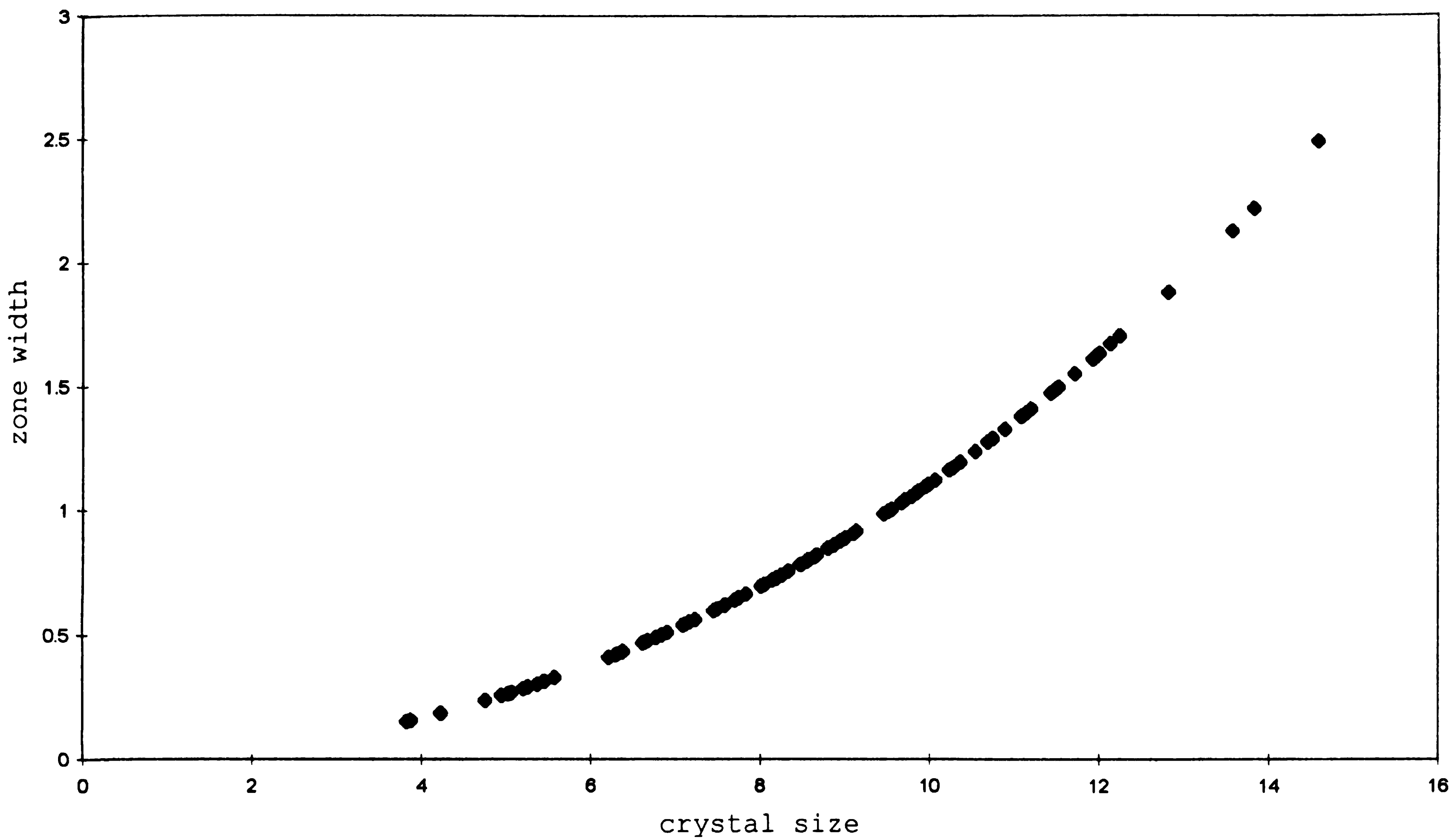

Figure 2. Population Trend for Mononuclear Crystal Growth

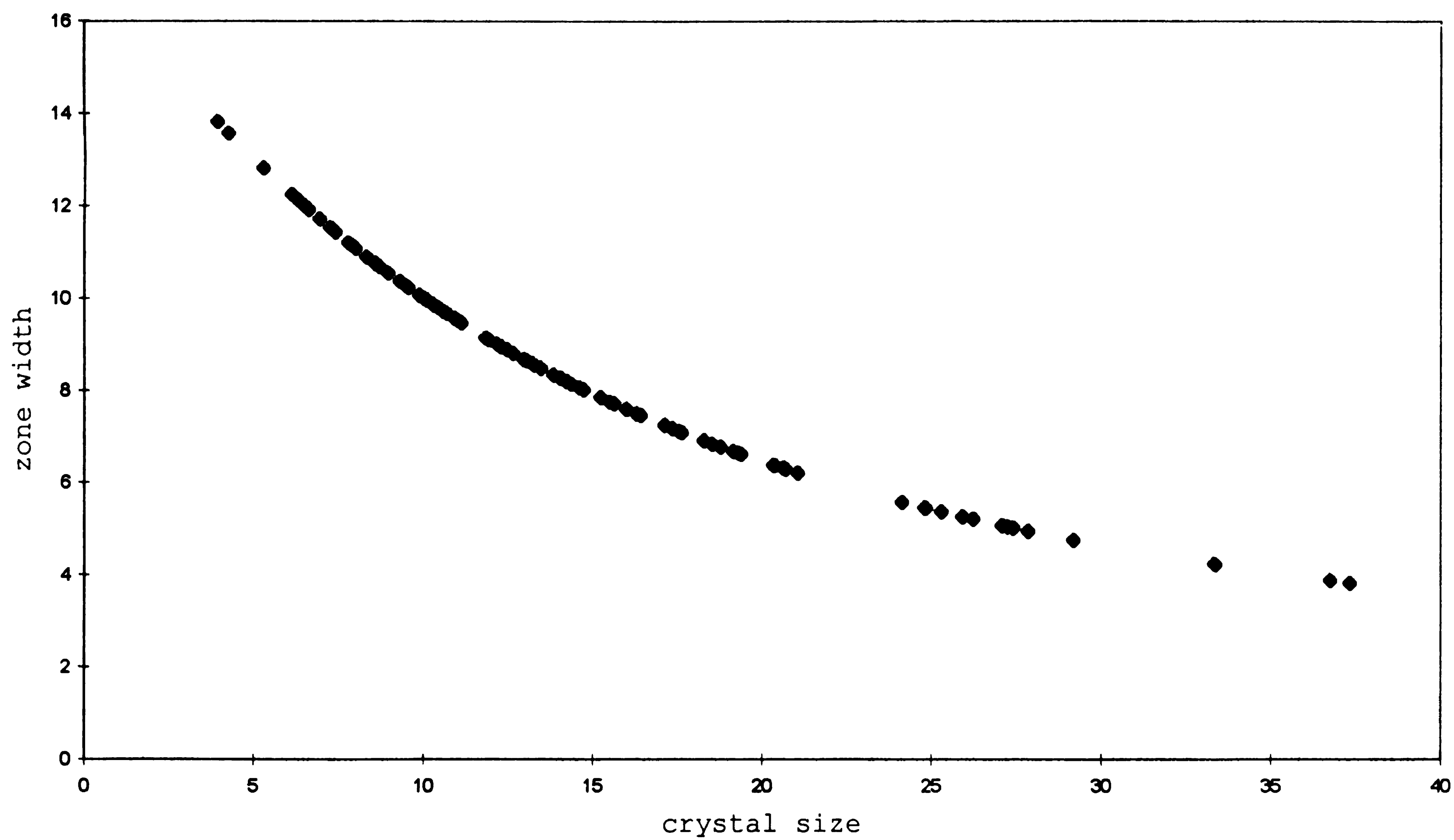

Figure 3. Diffusion Limited Growth Model for a Crystal Through Time

relati
boundar
from th
the fir
is inb
deriat
of it =
polym
crysta
growth,
growth,
stra[illegible]
but s
the
both
a cry
size,
in th
secon
const
nucle
to ta
surf
time
rate

relationship between the initial crystal size and rate of boundary layer formation. If the crystals are precipitating from the same solution on the same substrate, the rate of the formation of boundary layer per unit area per unit time is independent of the initial crystal size when the mechanism switches to diffusion-limited growth. Therefore, $dr/dt = k$ represents diffusion-limited growth as well as polynuclear growth and spiral growth for populations of crystals (Figure 4). In the case of birth and spread growth, a hybrid case between mononuclear and polynuclear growth, a population of crystals would also appear as a straight line, $dr/dt = k$, on a zone-width vs. crystal-size plot since the zone width, new precipitate added per unit of time (growth rate), does not change with crystal size. In birth and spread growth, two critical assumptions result in a crystal growth equation that is independent of crystal size. The first assumption is that nuclei can form anywhere on the surface (Nyvlt 1985, Ohara and Reid 1973). The second critical assumption is the rate of growth of faces is constant (Nyvlt 1985, Ohara and Reid 1973). Since nucleation is the rate-limiting step and nuclei are assumed to have an equal probability of forming anywhere on the surface, the rate of nuclei formation per unit area per unit time is independent of crystal size. Therefore, nucleation rate would not vary with crystal size even though it does

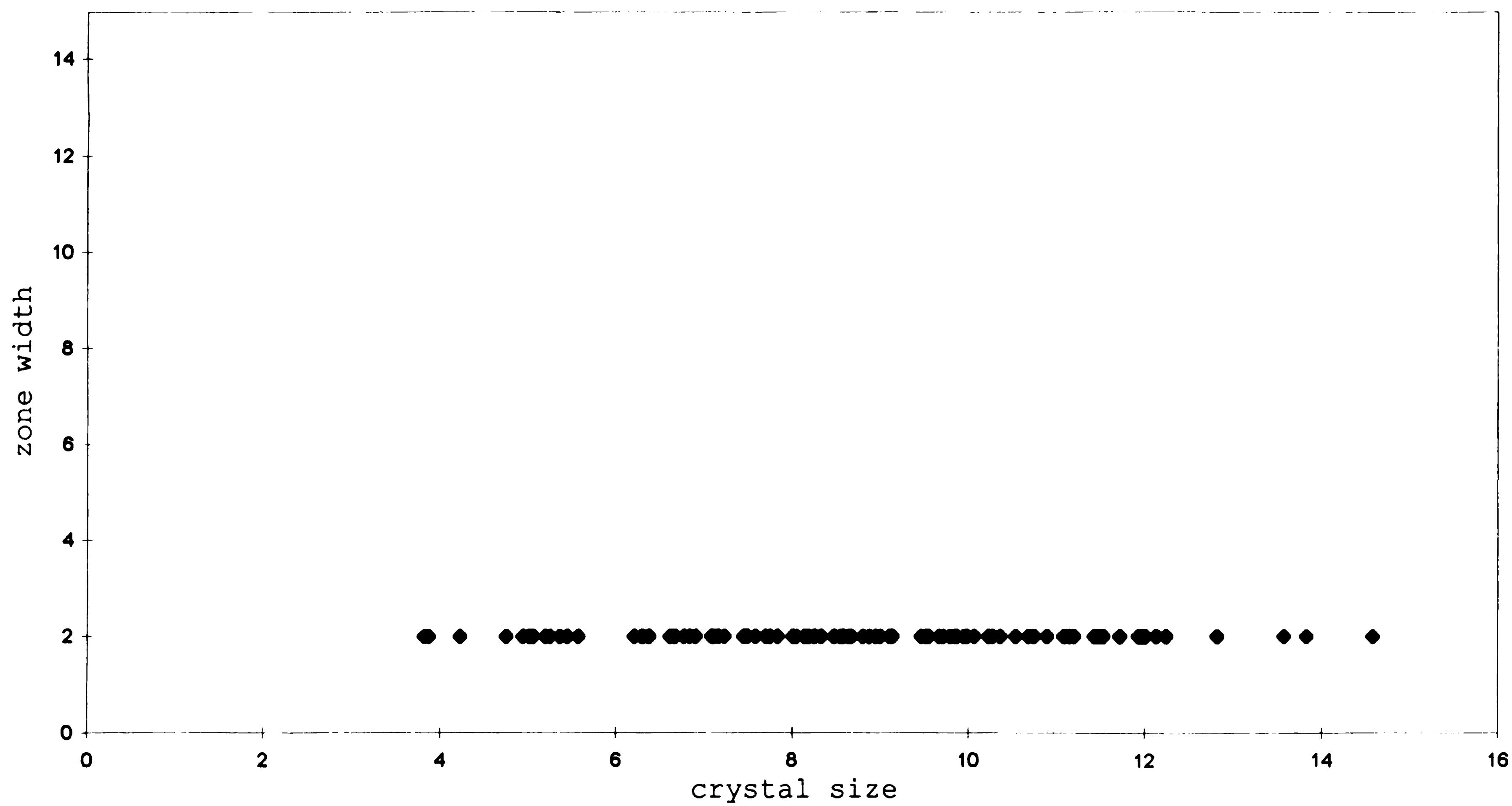

Figure 4. Population Trend for Polynuclear, Birth and Spread, Spiral and Diffusion-Limited Growth Models

vary with solute concentration for the birth and spread growth model similar to polynuclear growth.

For the two trends (mononuclear growth, Figure 2 and all other growth models, Figure 4), the crystal growth equation represented by the zone-width vs. crystal-radius plots would fit $dr/dt = kr^2$ or $dr/dt = k$. For mononuclear growth, a series of equations with a variable distance to the vertex would comprise the function family (Figure 5). For polynuclear, birth and spread, diffusion-limited or spiral growth, the series of equations would consist of horizontal lines (Figure 6).

If k is spatially heterogeneous, the expected trend would be different equations from one family of functions (one crystal growth mechanism) or multiple families of functions (multiple crystal growth mechanisms). If each mechanism can be represented by a range of k values, or growth conditions, and each mechanism has different k ranges (Sunagawa 1984), then k varies with mechanism as well as within a mechanism. Thus, the magnitude of variation in k, or growth conditions determines whether the trend is: 1) different equations from a family of functions representing one crystal growth mechanism, or 2) different equations from different families of functions representing multiple crystal growth mechanisms. The latter can be tested by comparing crystal growth mechanisms, or different zone width-crystal size trends, $dr/dt=k$ or $dr/dt=kr^2$, spatially.

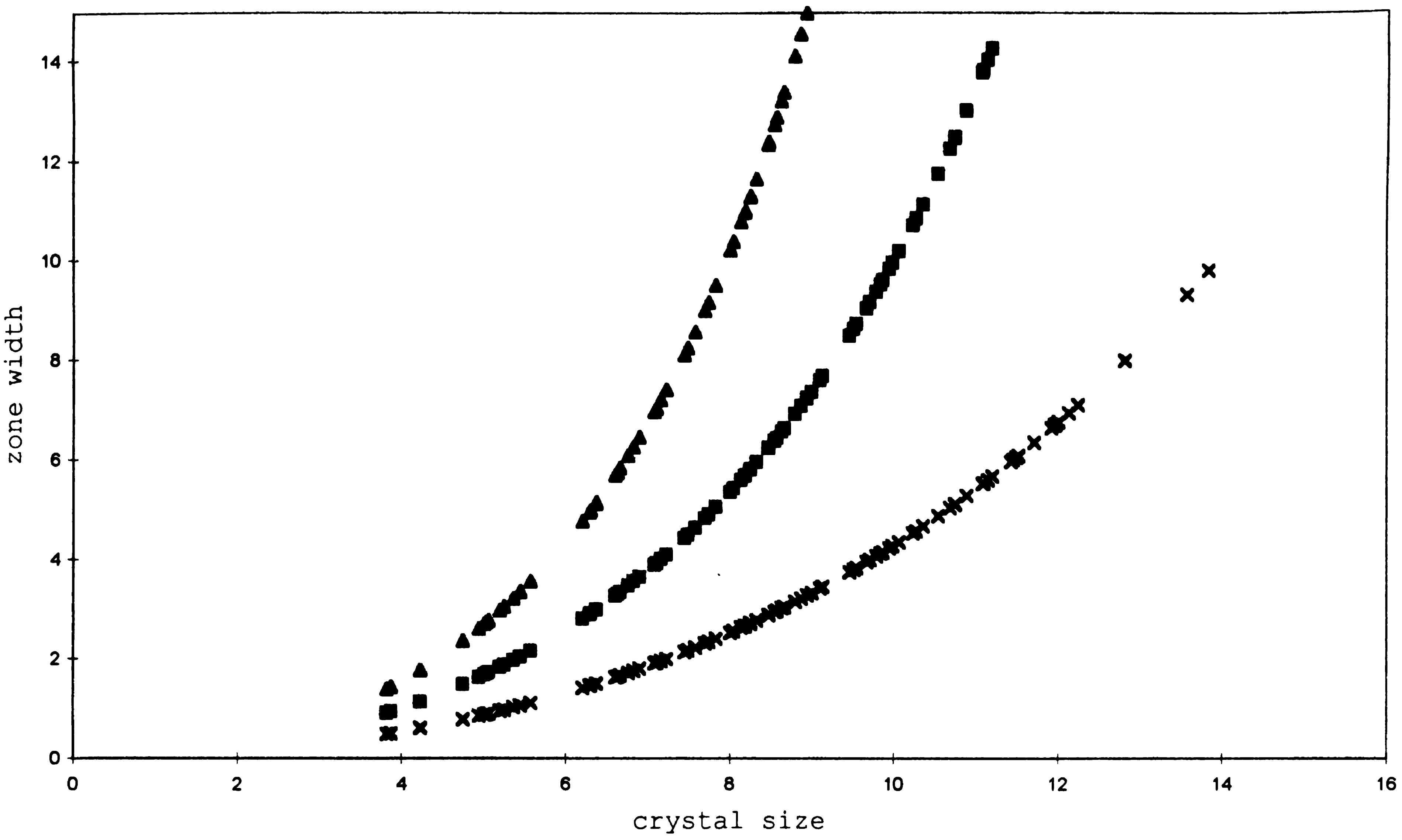

Figure 5. Family of Trends for Mononuclear Crystal Growth

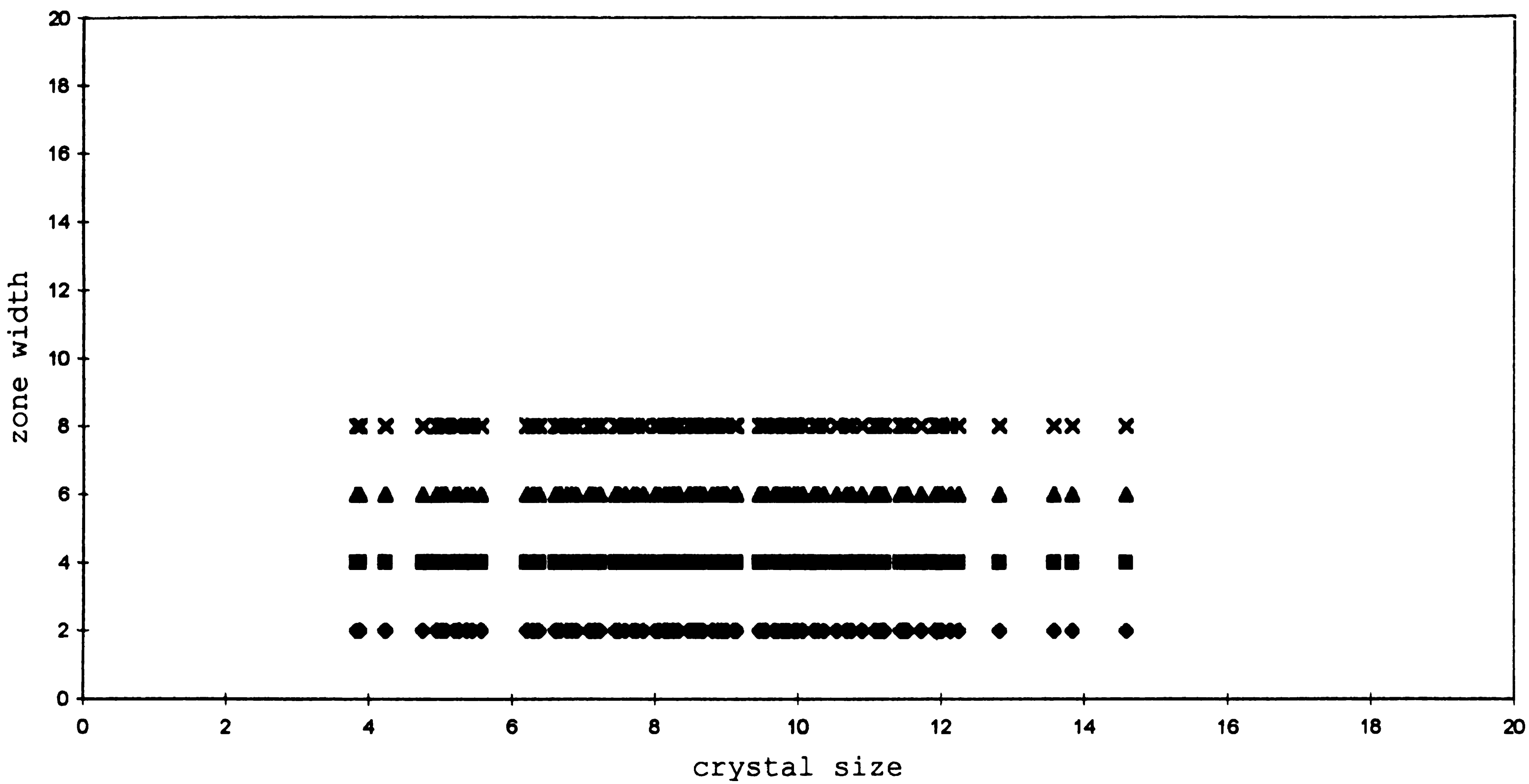

Figure 6. Family of Trends for Polynuclear, Birth and Spread, Spiral and Diffusion-Limited Growth Models

For spa

mechani

& for e

a singl

is exp

to pro

Geolog

T

Ordov

and Se

metho

Fe

Outcr

Ones

White

Ones

Ore

to ap

Meas

The

Cons

Burl

Out

Miss

For spatial comparisons involving one crystal growth mechanism, the variation of the basic equation type, dr/dt = k for example, represents variable crystal growth rates from a single crystal growth mechanism. Intuitively, the latter is expected, since each crystal growth mechanism is expected to cover a range of growth conditions (Sunagawa 1984).

Geologic Setting

The Saluda Formation (Ordovician), Whitewater Formation (Ordovician), Burlington-Keokuk Formation (Mississippian) and Seroe Domi Formation (Miocene) exhibit concentric cathodoluminescent zoning with multiple light (Mn) and dark (Fe) zones. Zones can be correlated on the scale of an outcrop for the Burlington-Keokuk and Seroe Domi formations. Zones can be correlated between outcrops for the Saluda and Whitewater Formations. These formations exhibit intact, zoned rhombs with minimal subsequent alteration at one or more outcrops of each formation. Since zone width is used to approximate growth rate, the same zone needs to be measured within each formation. This condition constrains the choice of formations to dolomites with spatially consistent zonal stratigraphy.

Burlington-Keokuk Formation

The Burlington-Keokuk formation (Mississippian) crops out across northwestern Illinois, southeastern Iowa, and Missouri (Banner *et al.* 1988). The Burlington-Keokuk is

[illegible]
[illegible]
[illegible]
[illegible]
[illegible]
[illegible]
[illegible]
[illegible]
al.

[illegible]
[illegible]
Gene
Gener
Data
al. [illegible]
and g
Gener
Colum
Chart
exhi
Vari
Vari
Cat
Fig.
Cat

conformably overlain by the Warsaw Shale Formation (Mississippian) and unconformably overlies the Hampton Formation (Mississippian) (Harris 1982). The Burlington-Keokuk consists of shallow marine deposits on an intracratonic shelf, which was subsequently buried by a prograding delta depositing the Warsaw Shale (Lane and DeKeyser 1980). The unit is characterized as dolomitized mudstones and crinoidal wackestones to packstones (Banner *et al.* 1988, Cander *et al.* 1988).

The Burlington-Keokuk dolomites can be divided into three separate dolomite generations based on zonal stratigraphy: 1) a concentrically-zoned rhombic generation (generation I), 2) a brightly-luminescent, rhombic generation, which is not zoned (generation II), and 3) a dark nonluminescent generation (generation III) (Cander *et al.* 1988). Generation II dolomite replaced generation I, and generation III replaced both generation I and II. Generation I had undergone dissolution at most outcrops of dolomitized Burlington-Keokuk. Samples from the Dallas City Quarry (Illinois) and outcrops in Illinois and Missouri exhibit dissolution and replacement of Generation I to various degrees (Figure 7). The zonal stratigraphy also varies from outcrop to outcrop in detail and number of zones (Cander *et al.* 1988). The type of dissolution seen in Figure 7 is characteristic of most outcrops to some degree (Cander *et al.* 1988). A single outcrop in Eastern Missouri

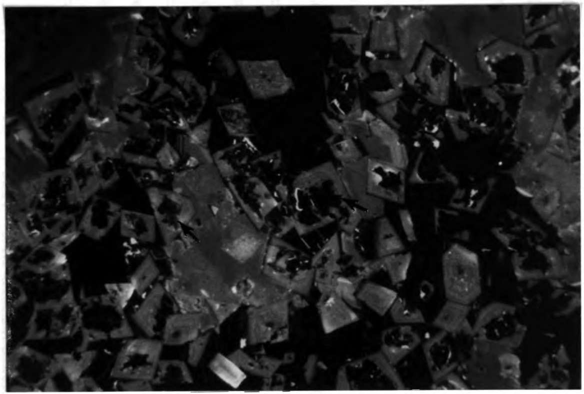

Figure 7. Cathodoluminescent image of Burlington-Keokuk sample from the Dallas City Quarry. Arrows point to dissolution of dolomite cores (1 inch = 100 microns).

[illegible]

that e

Genera

its in

site,

[illegible]

[illegible]

of ge

relat

Sam

Rete.

the

Varia

Miss

Appr

Weig

are

[illegible]

[illegible]

at

[illegible]

[illegible]

[illegible]

Val

(Highway 61, north of Bowling Green, Missouri) was found that exhibits minimal to no evidence of dissolution of Generation I across the entire outcrop. This outcrop with its intact zones was used for the study. At this particular site, the Burlington-Keokuk consists of a unimodal, planar dolomite with fossil molds and is interpreted as a dolomitized crinoidal wackestone (Figure 8, 9).

The isotope values for the concentrically zoned rhombs of generation I indicate a depletion in $\delta^{13}C$ and $\delta^{18}O$ relative to expected marine dolomite of Mississippian age (Banner *et al.* 1988). This was interpreted to represent a meteoric component mixing with seawater after deposition of the Burlington-Keokuk. The variation in $\delta^{18}O$ without variation in $\delta^{13}C$ could also result from normal Mississippian marine waters with temperature fluctuations of approximately 20 degrees Celsius (Figure 10) (Tucker and Wright 1990). However, normal Mississippian marine waters are expected to result in dolomite crystals with higher Sr concentration and lower Fe and Mn concentrations than the Burlington-Keokuk generation I dolomite. Generation I has an Fe concentration range of 500 to 3000 ppm (expected marine value, 16 to 57 ppm), a Mn concentration range of 600 to 1100 ppm (expected marine value, 19 to 22 ppm), and a Sr concentration range of 108 to 123 ppm (expected marine value, 150 to >200 ppm) (Banner *et al.* 1988). The $^{87}Sr/^{86}Sr$

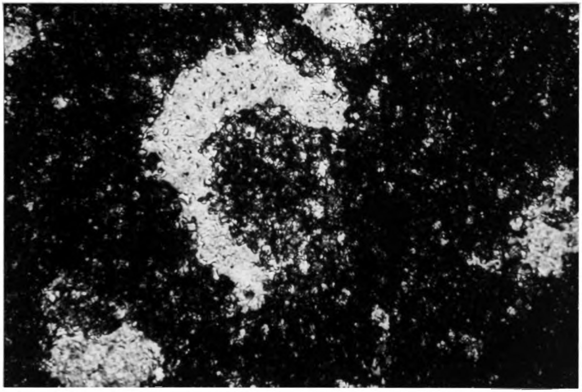

Figure 8. Partially crossed polars view of Highway 61 Burlington-Keokuk sample (Missouri). Arrow points to crinoid fossil mold (1 inch = 200 microns).

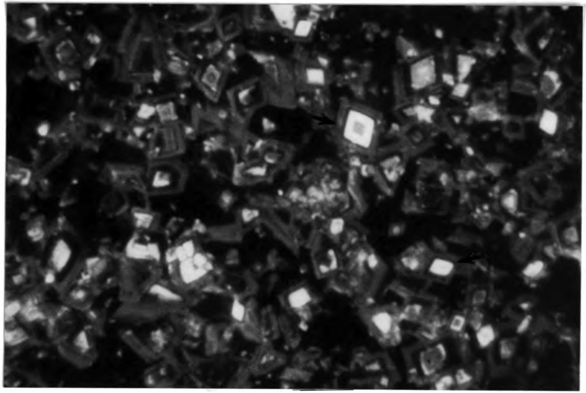

Figure 9. Cathodoluminescent view of Highway 61 Burlington-Keokuk sample. Arrows point to slices of dolomite rhombs that exhibit all the zones encountered. (0.75 inch = 100 microns).

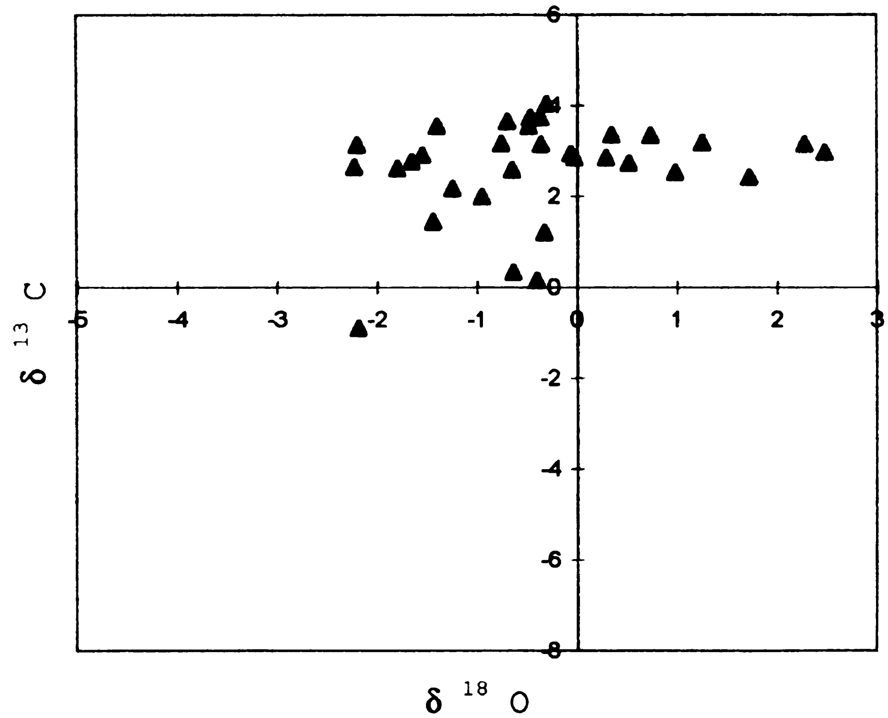

Figure 10. Burlington-Keokuk Isotope Data, $\delta^{18}O$ versus $\delta^{13}C$ (after Banner *et al.* 1988)

atto co

umber

al. 14

neip.

eplac

ugh o

the

Or

for t

aters

ower

et al.

Serre

Capo

Stand

Attl

Germ

Libi

Firs

St.

Up

[illegible]

Ted

Fo

ratio of generation I (0.70757 to 0.70808) is only slightly higher than the expected marine value (0.7076) (Banner *et al.* 1988). Mixing meteoric water with seawater and precipitating dolomite from a high water/rock ratio would explain: 1) the depletion and range of $\delta^{18}O$ and $\delta^{13}C$, 2) the high concentrations of Fe and Mn relative to seawater, and 3) the depleted Sr concentration and only slightly higher $^{87}Sr/^{86}Sr$ ratio (Banner *et al.* 1988). The latter results from the low concentration of Sr in freshwater and meteoric waters enriched in radiogenic Sr from interaction with the lower Paleozoic rocks of the Transcontinental Arch (Banner *et al.* 1988).

Seroe Domi Formation

The Seroe Domi formation represents a foreslope to lagoonal deposit overlying Cretaceous basalts at the Seru Blandan and St. Michielsberg outcrops, Curacao, Netherland Antilles (Miocene). The tops of the inclined beds of the Seroe Domi are partially dolomitized (Fouke *et al.* 1996, Lucia and Major 1994). Completely dolomitized sections of first generation Seroe Domi dolomite at the Seru Blandan and St. Michielsberg outcrops occur as lenses of dolomite that dip seaward (Fouke *et al.* 1996, Lucia and Major 1994, Sibley 1980). The Seroe Domi Formation includes foram wackestones, red algal packstones, coralgal grainstones and boundstones (Fouke *et al.* 1996). Three generations of dolomite have

been recognized in the Seroe Domi outcrops on the island of Curacao: 1) a yellow-orange, concentrically-zoned generation (generation I), 2) an orange-brown generation with sectoral zoning (generation I'), and 3) a dull orange luminescent generation (generation II) (Fouke *et al.* 1996). All three occur as both cements and replacement of calcium carbonate substrate (Fouke *et al.* 1996). Generation I dolomite was used for this study because of its zoned, planar rhombs (Figure 11). The yellow-orange concentrically zoned generation I occurs as dolomite lenses near the base of the section (Fouke *et al.* 1996). Generation I' which exhibits uniform zones most often occurs as a pore-lining cement and rarely exhibits complete rhombs and exhibits sectoral zoning. Generation II does occur as planar rhombs contains but does not have internal zones.

The first generation of dolomite is a unimodal planar dolomite that obliterates the texture of the precursor substrate (Figure 12). The dolomite (generation I) has also being partially replaced by generation II (Figure 13) and has undergone dissolution (Figure 14). The dissolution patterns in Figure 14 are consistent with dissolution of Ca-rich cores and inclusions (Figure 15).

Isotope data have been interpreted as a freshwater-marine mixing zone (Fouke *et al.* 1996, Sibley 1980) and as

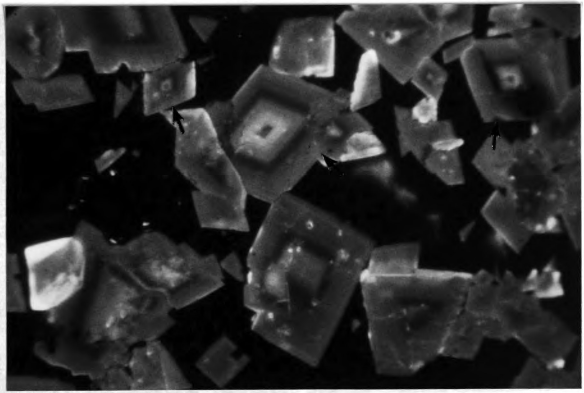

Figure 11. Cathodoluminescent image of Seroe Domi Generation I dolomite crystals. Arrows point to crystals that exhibit all of the zones encountered (1 inch = 50 microns).

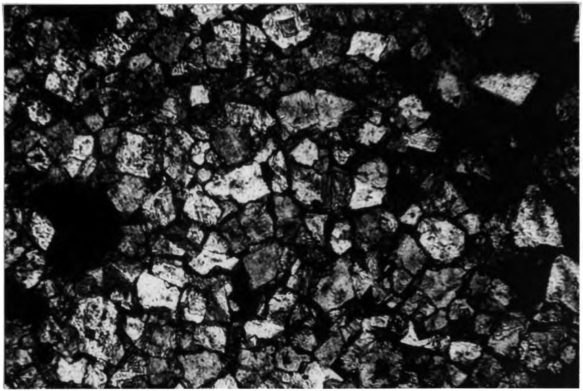

Figure 12. Partially-crossed polars view of Seroe Domi unimodal planar dolomite (0.75 inch = 100 microns).

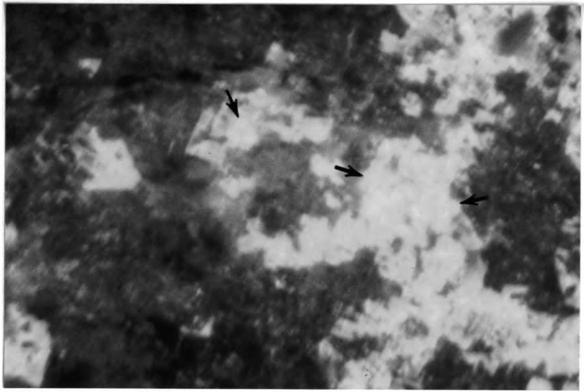

Figure 13. Cathodoluminescent image of Seroe Domi sample showing brightly luminescent dolomite generation II replacing generation I dolomite (1 inch = 100 microns).

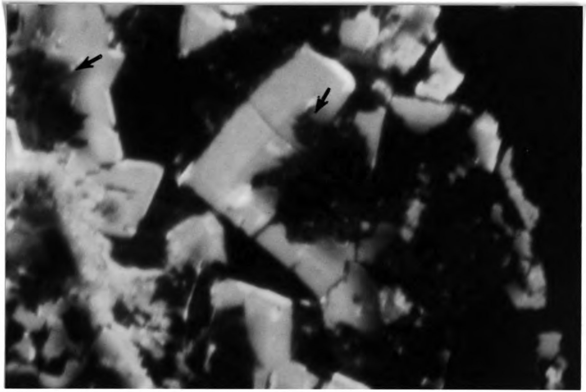

Figure 14. Cathodoluminescent image of Seroe Domi sample exhibiting dissolution of dolomite cores. Arrows point to edge of interior dissolution of generation I dolomite crystals (1 inch = 50 microns).

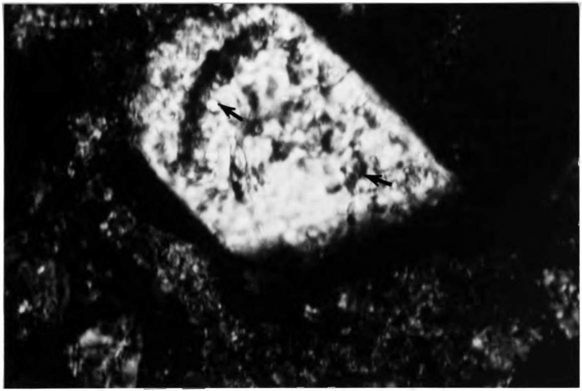

Figure 15. Cathodoluminescent image of Seroe Domi sample exhibiting inclusions and dissolution. Left arrow points to an inclusion. Right arrow points to dissolution (1 inch = 50 microns).

hypersaline seawater (Lucia and Major 1994). Evidence in favor of a mixed freshwater-marine interpretation include $\delta^{18}O$ values that are consistent with normal surface temperatures and $\delta^{13}C$ variation similar to modern seawater-freshwater mixing environments (Fouke *et al.* 1996, Machel and Burton 1994, Machel 1989). Evidence in favor of hypersaline seawater dolomitization is based on the geometry of the dolomitized lenses. A zone of undolomitized limestone that should comprise the upper freshwater lens is absent. In addition, dolomitization does not crosscut beds as expected for a mixing lenses moving deeper into the section as regresssion of seawater occurred (Lucia and Major 1994). Evidence against hypersaline seawater dolomitization is that the shape of the dolomitized lenses is a result of dolomite selectivity (Fouke *et al.* 1996). Fouke *et al.* (1996) argue that precursor beds for the stratiform dolomite bodies were more readily dolomitized than the surrounding limestone precursor. In addition, concentrations of the trace elements Na, Cl and SO_4 are lower than expected for a dolomite precipitating from evaporated seawater (Fouke *et al.* 1996). Further evidence in support of mixed seawater-meteoric dolomitization includes: 1) $\delta^{13}C$ and $\delta^{18}O$ values lighter than the estimated marine dolomite and 2) low Mg calcite cements encrusted by generation I dolomite (Fouke *et al.* 1996). The latter

suggests a period of subaerial exposure immediately prior to precipitation of generation I dolomite. The variation in $\delta^{13}C$ and $\delta^{18}O$ has also been suggested to represent mixing of marine and freshwater with different total dissolved carbon concentrations and soil-derived CO_2 (Fouke *et al.* 1996) (Figure 16). If the two fluids mixing had the same total dissolved carbon concentration, a plot of $\delta^{18}O$ vs. $\delta^{13}C$ values would fall on a line with a slope of 1. In this case, the freshwater has a higher total dissolved carbon concentration since it: 1) does not have a slope of 1 and 2) the $\delta^{13}C$ signature is lighter indicative a freshwater influence.

Saluda/Whitewater Formations

The Saluda Formation (Ordovician) is a massive dolomite overlain by partially dolomitized, marine limestones of the Whitewater Formation (Ordovician) and underlain by interbedded, marine limestones and shales of the Dillsboro Formation (Ordovician)(Brown and Lineback 1966). The Saluda and Whitewater Formations extend into southern Ohio and Kentucky. The Saluda Formation has also been recognized as a member of the Whitewater Formation based on its restricted extent (Gray 1972). The Saluda dolomite has been interpreted as a lagoonal deposit with dolomitization occurring from hypersaline solutions resulting from evaporation of seawater (Martin 1975, Hatfield

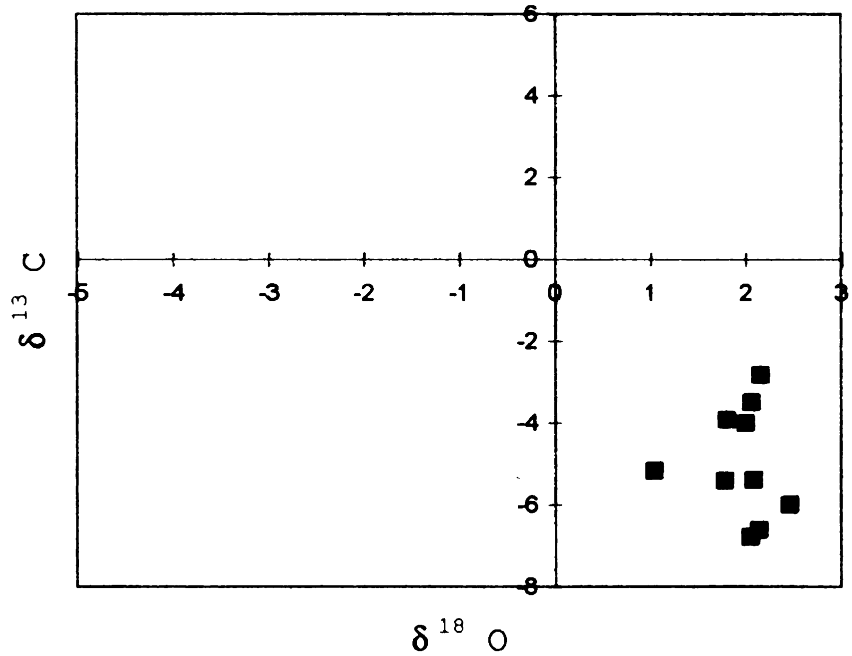

Figure 16. Seroe Domi Isotope Data, $\delta^{18}O$ versus $\delta^{13}C$ after Fouke *et al*. 1996

1968). The depositional model is based on the presence of large corals, *Tetradium* and *Favistella,* which surrounded the dolomitized lens of the Saluda Formation off the Cincinnati arch, and acted as a barrier to seawater (Hatfield 1968). Further evidence in support of a hypersaline interpretation is the presence of the ostracodes, *Leperditia* and *Leperditella*, which prefer a hypersaline environment (Hatfield 1968). In the Madison, Indiana area, the Saluda formation varies from interbedded, partially dolomitized fossiliferous grainstones and dolomicrite near the base to a massive laminated dolomicrite comprising the upper portion of the Saluda formation. The overlying marine limestones of the Whitewater Formation are partially to completely dolomitized peloidal grainstones.

Three outcrops (Highway 421, Hwy 7 and Hwy 56 outcrops; Madison, Indiana) were compared (see Sampling Locations section for locator map). The Highway 421 outcrop has the most complete and thickest section of the Saluda and Whitewater Formations. At this locality, there is approximately 16 feet of vertical section of the Saluda Formation and 20 feet of vertical section of the Whitewater Formation. The transition between the Saluda (dolomicrite) and the Whitewater (peloidal grainstone with abundant ostracods) is gradational over 8 feet of section. The upper portion of the Whitewater changes from a massive partially dolomitized limestone to interbedded shales and limestones.

The Saluda consists of the upper massive dolomicrite, which contains minor laminations and the lower interbedded partially dolomitized grainstones and dolomicrite at the base. The predominant fossils in the partially dolomitized grainstones are brachiopods, bryozoans, crinoids and trilobites. The massive dolomicrite represents approximately 10 feet of vertical section and the lower interbedded section represents 6 feet of vertical section. In the lower section, the interbedded dolomicrite persists laterally. The grainstones occur as irregular, discontinuous lenses ranging from 4 to 22 feet laterally. Both the interbedded grainstones and dolomicrites thickness vary between 1 and 3 feet vertically. There are sharp boundaries between the interbedded grainstones, interbedded dolomicrites, and massive dolomicrite.

At the Highway 7 and 56 outcrops, the total section is thinner. Cores of this section also indicate thinning eastward (Gray 1972, Brown and Lineback 1966). At the Highway 7 outcrop, formations above the Saluda have been eroded. There is approximately 10 feet of vertical section of the Saluda present. The interbedded grainstones and dolomicrites have the same lateral extent but do not exceed 1.5 feet vertically. The lower portion of the Saluda comprises only 4 vertical feet of section. At the Highway 56 outcrop, both the Saluda and Whitewater Formations are present. The Saluda at this outcrop is represented by 4

vertical feet of section. Half of the Saluda section is represented by interbedded grainstones and dolomicrites. Individual beds range from a few inches to 2 feet thick. The transition between the Saluda and the Whitewater is gradational, similar to the 421 outcrop. Approximately 10 vertical feet of the Whitewater Formation (peloidal grainstone) overlies the Saluda Formation. At both the Highway 421 and 56 outcrops, the Whitewater Formation is overlain disconformably by Silurian limestones.

Dolomite crystals in the Saluda Formation and overlying Whitewater Formation share the same zonal stratigraphy (Figure 17, 18). The same zone patterns indicate the two formations were dolomitized by the same solution (Sibley *et al.* 1993, Meyers 1974). Dolomitization of the Saluda and Whitewater Formations concurrently is in direct contrast to the idea the Saluda Formation was dolomitized penecontemporaneoulsy with deposition of the fine lime mud in a hypersaline environment (Martin 1975, Hatfield 1968). This does not indicate the Saluda precursor limestone was not deposited in a hypersaline environment but that dolomitization occurred after deposition of both the Saluda and Whitewater formations. The linear covariance between $d^{13}C$ and $d^{18}O$ values is consistent with dolomitization from a mixed meteoric-marine water rather than hypersaline solution (Figure 19, Table 3) (Lu and Meyers 1998, Frank *et al.* 1995). In this particular case, the total dissolved carbon

Figure 17. Cathodoluminescent view of Saluda dolomite crystal. Arrows point to crystals exhibiting all encountered zones (1 inch = 80 microns).

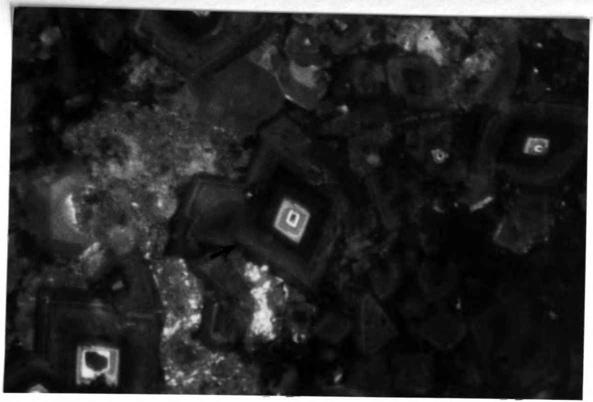

Figure 18. Cathodoluminescent view of Whitewater dolomite crystal. Arrow points to crystal exhibiting all encountered zones (1 inch = 100 microns).

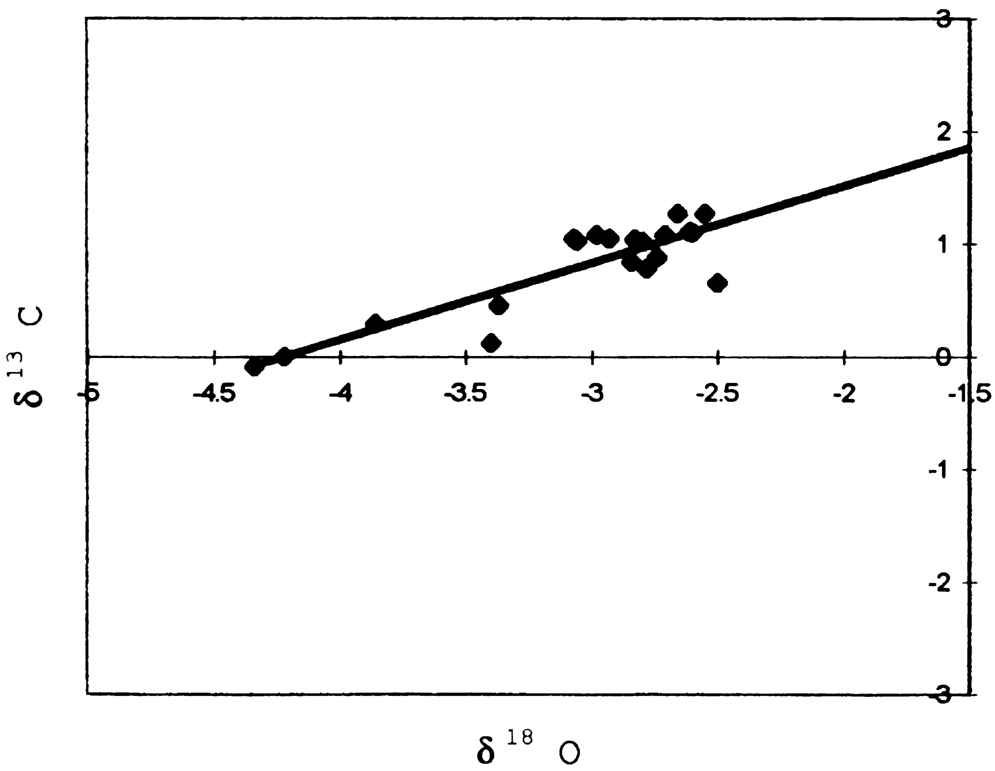

Figure 19. Saluda and Whitewater Isotope Data
$\delta^{18}O$ versus $\delta^{13}C$

Table 3. Carbon and Oxygen Isotope Data for Saluda and Whitewater Formations

Sample ID	$\delta^{13}C$ (VPDB)	$\delta^{18}O$ (VPDB)
M34	0.78	-2.78
G8	1.05	-3.07
P37	.12	-3.40
SD13	1.03	-3.06
P27	-0.09	-4.34
P17	0.29	-3.86
SD23	0.45	-3.37
SD3	0.84	-2.84
M4	1.04	-2.83
M11	0.88	-2.74
M20	1.02	-2.80
G5	0.65	-2.50
G4	1.05	-2.93
D8	1.27	-2.55
D10	1.27	-2.66
G3	1.11	-2.61
G6	1.10	-2.60
D6	1.08	-2.98
P2	0.00	-4.22
M42	1.08	-2.71

W
a
a
W
re
Wi
Jo
cs
F
Wi
do
do
For
Ler
Pac
29,
Hi

concentrations of the two fluids would be the same. The $d^{13}C$ and $d^{18}O$ values also fall within the range expected for precipitation from late Ordovician seawater. However, this is inconclusive based on the large ranges in $d^{13}C$ and $d^{18}O$ (4 and 6 $^{o}/_{oo}$ ranges) obtained from brachiopods (Qing and Veizer 1994) and the general disagreement between workers on the best isotope values for Ordovician seawater.

The massive dolomicrite is a unimodal planar dolomite with minor bioturbation and lamination and is interpreted as a massive mudstone (Figure 20). The Whitewater Formation is also comprised of a unimodal planar dolomite. In the Whitewater, ostracodes are only partially replaced and relict outlines of peloids are common (Figure 21). The Whitewater is interpreted as a peloidal grainstone. Dolomite rhombs nonmimetically replacing compacted ostracodes indicates dolomitization was postdepositional (Figure 22, 23, 24). The boundary between the Saluda and Whitewater is marked by a transition from laminar dolomicrites lacking fossil evidence to the partially dolomitized peloidal grainstones in the Whitewater Formation. In the lower section of the Saluda, grainstone lenses grade eastward from the Highway 421 outcrop into packstones (Figure 25, 26) and wackestones (Figure 27, 28, 29, 30) interbedded with dolomitized mudstones at the Highway 56 and 7 outcrops.

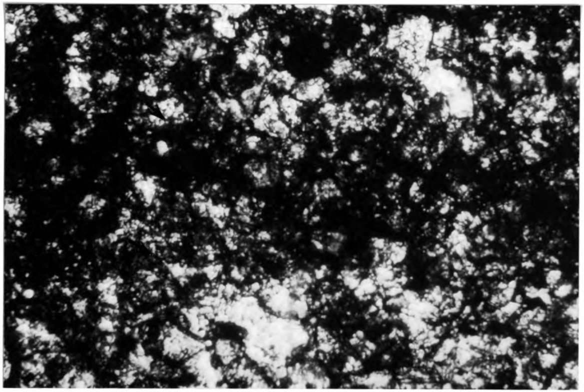

Figure 20. Plain light view of Saluda mudstone. Arrows point to top and bottom of lamination (1 inch = 200 microns).

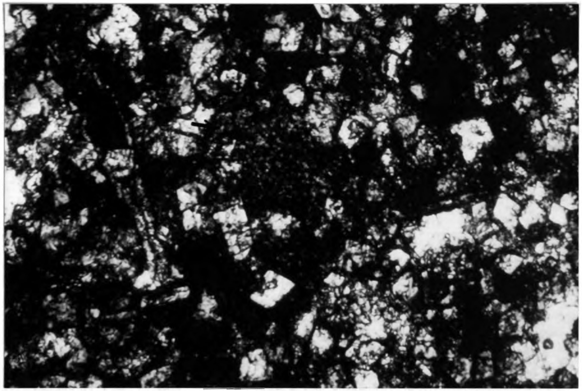

Figure 21. Partially crossed polars view of Whitewater peloidal grainstone. Arrow points to relict outline of peloid (1 inch = 100 microns).

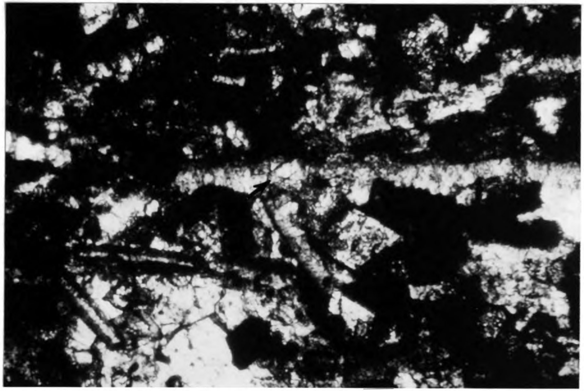

Figure 22. Plain light view of Whitewater peloidal grainstone. Dolomite rhomb (indicated by arrow) is replacing compacted ostracodes (1 inch = 100 microns).

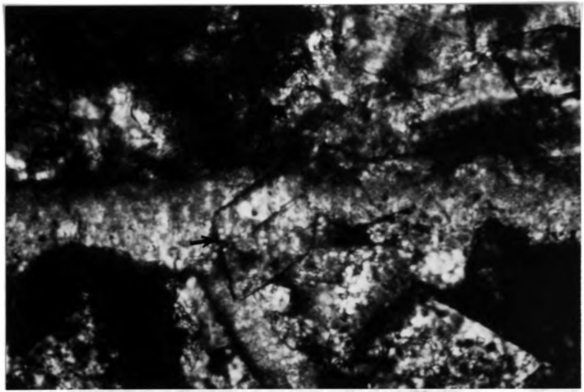

Figure 23. Closeup view of dolomite rhomb in Figure 22 (1 inch = 50 microns).

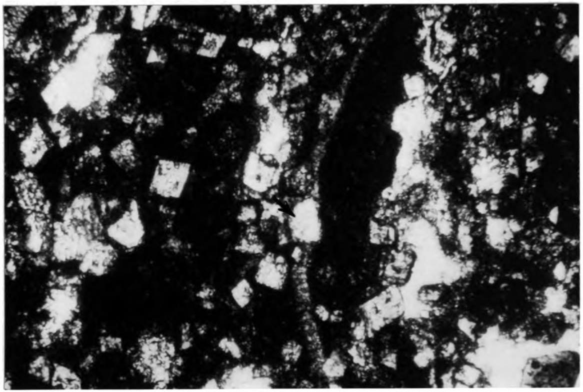

Figure 24. Plain light view of Whitewater peloidal grainstone. Arrow points to dolomite rhomb replacing an ostracode (1 inch = 200 microns).

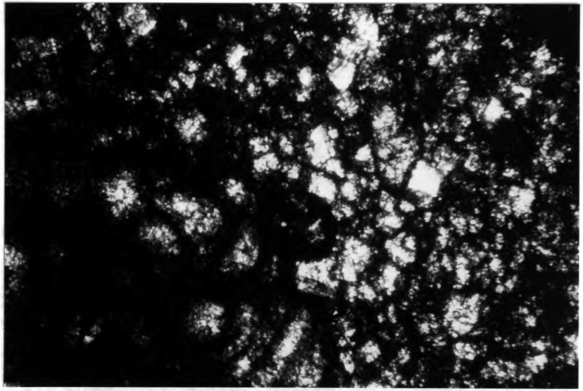

Figure 25. Partially crossed polars view of Saluda packstone. Arrow points to fossil fragment (1 inch = 200 microns).

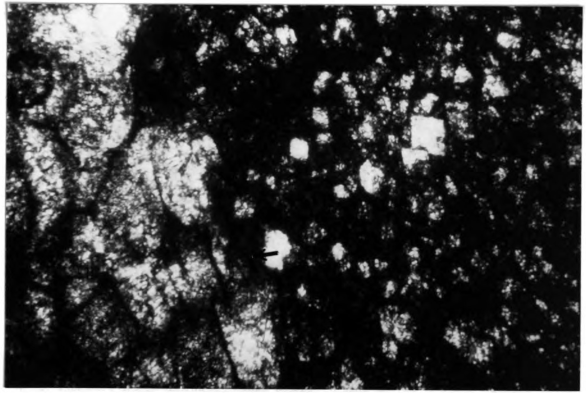

Figure 26. Partially crossed polars view of Saluda packstone. Arrow points to fossil fragment (1 inch = 200 microns).

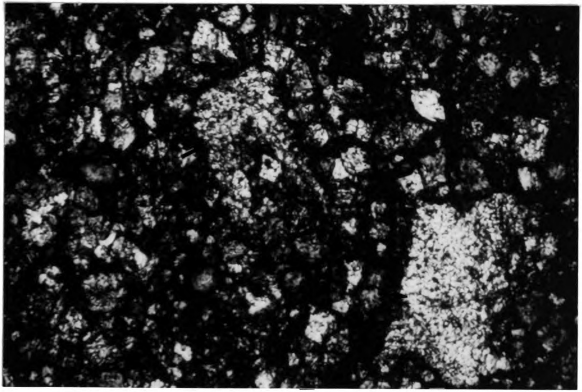

Figure 27. Partially crossed polars view of Saluda wackestone. Arrows point to crinoid fragments (1 inch = 200 microns).

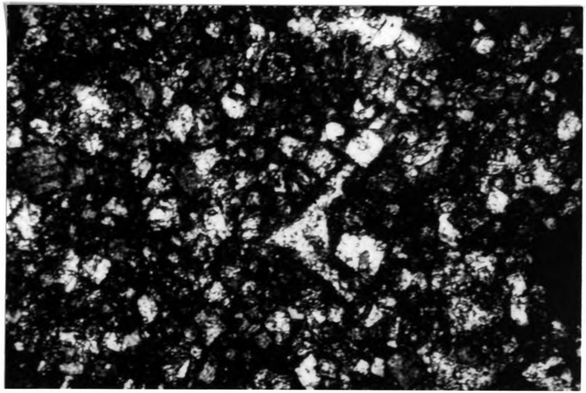

Figure 28. Partially crossed polars view of Saluda wackestone. Arrow points to crinoid fragment (1 inch = 200 microns).

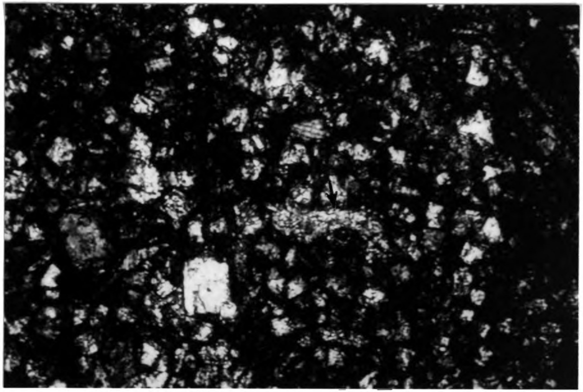

Figure 29. Partially crossed polars view of Saluda wackestone. Arrow points to crinoid fragment (1 inch = 200 microns).

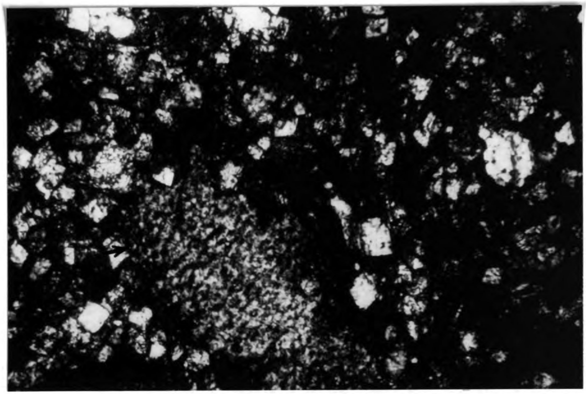

Figure 30. Partially crossed polars view of Saluda wackestone. Arrow points to bryozoan fragment (1 inch = 200 microns).

Methods

Dolomites representing different lithologies, ages and stable isotope signatures were chosen to compare zone-width (growth rate) vs. crystal-size relationships (Figure 31). The consistent zonal stratigraphy between the Whitewater Formation and Saluda Formation allowed comparison of mudstones, grainstones, packstones and wackestones. Wackestones from the Burlington-Keokuk and Saluda, which have distinctly different dolomitizing fluids, (based on stable isotope signatures) were used for comparisons between similar precursor lithologies of different ages (Figure 8, 27-30). The Seroe Domi exhibited more than one concentric zone free of zonal unconformities (episodes of alteration or dissolution between precipitation of individual zones) bounded by at least one internal and external zone. This allowed comparison of zone width-crystal size relationships through time.

Zone Selection

A zone must represent the entire period of precipitation, or be free of zonal unconformities, and be preceded and succeeded by a zone to accurately reflect growth rate. If the central zone is chosen, differences in time for primary nucleation could account for differences in zone width since the type of substrate has been shown to affect the length of the induction period, or time to first

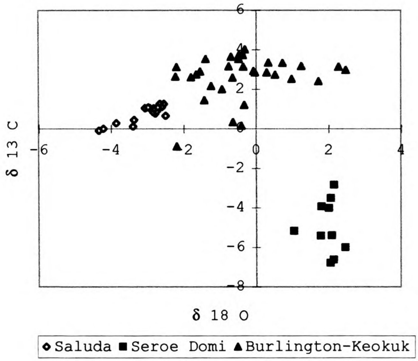

Figure 31. Isotope Data, δ18O versus δ13C

heterogeneous nucleation (Sibley *et al.* 1994). This effect is minimized during secondary nucleation of dolomite on dolomite. The outermost zone is commonly found to exhibit dissolution or intergrowth preventing an accurate measurement of zone width. In addition to these restrictions, only concentrically zoned, rhombic slices of the crystals in thin section are measured in order to convert apparent zone width to true zone width (see Geometric Corrections Section).

Sampling locations

Samples of the Saluda, Whitewater, and Burlington-Keokuk Formations were collected from four outcrops. Thin sections for the Seroe Domi Formation were provided by Bruce Fouke (see Fouke *et al.* 1996). The Saluda and Whitewater formations are represented by three outcrops along an east to west trend near Madison, Indiana (Figure 32). The Burlington-Keokuk Formation crops out along Highway 61 north of Bowling Green, Missouri (Figure 32). Samples were collected on a grid from the four outcrops (Figure 33, 34, 35 and 36). The Seroe Domi formation thin sections are from transits along two adjacent outcrops (Figure 37, after Fouke *et al.* 1996 and Fouke, unpublished field notes). Sample locations are indicated on the profiles of the three outcrops of the Whitewater and Saluda dolomite at the Highway 421, Hwy 7 and Hwy 56 outcrops in Southern Indiana

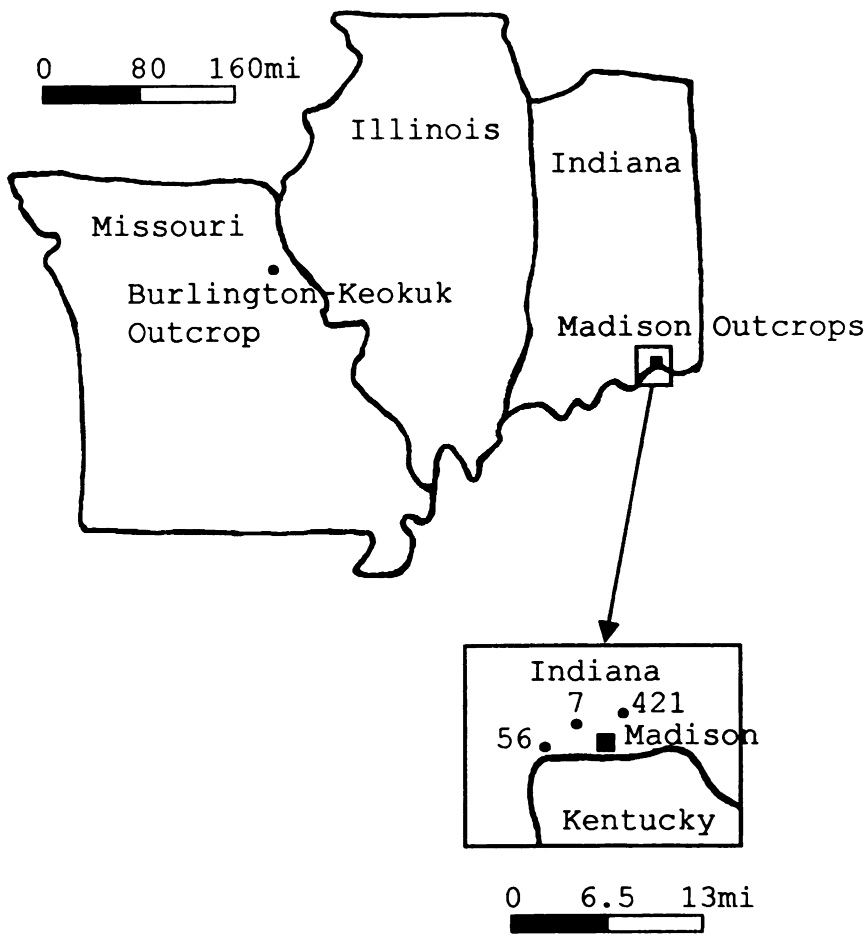

Figure 32. Location Map

Figure 33. Highway 421 Outcrop of Saluda and Whitewater Formations. Arrow points to coral layer at base of Saluda.

Figure 34. Highway 7 Outcrop of Saluda and Whitewater Formations. Arrow points to coral layer at base of Saluda.

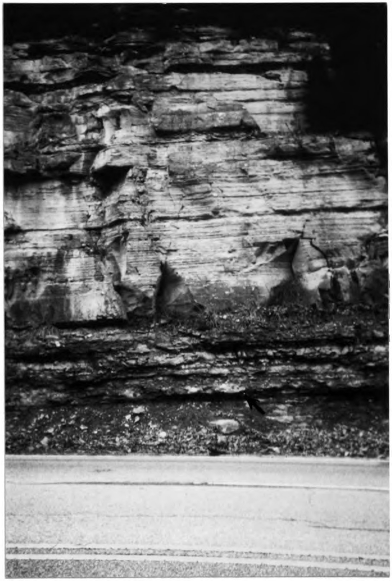

Figure 35. Highway 56 Outcrop of Saluda and Whitewater Formations. Arrow points to coral layer at base of Saluda.

Figure 36. Highway 61 outcrop of Burlington-Keokuk Formation.

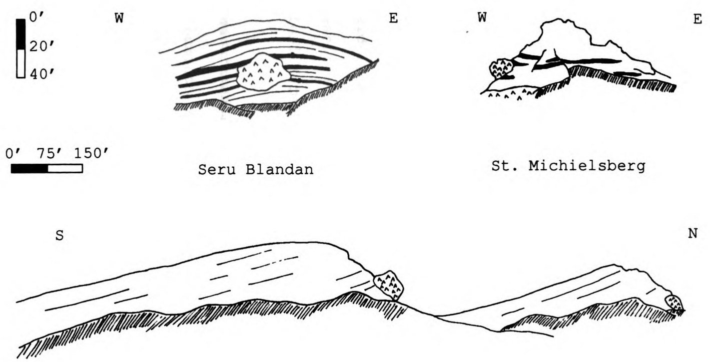

Figure 37. Seroe Domi, Seru Blandan and St. Michielsburg Outcrops, Curacao (after Fouke *et al*. 1996 and Fouke unpublished field notes)

(Figure 38, 39 and 40). The three outcrops occur across a transect approximately 5.5 miles in length (Figure 32). At the largest outcrop, the Highway 421 outcrop, samples were collected along 435 feet of exposure. Samples were collected in grids at a spacing of 3-5 feet vertically and horizontally where possible as indicated on the outcrop profiles (Figure 38, 39 and 40). A similar grid sampling was employed for collection at the Hwy 61 outcrop of the Burlington-Keokuk in Eastern Missouri covering a distance laterally of 363 feet (Figure 41). Samples from the Seroe Domi represent three small dolomitic lenses less than 15 feet long and 3 feet thick (shaded beds in Figure 37). Only three widely spaced samples were analyzed due to significant replacement and dissolution of generation I dolomite in the Seroe Domi Formation.

Zone Measurements

A Luminoscope Model ELM 3.3 operating at 16kV was used to observe the cathodoluminescence of dolomite in polished thin sections of the four formations. Color slide pictures were taken from thin sections of the samples. The slides were then examined with a light microscope for rhombic slices of dolomite. Rhombic slices of dolomite that exhibited concentric zoning and parallel zone apexes were measured (Figure 42). The length measurements A, B, C and E are used to correct slices that cut the center of the

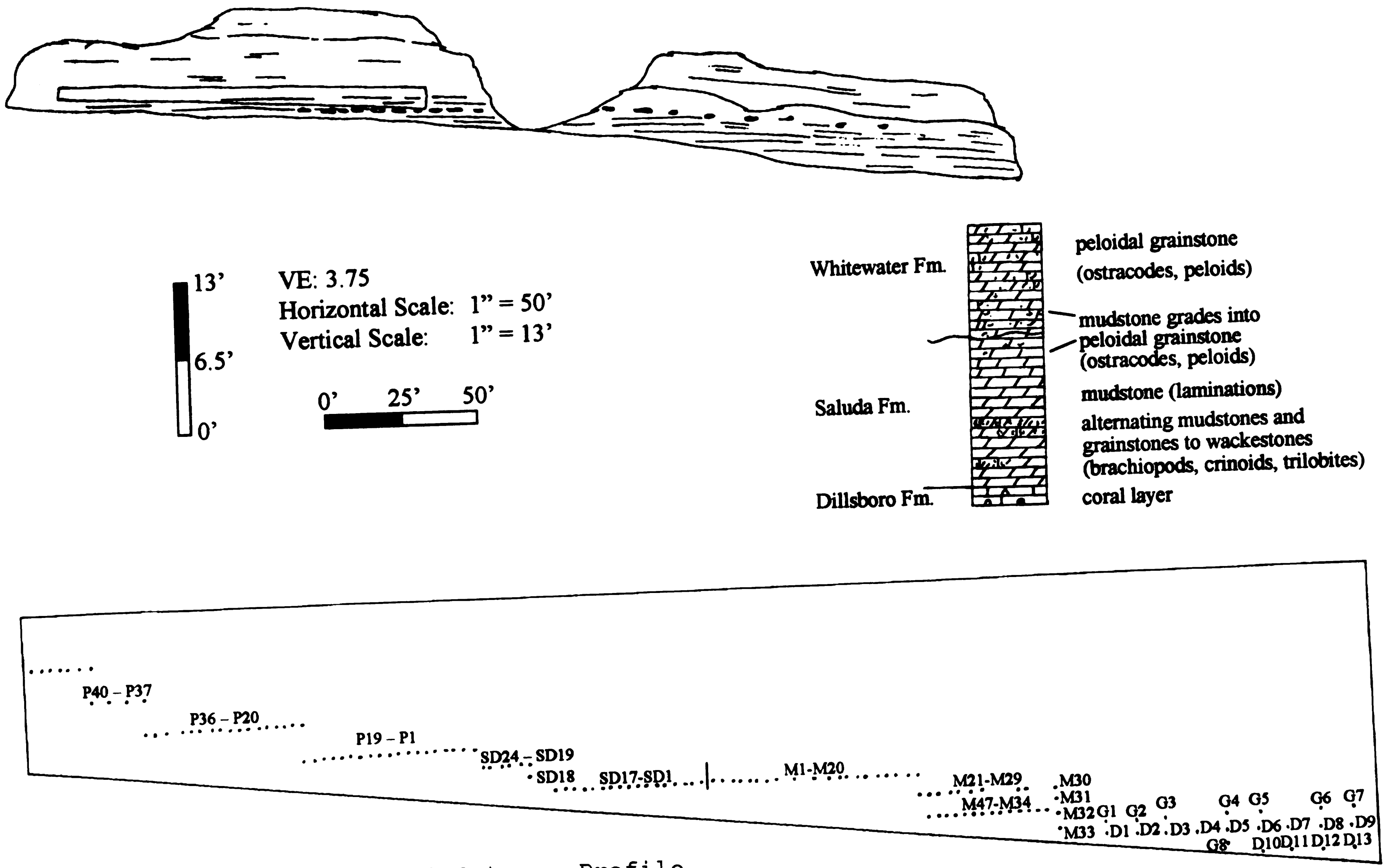

Figure 38. Saluda Hwy 421 Outcrop Profile

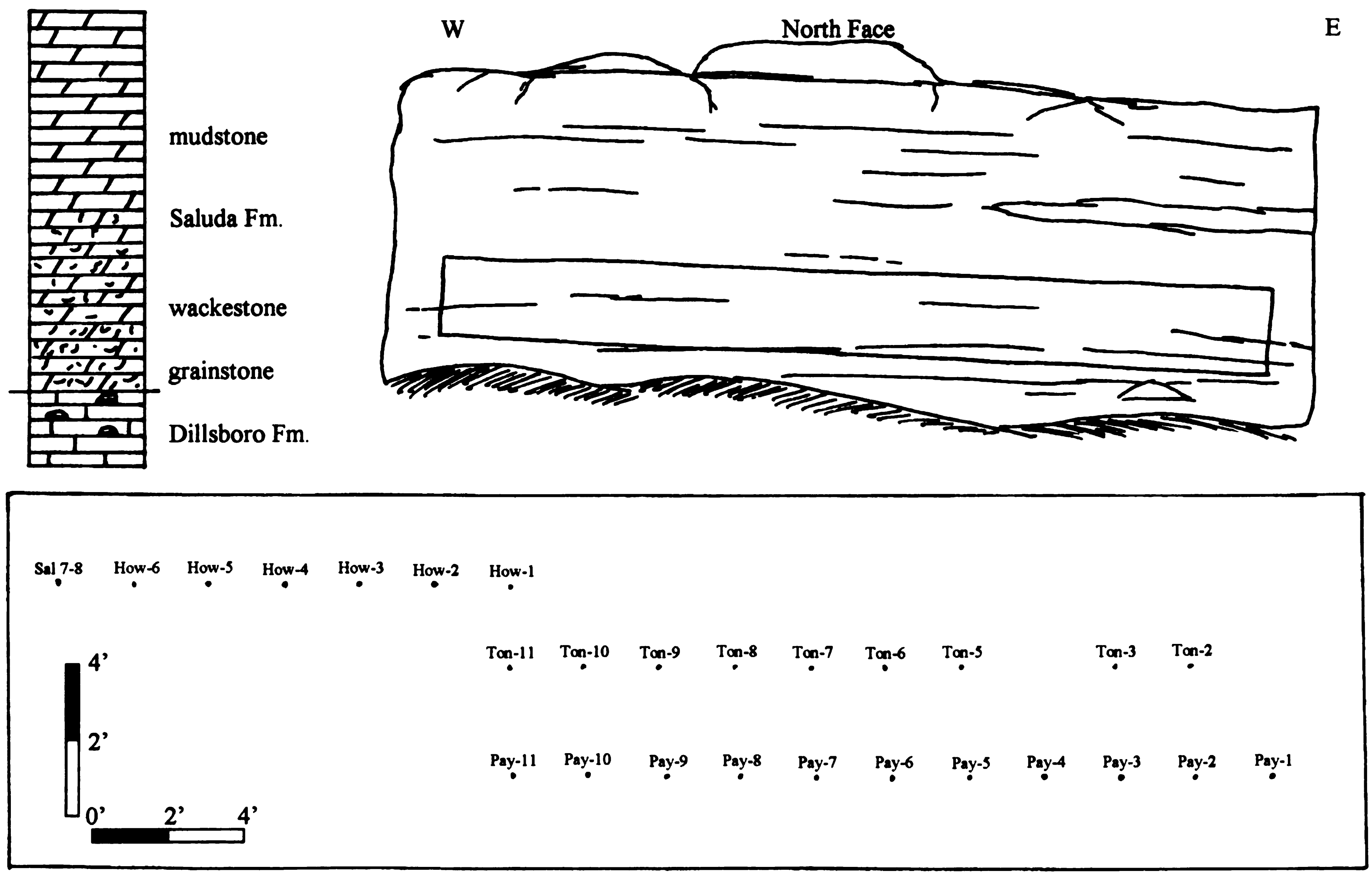

Figure 39. Saluda Hwy 7 Outcrop Profile

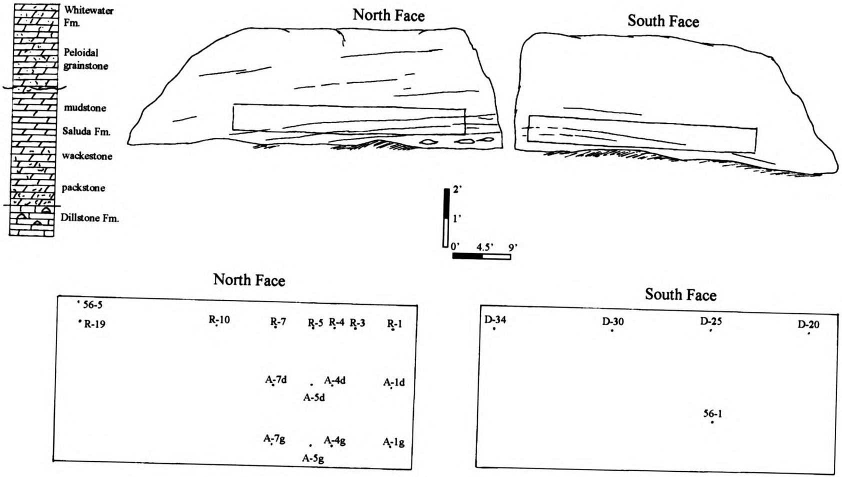

Figure 40. Saluda Hwy 56 Outcrop Profiles

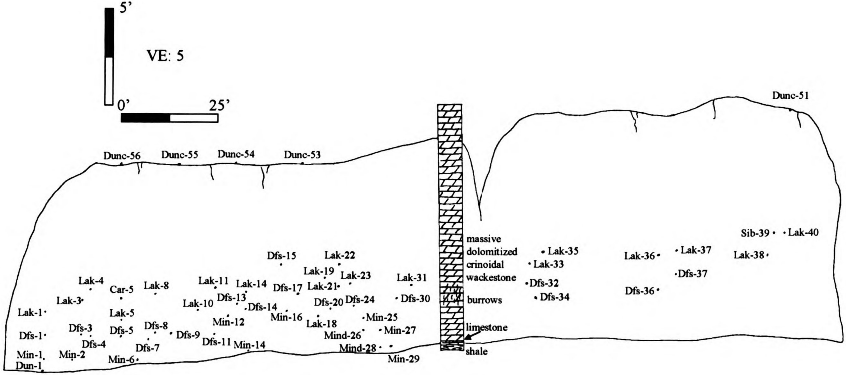

Figure 41. Burlington-Keokuk Hwy 61 Outcrop Profile

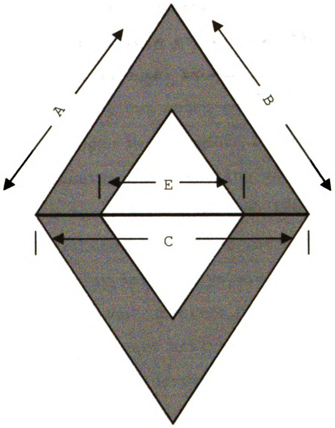

Figure 42. Zone measurements of rhombic slice
(shaded band represents zone measured)

crystal but not parallel to the $1\ 0\ \bar{1}\ 4$ face. Typically, zero to five crystals were found on each slide that cut through the center of the crystal at an angle to the $1\ 0\ \bar{1}\ 4$ face that could be corrected back to the $1\ 0\ \bar{1}\ 4$ reference plane (see Geometric Corrections section). Since all four formations lack an orientation of their crystals, each crystal has an equal probability of being cut in an orientation that allows measurement. Comparison for precision in length measurements between two independent observers indicates a correlation of 99% (Figure 43). The difference in measurements between the two observers is normally distributed indicating the error is not skewed towards smaller or larger crystals. Replicate analyses for the first independent observer have a 99% correlation (Figure 44). Replicate analyses for the second independent observer have a 98.5% correlation (Figure 45). The precision error on any single length measurement is +/- 1 tic unit. The precision error on the corrected zone width and crystal radius values is also +/- 1 tic unit.

Geometric Corrections

Three categories of slice orientations can be used to calculate back to the $1\ 0\ \bar{1}\ 4$ reference plane. Each of the three types of slices must cut through the center of the crystal. In order to insure this condition, samples from

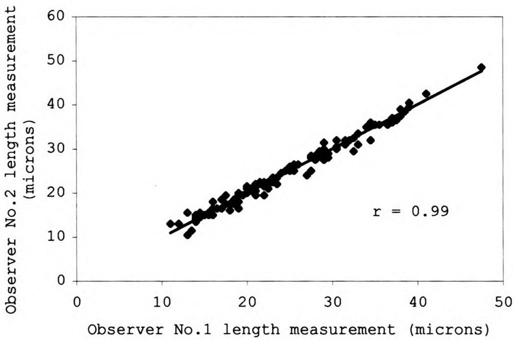

Figure 43. Comparison of length measurements between two observers

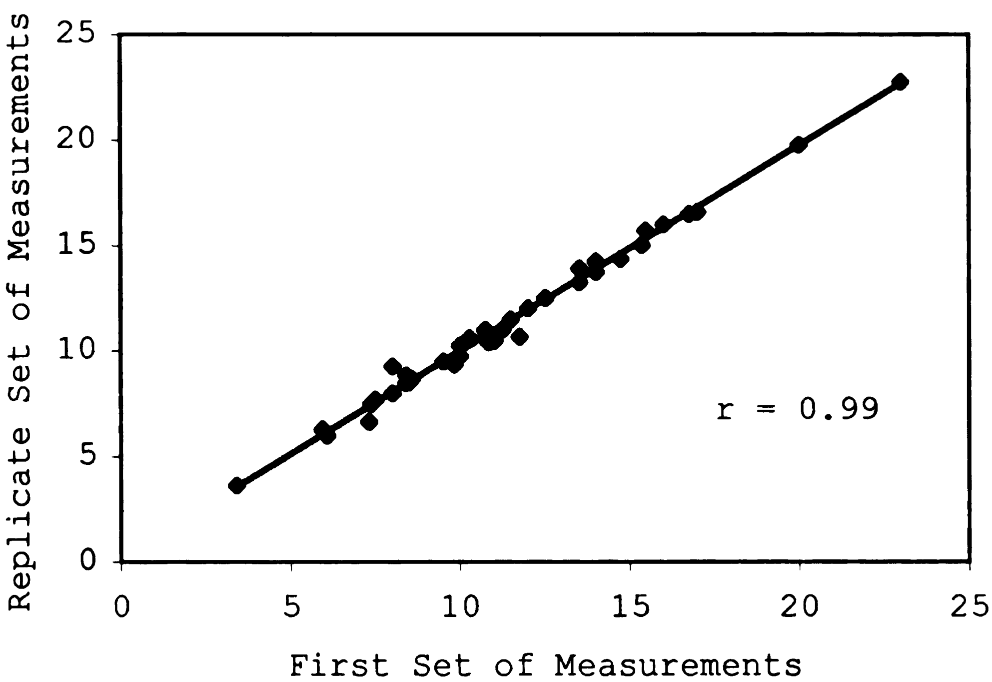

Figure 44. Comparison of replicate analyses for first observer

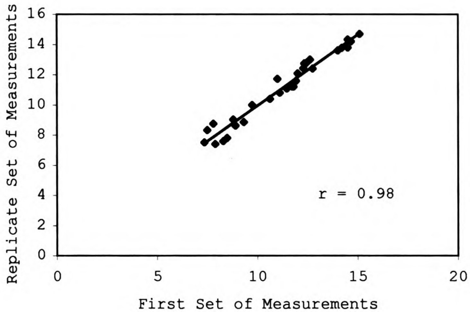

Figure 45. Comparison of replicate analyses for second observer

each formation were inspected for slices that included the greatest number of zones. Only slices that exhibited these zones were measured. Slices of crystals that did include all the zones and thus cut through the center could be divided into three general orientations: 1) rotation through the long diameter of a rhomb, 2) rotation through the short diameter of a rhomb, and 3) rotation through both the long and short diameter. From measurement of the apparent zone width (C-E, Figure 42), apparent crystal diameter (E, Figure 42) and zone boundaries (A and B, Figure 42), true zone width and crystal radius can be calculated. (See Appendix A for a detailed description of true zone width and radius calculations).

Statistical Methods

A minimum of 30 crystals from each sample with paired zone width and radius data were plotted. Normal probability plots were used to determine radius and zone width distributions. The Shapiro-Wilkes normality test was used to test for a normal distribution. Regression analysis included linear, quadratic, and exponential fits. Rearrangement of the complex quadratic mononuclear growth model equation to a linear function was used to distinguish this case (see previous Population Trend Section for equation). To determine the goodness of fit of a sample to a regression line, the correlation coefficient was

determined. To determine if the relationship between zone width and radius of crystals from a sample was statistically significant, an f test of the correlation coefficient was used with the null hypothesis of no correlation between zone width and radius, or no slope (Crow *et al.* 1960). To distinguish between different slopes generated from different samples, a t test of regression coefficients was used to compare variances of the radius populations between the two samples and the variances of zone width populations between the two samples (Crow *et al.* 1960). This t test is referred to as the significance of β t test and is used to determine if the slopes varied between samples at the 95 percent confidence interval (Crow *et al.* 1960). In the β t test, the null hypothesis was no variation between the two slopes, or a difference of slopes equal to zero.

Results

Paired zone-width vs. crystal-radius data from the Saluda, Whitewater, Burlington-Keokuk, and Seroe Domi Formations can be described by both normal and log normal distributions. Crystal measurements for each sample are reported in measured tic increments, conversion to microns can be obtained by multiplying Saluda, Whitewater and Seroe Domi data by 1.5 and multiplying Burlington-Keokuk data by 1.0 (or unity) (see Appendix B for measurements).

Histograms of crystal sizes for each of the four formations indicate a near-normal coarse skew nature (Figure 46, 47, 48, 49). The characteristic coarse skew is often found in carbonate rocks as wells as other rock types (Eberl *et al.* 1998, Sibley *et al.* 1993). All of the samples can be characterized by a normal distribution at either the 95% or 99% confidence intervals, which permits the use of the significance of **β** t test and the f test of the correlation coefficient. The f test of the correlation coefficient is sensitive to the condition of normality. Deviations from normality result in lower coefficient correlations.

Eighty-one percent of sample crystal sizes (r_1) yielded normal distributions at the 95 percent confidence interval using the Shapiro-Wilkes normality test (Table 4). Eighty-five percent of sample zone widths yielded normal distributions at the 95 percent confidence interval (Table 5). Samples that did not meet the condition of normality at the 95 percent confidence interval, did meet the condition of normality at the 99 percent confidence interval (Table 6). Likewise, ninety-two percent of the sample crystal sizes yielded log normal distributions at the 95 percent confidence interval (Table 4, 5 and 6, samples denoted by *) and eighty-eight percent of sample zone widths yielded log normal distributions at the 95 percent confidence interval (Table 4, 5 and 6, samples denoted by $^{+}$). All other samples can be described by a log normal distribution at the

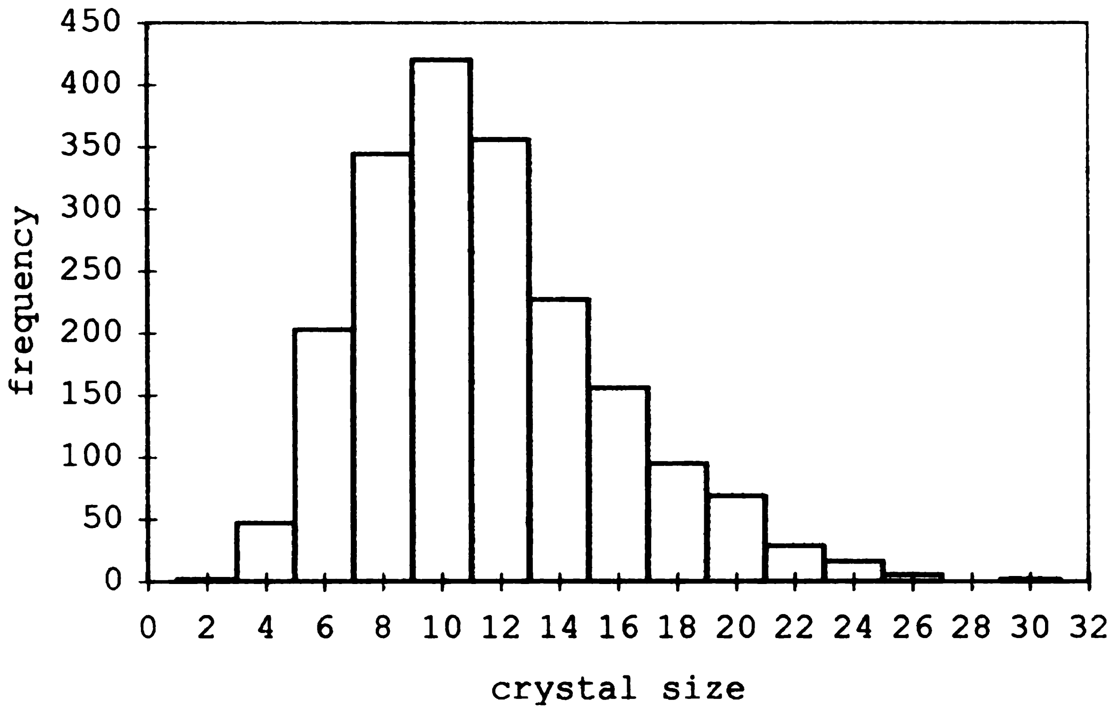

Figure 46. Saluda/Whitewater Formation crystal size frequency

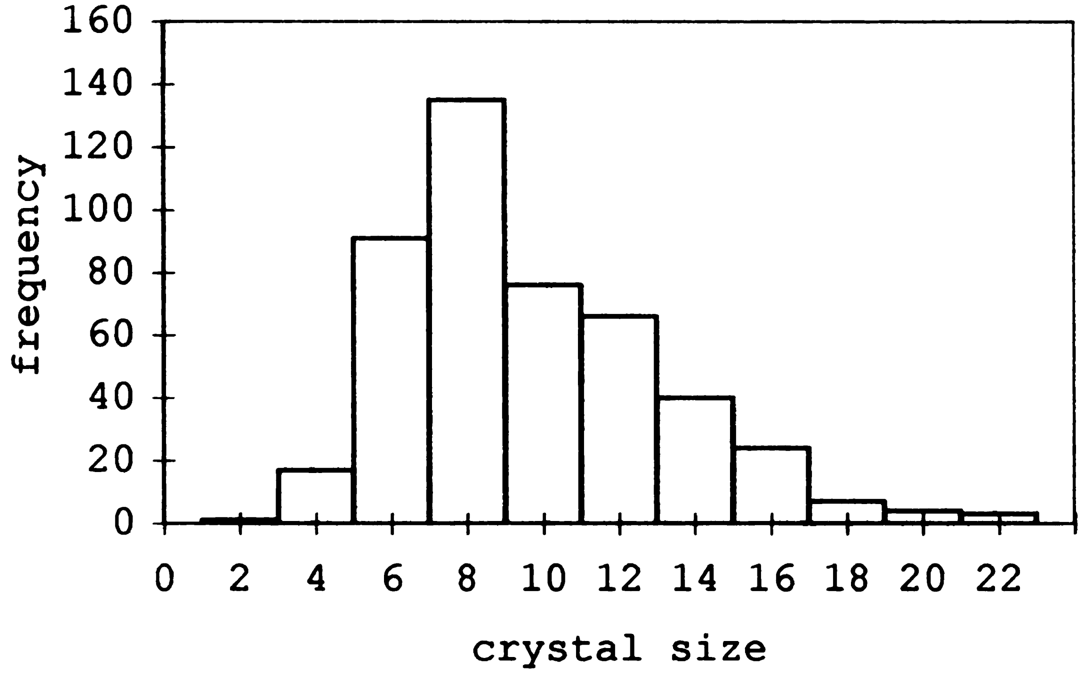

Figure 47. Burlington-Keokuk Formation crystal size frequency

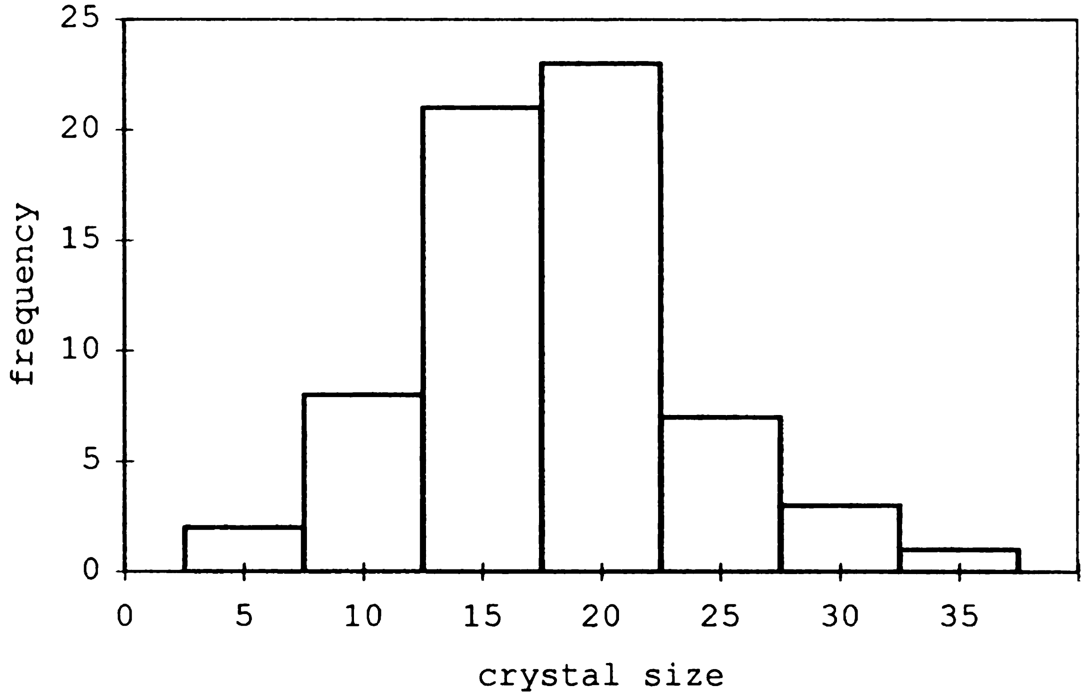

Figure 48. Seroe Domi Formation zone I crystal size frequency

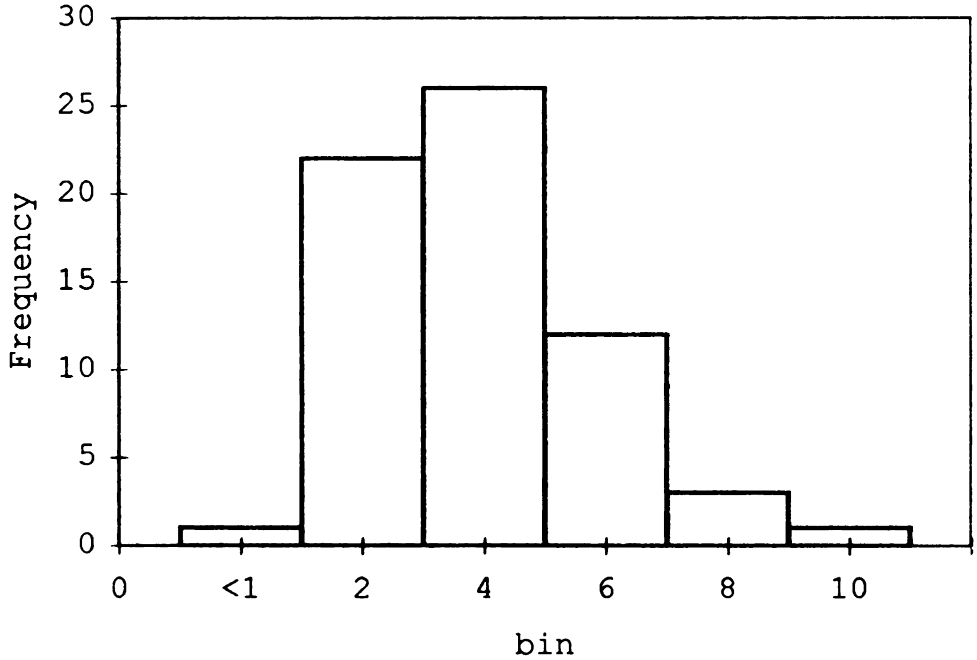

Figure 49. Seroe Domi Formation zone II crystal size frequency

Table 4. Samples with normal crystal size distributions at the 95% confidence interval

M1*	SD11*	P31*	D34*	56-5*	SB1 (zone II)*
M2	SD15*	SD13*	A7d*	PAY 11*	SB2 (zone I)*
M4*	P5*	SD7*	A5g*	SAL 7-8*	SM1 (zone I)*
M8*	P27*	D10*	PAY 1*	CAR 5*	SM1 (zone II)*
M26*	P34*	D8*	HOW 1*	LAK 22*	SB1 (zone I)*
M30*	P36*	D6*	HOW 6*	LAK 31*	
M34*	P40*	G8*	R 5*	LAK 40*	
G5*	P41*	G6*	R 10*	DFS 37*	
G7*	P45*	R1*	A7g*	LAK 10*	
SD3*	P37*	D25	56-1*	MIN 6*	

Table 5. Samples with normal zone width distributions at the 95% confidence interval

M1+	SD11+	DFS15+	D34	SB1 (zone II)+
P19+	SD15	MIN29+	A7d+	SB2 (zone I)
M4+	P5+	M20+	A5g	SM1 (zone I)+
M8	P27+	M11+	PAY 1+	SM1 (zone II)+
M26+	P34+	CAR 5+	HOW 1+	SB2 (zone II)+
M30+	P36+	LAK 22+	HOW 6+	P17+
M34	P40	LAK 31+	P2+	
G5+	P41+	LAK 40	D12+	
G7+	P45+	R1+	G4+	
SD3+	DFS1+	D25+	M42+	

Table 6. Samples with normal distributions at the 99% confidence interval

Crystal Size Distributions Samples		Zone Width Distributions Samples		
P19*	M21*	M2+	D10+	56-1
P17*	M20*	SD23+	D8+	56-5+
P2*	M11*	G3+	D6+	PAY 5+
SD23*	A1d*	G1+	G8+	PAY 11+
D12*	A5d*	M28+	G6+	TON 11+
G4*	PAY 5*	M21+	R5+	SAL 7-8+
G3*	TON 11*	P37+	R10+	DFS 24+
G1	DFS 1	P31+	A1d+	DFS 32+
M42*	DFS 15	SD13+	A5d+	DUNC 56+
M28*	MIN 29*	SD7+	A7g+	MIN 16+
DFS 24	DUNC 56*	LAK 36+	MIN 6+	SB1 (zone I)+
DFS 32*	MIN 16*	DFS 37+		
LAK36*	SB2 (zone II)*	LAK 10+		

99 percent confidence interval (Table 4, 5 and 6, samples not marked).

Zone width-radius scatter plots for 98% of all the samples indicate a statistically significant linear trend between zone width and crystal radius at the 95 percent confidence interval (Table 7). The slopes of individual samples from all four formations range from 0.05 to 1.53 with correlation coefficients ranging from 0.23 to 0.81 (Table 7). The mudstones, interbedded grainstones, packstones, wackestones and mudstones of the Saluda Formation each exhibit a linear correlation (Figure 50, 51, 52, 53, 54). Peloidal grainstones from the Whitewater Formation also exhibit a linear correlation (Figure 55). In addition, crinoidal wackestones from the Burlington-Keokuk and unimodal planar dolomites from the Seroe Domi exhibit a linear correlation (Figure 56, 57, 58). Plots of zone width-crystal radius (r_1) for all samples from each of the three dolomites (Saluda/Whitewater, Burlington-Keokuk, Seroe Domi) are fit best by the equation dr/dt = kr. The data is not best fit by the crystal growth equations for populations of crystals growing by mononuclear growth, polynuclear growth, spiral growth, diffusion-limited growth or birth and spread growth.

Table 7. Slope and correlation coefficients for all samples

Sample	Slope	r	Sample	Slope	r
M1^{Sm}	0.15	0.62	HOW 1^{Sm}	0.15	0.62
M2^{Sm}	0.22	0.76	HOW 6^{Sm}	0.16	0.58
M4^{Sm}	0.14	0.64	SAL 7-8^{Sm}	0.14	0.41
M8^{Sm}	0.10	0.45	PAY 11^{Sw}	0.21	0.74
M26^{Sm}	0.11	0.52	56-1^{Sw}	0.16	0.69
M30^{Sm}	0.18	0.73	R10^{Wo}	0.16	0.43
M34^{Sm}	0.12	0.47	R5^{Wo}	0.21	0.45
G5^{Sg}	0.11	0.47	TON 11^{Sm}	0.22	0.63
G7^{Sg}	0.15	0.65	PAY 5^{Sw}	0.16	0.61
SD3^{Sm}	0.11	0.66	A5d^{Sm}	0.11	0.44
SD11^{Sm}	0.19	0.69	A1d^{Sm}	0.21	0.62
SD15^{Sm}	0.13	0.44	56-5 *$^{\#Wo}$	0.11	0.27
P5^{Wo}	0.08	0.45	A7g *$^{\#Sp}$	0.12	0.35
P27^{Wo}	0.07	0.41	CAR 5^{Bc}	0.12	0.43
P36^{Wo}	0.16	0.65	LAK 22^{Bc}	0.13	0.37
P40^{Wo}	0.14	0.45	LAK 31^{Bc}	0.16	0.37
P41^{Wo}	0.19	0.50	LAK 40^{Bc}	0.16	0.46
P45^{Wo}	0.12	0.38	DFS 37^{Bc}	0.23	0.42
G6^{Sg}	0.14	0.69	LAK 10^{Bc}	0.22	0.37
G8^{Sg}	0.19	0.58	MIN 6^{Bc}	0.23	0.60
D6^{Sm}	0.26	0.81	DFS 24^{Bc}	0.21	0.68
D8^{Sm}	0.08	0.37	LAK 36^{Bc}	0.41	0.76
D10^{Sm}	0.12	0.43	MIN 16^{Bc}	0.14	0.37
SD7^{Sm}	0.17	0.71	DFS 1^{Bc}	0.18	0.44
P31^{Wo}	0.15	0.47	DFS 15^{Bc}	0.11	0.41
P37^{Wo}	0.21	0.67	DFS 32 *$^{\#Bc}$	0.11	0.26
P19^{Wo}	0.15	0.62	DUNC 56 *$^{\#Bc}$	0.05	0.23
P17^{Wo}	0.14	0.61	MIN 29 *$^{\#Bc}$	0.10	0.28
P2^{Wo}	0.06	0.41	SB1 (zone II)^{Du}	0.62	0.59
SD23^{Sm}	0.10	0.49	SB2 (zone I)^{Du}	0.13	0.79

Table 7 (cont'd).

Sample	Slope	r	Sample	Slope	r
G4^{Sg}	0.11	0.47	SM1(zone I)*$^{+Du}$	0.05	0.24
G1^{Sg}	0.15	0.78	SM1(zone II)*$^{+Du}$	0.87	0.34
M42^{Sm}	0.07	0.39	SB2 (zone II)^{Du}	1.53	0.78
M28^{Sm}	0.11	0.59	SB1 (zone I)^{Du}	0.19	0.43
M21^{Sm}	0.19	0.63	R1^{Wo}	0.17	0.47
D12^{Sm}	0.11	0.64	D25^{Wo}	0.14	0.56
M20^{Sm}	0.13	0.37	D34^{Wo}	0.16	0.58
M11^{Sm}	0.11	0.47	A7d^{Sm}	0.18	0.64
G3^{Sg}	0.23	0.61	A5g^{Sp}	0.17	0.64
P34 *$^{\#Wo}$	0.10	0.31	PAY 1^{Sw}	0.13	0.65
SD13 *$^{\#Sm}$	0.10	0.27			

* samples that have zero correlation at the 95 percent confidence interval

\# samples that have a significant correlation at the 89 percent confidence interval

$^{+}$ samples that have a significant correlation at the 80 percent confidence interval

S Saluda Formation samples
W Whitewater Formation samples
B Burlington-Keokuk Formation samples
D Seroe Domi Formation samples
c dolomitized crinoidal wackestone
u unimodal planar dolomite where original rock texture is completely obliterated by dolomitization
o dolomitized peloidal grainstone
m dolomitized mudstone
g partially dolomitized grainstone
w dolomitized wackestone
p dolomitized packstone

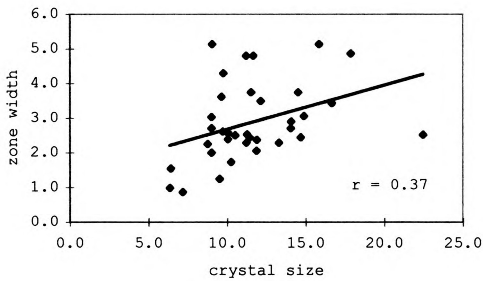

Figure 50. Saluda Mudstone (sample M20)

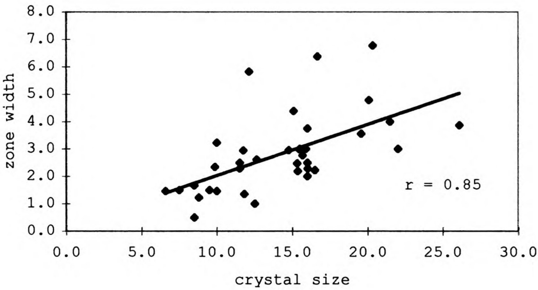

Figure 51. Saluda Grainstone (sample G8)

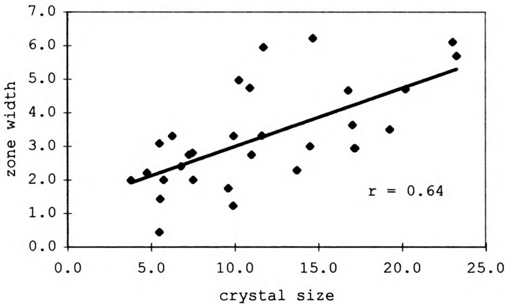

Figure 52. Saluda Packstone (sample A5g)

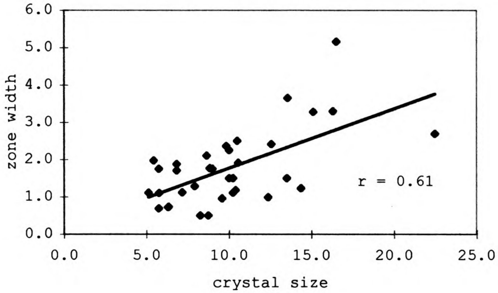

Figure 53. Saluda Wackestone (sample Pay 5)

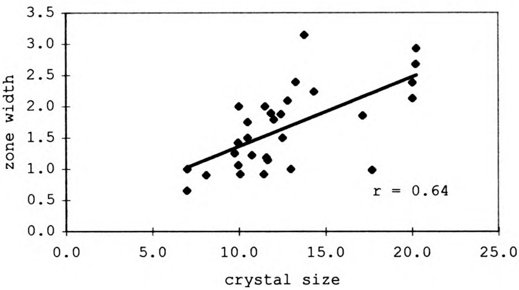

Figure 54. Saluda Interbedded Mudstone (sample D12)

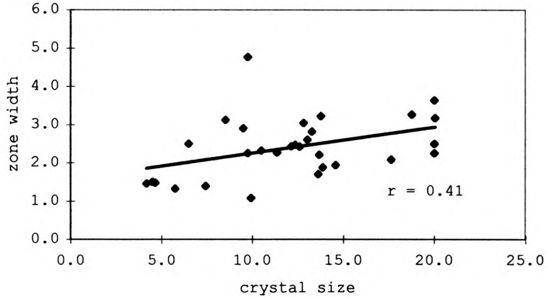

Figure 55. Whitewater Peloidal Grainstone (sample P 27)

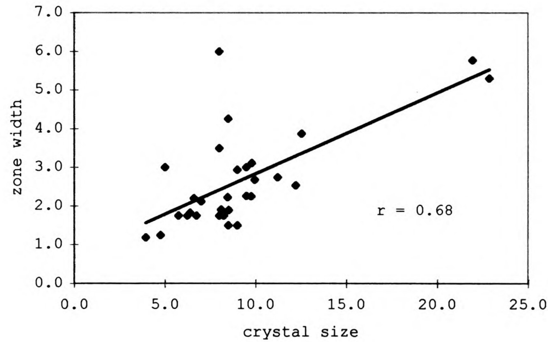

Figure 56. Burlington-Keokuk Crinoidal Wackestone
(sample DFS 24)

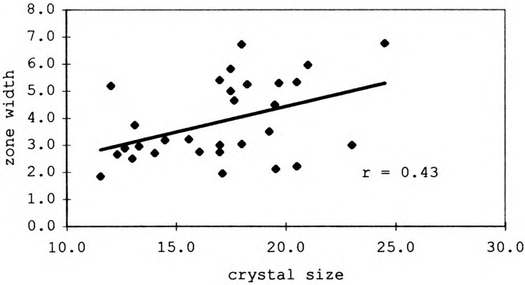

Figure 57. Seroe Domi Dolomite, Zone I (sample SB1)

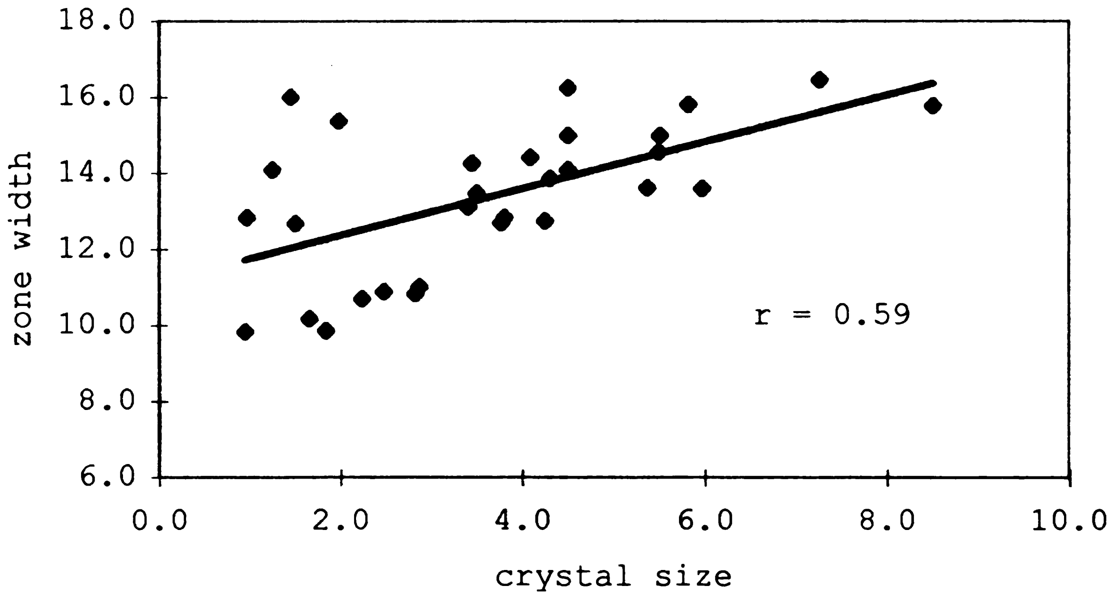

Figure 58. Seroe Domi Dolomite, Zone II (sample SB1)

Comparison of Crystal Growth Rate Equation among Lithologies of the Same Dolomite

In order to compare zone-width vs. crystal-size crystal growth equations among samples of the same lithology and samples of different lithologies, comparisons were made among samples of the Saluda and Whitewater formations since the same zone could be measured throughout the different lithologies of the two formations (dt is constant for samples compared). Because each sample is fit best with the equation $dr/dt = kr$, equations for different lithologies can be compared by slope. In the equation $dr/dt = kr$, k is the slope. However, unlike the other crystal growth equations for the crystal growth models previously discussed, the physical parameters that k signifies are unknown. In previous models, k is attributed to parameters such as solution chemistry and hydraulic properties. Because it is unclear what set of parameters k represents, k' will be used to denote the slope in the empirically determined crystal growth equation, $dr/dt = k'r$. Comparisons of k' among samples within a specific lithology and between samples of different lithologies indicated the slopes were not statistically different at the 95 percent confidence interval using the β significance test for slopes (Table 7). In addition, the mudstones and grainstones of the Saluda Formation and the grainstones of the Whitewater Formation sample slopes did not vary among or between

formations despite statistically different crystal size populations. Different rock types dolomitized concurrently did not exhibit a difference in the correlation between zone width and radius.

Comparison of Crystal Growth Rate Equation between Different Dolomites

The Saluda/Whitewater Formations, Burlington-Keokuk Formation and Seroe Domi all exhibit similar linear trends of crystal growth rate and crystal size. Each of the dolomites has a different zonal stratigraphy (dt is not assumed constant between different dolomites). Since the Burlington-Keokuk and Seroe Domi samples are also best fit by the equation $dr/dt = k'r$, comparison of crystal growth equations is accomplished by comparing the slopes. The slopes of the samples in the Burlington-Keokuk do not vary from the slopes of the Whitewater and Saluda Formations at the 95 percent confidence interval using the β significance test for slopes. The slopes of the Seroe Domi Zone I samples do not statistically vary from the slopes of the Whitewater, Saluda, and Burlington-Keokuk Formations at the 95 percent confidence interval using the β significance test for slopes. The slopes of the Seroe Domi Zone II samples do vary at the 95 percent confidence interval using the using the β significance test for slopes when compared to the Whitewater, Saluda, Burlington-Keokuk and Seroe Domi Zone I

samples. The mean zone widths for the Whitewater, Saluda, Burlington-Keokuk, Seroe Domi Zone I, and Seroe Domi Zone II do vary statistically from each at the 95 percent confidence interval using a two-sample t test comparing two formations at a time.

Temporal Comparisons within the Seroe Domi Formation

The unimodal planar crystals in the Seroe Domi Dolomite I exhibit two zones that can be measured. A dark zone and a light zone adjacent to each other in the crystals were measured (Figure 11). As previously stated, the slopes of Zone I and Zone II statistically vary from each other. The interior zone (Zone II) is a thick bright zone. The next zone precipitated is Zone I, a dark zone. Zone II is thicker than Zone I. Zone II is potentially composed of multiple thinner zones (Figure 11). These zones are individually not resolvable for measurement due to the difficulty in picking zone boundaries and the limit of magnification. Zone II samples have a greater slope than Zone I samples (Table 7).

Comparison of Crystal Growth Equations for Adjacent Crystals in Thin Section

Subsets of the Saluda and Burlington-Keokuk Formations were obtained by selecting crystals that share the same pore space or are in direct contact with each other (Figure 59). Plotting zone-width vs. crystal-size data for pairs of adjacent crystals results in a statistically significant

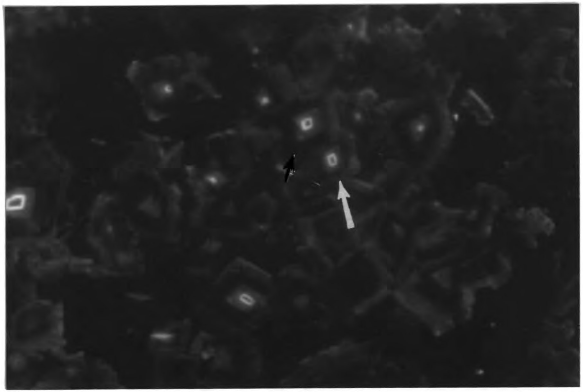

Figure 59. Cathodoluminescent view of Saluda dolomite sample. Arrows point to adjacent (paired) crystals (1 inch = 100 microns).

linear trend at the 95 percent confidence interval (Figure 60, 61). The Burlington-Keokuk subset was selected from data on samples LAK-22, MIN-16, and DFS-24. The Saluda subset was selected from data on samples M2, M1, M4, and SD3.

Discussion

The zone-width vs. crystal-radius plots indicate a similar linear trend, $dr/dt = k'r$, for all four formations. However, the linear crystal growth equation does not correspond to any of the published crystal growth mechanisms. The crystal growth equation $dr/dt = k' r$ does extend spatially on the scale of an individual outcrop and on the scale of multiple outcrops separated by approximately five miles. Because the three different dolomites studied share the same general crystal growth equation, $dr/ dt = k'r$, the crystal growth mechanism can be said to be independent of lithology variation over the fluid composition range of dolomitizing fluids represented by the Saluda/Whitewater, Burlington-Keokuk and Seroe Domi dolomites. The extent to which k' represents solution variation when comparing formations or different zones from the same formation is unknown since dt cannot be assumed to be the same between different zones or formations. The variation in the slope k' could result from solution variation, changes in dt, or some combination of the two

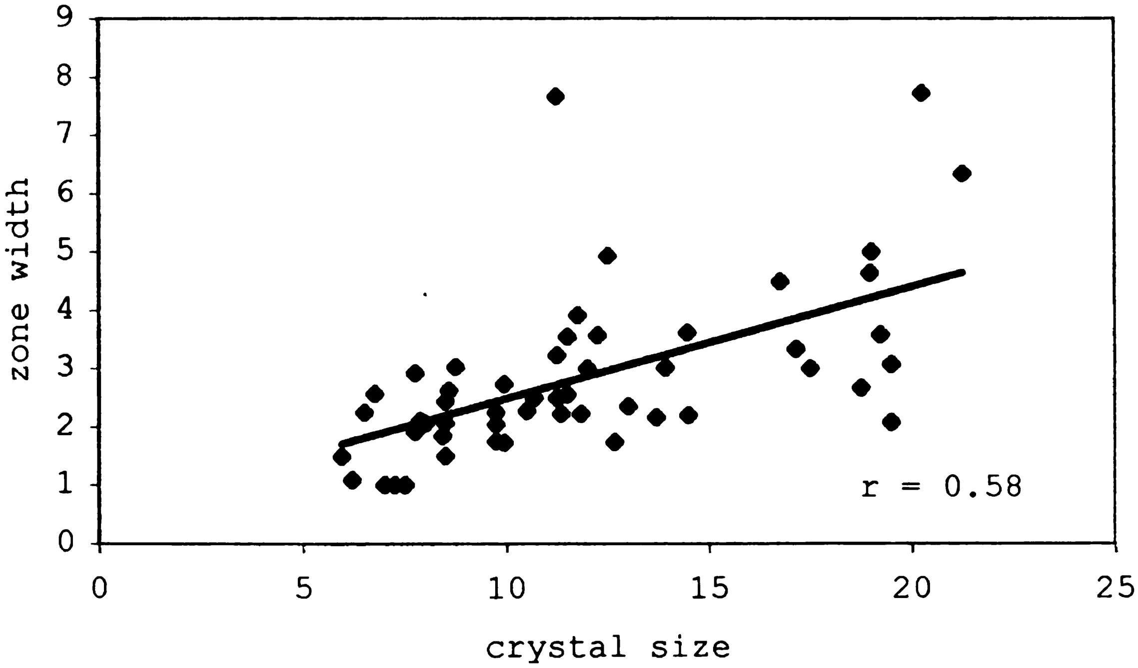

Figure 60. Saluda Paired Crystals

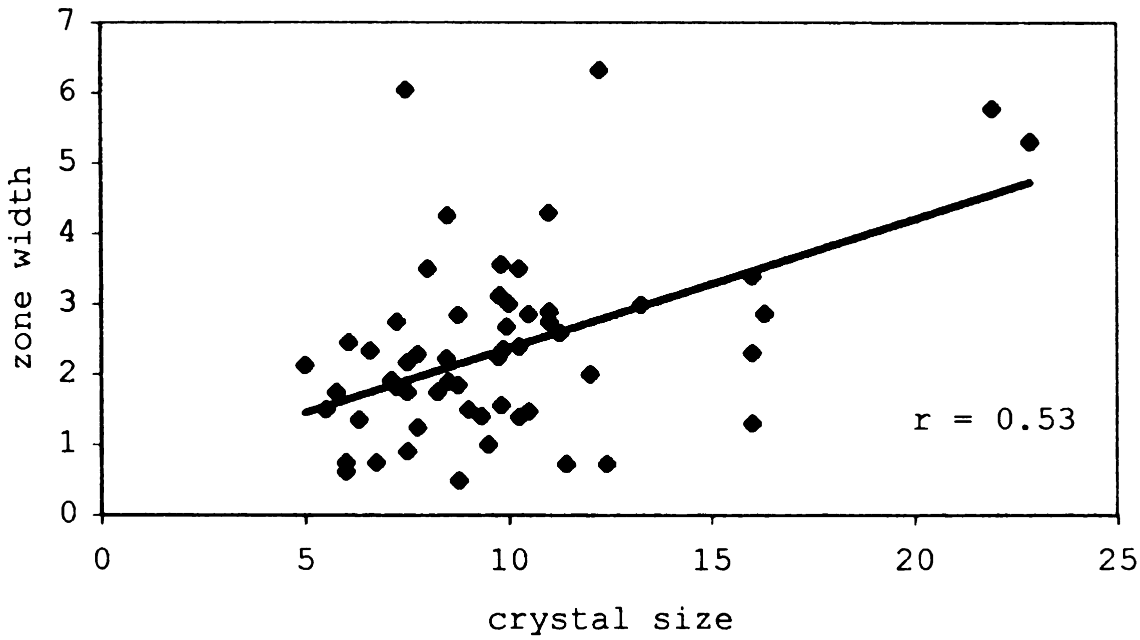

Figure 61. Burlington-Keokuk Paired Crystals

factors unless the comparison of k′ is of values from the same dolomite and same zone such as the Saluda/Whitewater samples. Thus, the variation of k′ between Seroe Domi zone II samples and all other samples may be attributed to both or either solution variation or a change in dt relative to the other samples.

Crystal Growth Equation and Crystal Growth Mechanism

The fact the relationship between zone width and crystal radius is linear and is not represented by any known crystal growth mechanism indicates either: 1) the linear relationship found represents a new mechanism or combination of mechanisms not investigated previously or 2) the assumption of isochronous zones commonly made in carbonate petrography is wrong.

The assumption of isochronous zones can be made based on the assumption that changes in solution cause variations in zone intensity and color across the outcrop in a shorter period of time than the induction period for dolomite. Abrupt dolomite/limestone contacts and the lack of partially dolomitized rocks as well as experimental high temperature dolomitization of calcite indicate a long induction period for dolomite (Sibley *et al.* 1994, Sibley 1990, Sibley and Bartlett 1987, Sibley *et al.* 1987). Experimental studies also imply dolomite precipitating on dolomite seeds has a long induction period (Gaines 1980). This is consistent with the idea that changes in stochiometry of dolomite factors unless the [illegible] values from the same dolomite and some [illegible] Whitewater samples. Thus, the [illegible] zone II samples and al[illegible] attributed to both or either solution [illegible] relative to the other samples.

Crystal Growth Equat[illegible] Growth Mechanism

The fact the relationship between [illegible] width and crystal radius is [illegible] and is not represented by any known crystal growth mechanism implies either: 1) the linear relationship found represents a new mechanism or combination of mechanisms not investigated previously or 2) the assumption of isochronous zones commonly made in carbonate petrography is wrong.

The assumption of isochronous zones can be made based on the assumption that changes in solution cause variations in zone intensity and color across the outcrop in a shorter period of time than the induction period for dolomite. Abrupt dolomite/limestone contacts and the lack of partially dolomitized rocks as well as experimental high temperature dolomitization of calcite indicate a long induction period for dolomite (Sibley et al. 1994, Sibley 1990, Sibley and Bartlett 1987, Sibley et al. 1987). Experimental studies also imply dolomite precipitating on dolomite seeds has a long induction period (Gaines 1980). This is consistent with the idea that changes in stochiometry of dolomite (percent molar Mg) affect the surface free energy requirement for precipitation. Thus, changes in stochiometry of dolomite with changes in solution could create induction periods between zones. Another argument that initial start times for zones are isochronous is the fact a random plot would be expected as a result of different-sized crystals starting at random times.

While the previous argument indicates the initial time of each zone may be isochronous, the end time of each zone may still vary. If the final time for each zone is not the same, then a linear trend can be created by allowing the larger crystals a longer period of growth. However, if we look at actual data, this trend is found in each sample. So, if it is a matter of the larger crystals having grown for a longer time, then on the scale of a thin section, larger crystals grew for a longer time than other crystals in the area represented by a thin section. Pairs of adjacent crystals indicate the larger crystals either in the same pore or in direct contact with smaller crystals have thicker zone widths. Thus, the larger crystal is either 1) growing faster than the smaller crystal or 2) growing for a longer period of time. The latter would indicate the fluid around the large crystal was more saturated than the fluid around the small crystal and thus took a longer time to deplete even though the crystals share the same pore space. This of course, assumes the fluid between the adjacent

crystals was heterogeneous and not mixing, or solution in the pore was heterogeneous. This idea is rejected in favor of isochronous final times for zone widths. If large crystals were growing for a longer period of time due to solution heterogeneity, one would expect this trend to result from large crystals near pores. Petrographically, on the scale of a thin section there is no relationship between the large crystals and porosity (Figure 62). Large crystals and small crystals adjacent to each other that have no spatial bias to porosity and exhibit a linear trend between zone width and crystal radius, are readily found as indicated by the adjacent crystal pair plots (see Results Section).

If the zones are isochronous as argued, the linear relationship found represents either a new surface-limited growth mechanism not previously considered, or a combination of crystal growth mechanisms that leads to a linear trend. Mononuclear, polynuclear and spiral growth mechanisms or any combination of these mechanisms will not result in a linear trend between zone width and radius among a population of crystals as the models are previously presented in the crystal growth literature. Diffusion-limited growth also does not result in a linear trend for a population of crystals. Birth and spread growth cannot be attributed to a linear trend among zone width and radius. Birth and spread growth assumes a constant nucleation rate/unit area and a

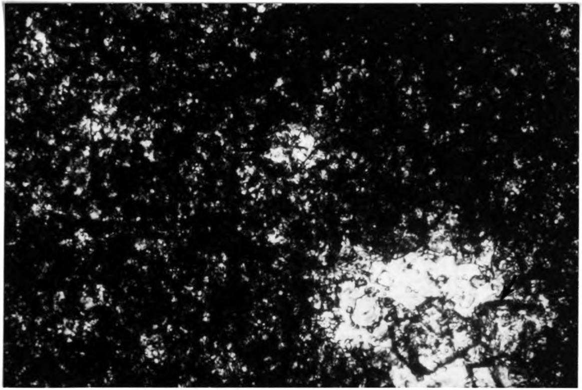

Figure 62. Partially crossed polars view of Burlington-Keokuk sample. Arrows point to large crystals near pore and within matrix (1 inch = 100 microns).

constant radial rate/unit area (Nyvlt 1985, Ohara and Reid 1973, Nielson 1964). In order to get a linear trend, nucleation rate or radial rate per unit area would have to vary from crystal to crystal. The saturation state would have to vary for adjacent crystals on a thin section for the nucleation or radial rate per unit area to vary for the previously published models. The latter variation in saturation state is rejected here for the same reasons it was rejected in the argument of isochronous final times for zone widths. There is no inherent property in any of the current growth mechanisms that would lead to a linear zone width-radius relationship in a population of crystals.

An alternative, consistent with the data, is any combination of polynuclear or birth and spread growth with a modified spiral growth model or a modified spiral growth itself. The spiral growth mechanism varies only with saturation state or solution properties which effect precipitation (Christian 1975, Ohara and Reid 1973, Burton *et al.* 1951). The spiral growth model is independent of defect density to the extent that groups of defects or single defects on the surface independently contribute to the overall growth rate. In Burton *et al.* (1951), the rate of spiral growth is determined by the distance between steps of the spiral where the rate increases with the distance between steps:

$R = d\ (v_{\infty} / \lambda_0)$ (Bennema 1984, Burton *et al.* 1951)

where λ_0 is the distance between each arm of the spiral, d is the thickness of the layer (step), and v_∞ is the advance velocity of the steps (dependent on saturation state). The distance between steps produced by a spiral is given by the rate of step advance (v_∞) per number of steps (determined by the distance between arms of the spiral) or the flux of steps, v_∞/λ_0 (Bennema 1984, Burton *et al.* 1951). A decrease in the distance between steps results in a solute uptake by the steps greater than solute delivery from solution. Thus, the crystal growth rate is dependent on the interrelationship between step distance and saturation state. As saturation state increases, the minimum distance between steps necessary to maintain a concentration of adsorbed ions around the step decreases.

Burton *et al.* (1951) do indicate a range in growth rate is possible when more than one defect is present on the surface. In the case of a group of defects, Burton *et al.* (1951) divide the surface into groups of defects intergrowing and acting as one defect. In this case, the perimeter of each step is larger and overall growth is greater. However, growth is still limited by saturation state and the distance between steps resulting in the basic equation $dr/dt = k$. In either the case of single defects or groups of defects acting as one (due to intergrowth), if the distance between the defect centers or centers of defect

groups is great enough such that the center of the defects or defect groups do not intergrow then the total perimeter of steps is increasing. Simply, if the number of defects, whether single defects or group defects, on the surface is increasing, the rate of growth increases as the amount of step edge available or total step perimeter increases. Therefore, growth rate is dependent on defect density as well as distance between steps and saturation state. The crystal growth rate for a population of crystals interacting with the same solution would equal a constant, $dr/dt = k$, if the defect density/unit area/unit time did not vary from one crystal to another crystal. If the defect density/unit area/unit time increased with crystal size, then the crystal growth rate for a population of crystals interacting with the same solution could be represented by $dr/dt = k^*r$ where k^* represents solution conditions, mineralogy, and defect density/unit area/unit time. Thus, crystals growing by the spiral growth mechanism in a homogeneous solution can still exhibit a linear population trend between zone width and crystal size where the larger crystals are growing faster by varying defect density. This could be accomplished in two ways: 1) an increase in defect density/unit area with crystal size or 2) increasing distance from defects originating in the center of the face to the edge of the face (an increase in defect density/unit area/unit time).

groups is great enough such that the number of the defects or defect groups do not increase, when the total perimeter of steps is increasing. Simply, if the number of defects, whether single defects or group defects, on the surface is increasing, the rate of growth increases as the amount of step edge available or total step perimeter increases. Therefore, growth rate is dependent on defect density as well as distance between steps and saturation state. The crystal growth rate for a population of crystals interacting with the same solution would equal a constant, $dr/dt = k$, if the defect density/unit area/unit time did not vary from one crystal to another crystal. If the defect density/unit area/unit time increased with crystal size, then the crystal growth rate for a population of crystals interacting with the same solution could be represented by $dr/dt = k^*t$ where k^* represents solution conditions, mineralogy, and defect density/unit area/unit time. Thus, crystals growing by the spiral growth mechanism in a homogeneous solution can still exhibit a linear population trend between zone width and crystal size where the larger crystals are growing faster by varying defect density. This could be accomplished in two ways: 1) an increase in defect density/unit area with crystal size or 2) increasing distance from defects originating in the center of the face to the edge of the face (an increase in defect density/unit area/unit time).

First, if the defect density/unit area varied with crystal size, defect-ridden crystals would grow faster because the total step perimeter would be larger. Previously reported empirical evidence indicates larger crystals have a greater stress field to induce defects (Hull 1965). In addition, Randolph and Larson (1965) have indicated by observation some crystals inherently have more defects than others. Experimental evidence indicates a correlation between increasing defects and increasing growth rates (Ristic *et al.* 1991). Ristic *et al.* (1991) found an increase in the overall growth rate of potash alum crystals when incrementally increasing the strain on growing crystals. The increase in rate was attributed to an increase in dislocations observed petrographically on the growing crystals. Studies by White *et al.* (1974), Ottens *et al.* (1972), and Jancic and Garside (1975) also indicate an increase in crystal growth rate with crystal size but did not demonstrate a cause for the size-dependent growth. However, even if defect density/unit area was the same for all crystals, larger crystals could still grow faster if the defect density/unit area/unit time varied. A screw dislocation, the defect that causes spiral growth, is a slip plane in a crystal that occurs at an angle to the growing crystal face. The screw dislocation perpetuates in time by constantly supplying new low-energy sites for ions to attach to the surface relative to the formation of a

two-dimensional nucleus on a flat surface. As the defect perpetuates through time it grows at an angle to the growing face giving the appearance of migrating to the edge of the crystal surface. At the end of the life span of the screw dislocation it will intersect the edge of the growing crystal and the screw dislocation defect will become an edge defect that will not continue to propagate. To illustrate this point, the surface of a large crystal (crystal A, Figure 63) and a small crystal (crystal B, Figure 64) are divided into square unit areas and are given the same defect density/unit area. The lifespan of screw dislocations in the center of the larger crystal will be longer than the lifespan of screw dislocations in the center of smaller crystals. Thus, even if defects had an equal chance of occurrence/unit area (defect density/unit area is constant), larger crystals could still be growing faster than smaller crystals because the number of defects/unit area/unit time would be greater for the larger crystals. This is one alternative hypothesis for the physical model of the crystal growth mechanism represented by the equation $dr/\ dt = k'r$ determined from the empirical data in this study.

Spatial and Temporal Crystal Growth Trends

A crystal growth mechanism as described previously in the Population Trends for Crystal Growth Mechanisms section can be represented by a family of related functions since a crystal growth mechanism can occur over a range of solution

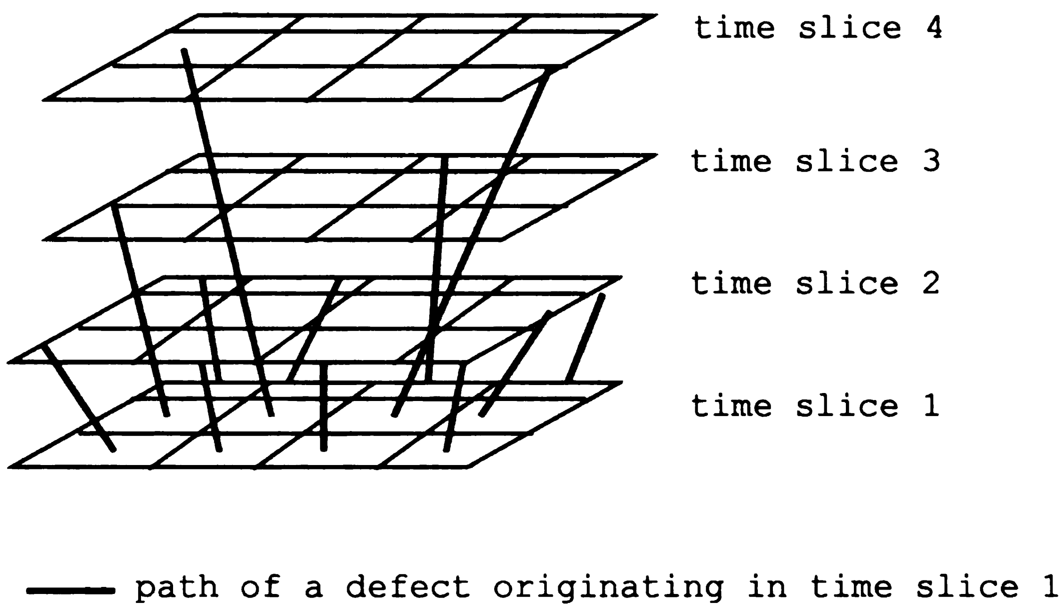

Figure 63. Crystal A

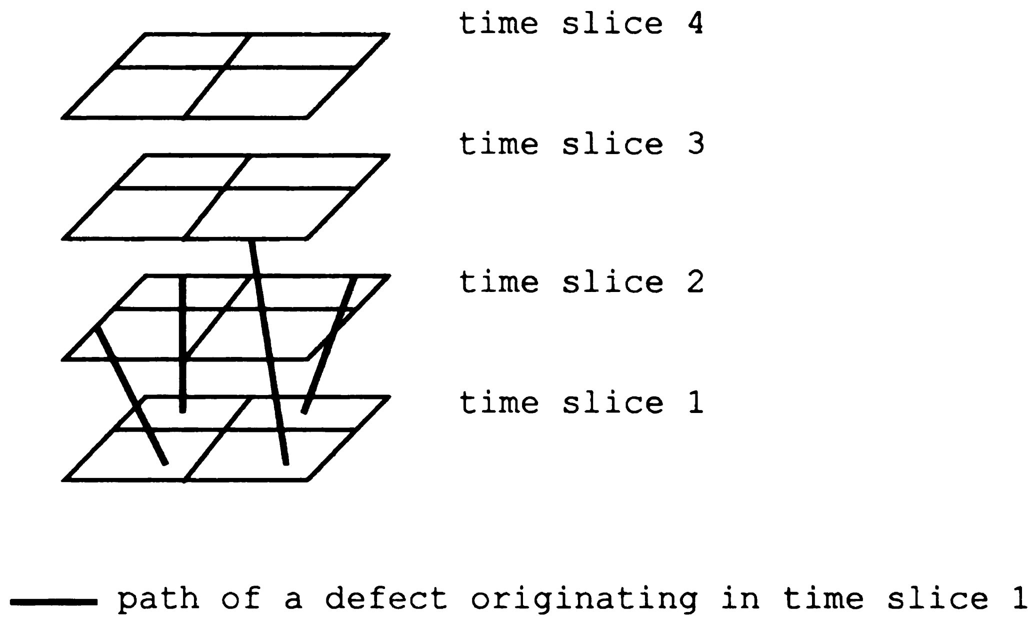

Figure 64. Crystal B

conditions. Also, when comparing formations, the period of time a zone grows can change the slope of the function but not the general function type. Thus, the four formations can all be described by the same general function type or crystal growth mechanism. The data indicate that bodies of rock on the scale of an outcrop that have the same *net* rock-water interaction and crystal growth mechanism, exist and are spatially mappable. Different lithologies within the Saluda/Whitewater Formations, different dolomites (Saluda/Whitewater, Burlington-Keokuk and Seroe Domi), and different zones from the same dolomite (Seroe Domi) have the same crystal growth mechanism, $dr/dt=k'r$. The slope of the fitted lines does not vary statistically from samples of one lithology to samples of another lithology. Thus, the crystal growth mechanism represented by the linear trend is not influenced by the range of the lithologies, rock ages or carbon and oxygen isotopes represented by the samples tested.

Variance in Crystal Growth Equations

In the crystal growth equations, we find low to moderate correlation coefficients even though the trend itself is statistically significant. This variance from the fitted line may result from experimental error, solution variation across the thin section (distances much greater than the size of a pore) or variation in the amount of time

the zone precipitates. First, the experimental error is discussed in the methods section and is less than the variation represented. Second, even though the pairs of adjacent small and large crystals in contact or within a pore indicate solution heterogeneity is not the cause of the linear trend, the variation from the trend may result from pore to pore solution heterogeneity. For example, if pore A solution has a higher saturation state than pore B solution, small and large crystals in pore A will grow faster than small and large crystals in pore B while the large crystals in both pores are growing proportionately faster than their smaller crystal counterparts. Arguments for the isochronity of initial and final times of zone widths are presented earlier. The constraint of a third unknown variable such as any solution concentration parameter (saturation state for example) for the zone measured and its relationship to the zone-width vs. crystal-radius function could result in a more accurate function with a corresponding higher correlation coefficient.

In the Saluda/Whitewater dolomite, even though the slopes of the Whitewater samples and Saluda samples are the same, the mean zone width is greater for the Whitewater samples. This could be accomplished in two ways: 1) the saturation state was higher in the Whitewater samples and/or 2) the Whitewater samples were in contact with the dolomitizing solution for a longer period of time. In

either case, the trend of larger crystals growing faster than smaller crystals still occurs (Figure 65).

Conclusions

The Saluda/Whitewater, Burlington-Keokuk, and Seroe Domi Formations are growing by a similar mechanism as demonstrated by the same statistically significant linear trend, $dr/dt = k'r$, between zone width and crystal size for all four formations. The heterogeneity of the four formations compared agrees with previous work that indicates a single mechanism can operate over a range of solution conditions (Sunagawa 1984). The crystal growth equation does not statistically vary within a particular lithology or between lithologies when comparing the same zone. When comparing different formations, the same linear trend exists between two different zones. The crystal growth equation $dr/dt = k'r$ also best represents zone-width vs. crystal-size plots of pairs of adjacent crystals. In addition, the data demonstrate the Saluda and Whitewater formations share the same zonal stratigraphy. From these observations, the following conclusions are drawn:

1) a body of rock greater than the scale of outcrop can be described by a single crystal growth equation,
2) the crystal growth mechanism represented by equation $dr/dt = k'r$ operates over a range of conditions as represented by the variation in lithology, age,

either case, the trend [illegible] crystal growth, faster than smaller crystals [illegible] (Figure 6-7).

Conclusions

The Saluda/Whitewater [illegible] and Sevier Domi Formations are grown [illegible] as demonstrated by the same [illegible] linear trend, dr/dt = k'r, between [illegible] crystal-size for all four formations. The [illegible] formations compared agrees with previous work that [illegible] a single mechanism can operate over a range of solution conditions (Sunagawa 1984). The crystal growth equation does not statistically vary within a particular lithology or between lithologies when comparing the same zone. When comparing different formations, the same linear trend exists between two different zones. The crystal growth equation dr/dt = k'r also best represents zone-width vs. crystal-size plots of pairs of adjacent crystals. In addition, the data demonstrate the Saluda and Whitewater formations share the same zonal stratigraphy. From these observations, the following conclusions are drawn:

1) a body of rock greater than the scale of outcrop can be described by a single crystal growth equation,

2) the crystal growth mechanism represented by equation dr/dt = k'r operates over a range of conditions as represented by the variation in lithology, age,

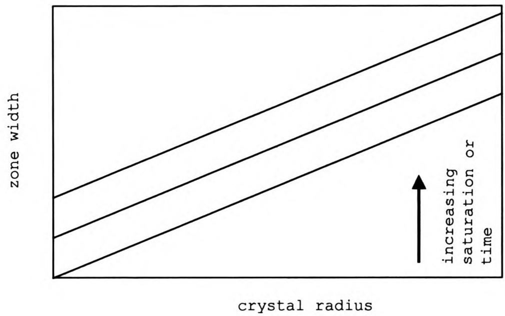

Figure 65. Family of functions for dr/dt = k'r

carbon isotopes and oxygen isotopes of the Saluda, Whitewater, Burlington-Keokuk, and Seroe Domi Formations,

3) the higher growth rate of larger crystals is not a result of thin section-scale solute flux, and

4) the Saluda Formation was dolomitized after deposition of the Whitewater Formation in contrast to published work suggesting the Saluda was dolomitized in a hypersaline environment concurrently with deposition.

While no current size-dependent crystal growth mechanism exists which can be ascribed to the equation $dr/dt = k'r$, this linear trend is found in similar data from Ristic *et al.* (1991), White *et al.* (1974) and Nordeng and Sibley (1996). A possibility suggested for the mechanism is a polynuclear, birth and spread and modified spiral growth or modified spiral growth with increasing defect density with time on the larger crystals.

APPENDIX A

APPENDIX A

Geometric Correction to Slice of Rhombic Face

Three lengths and one angle (A, B, C, β) were measured for each concentrically-zoned slice of the rhomb face $(1\ 0\ \bar{1}\ 4)$ as illustrated in Figure 66. Measurement of β was used as an internal check on data precision since it can also be calculated from the three measured values of A, B, and C. The value of β calculated from A, B, and C in Equation 1 (Law of Cosines) was used to solve for the true lengths of A, B, and C referred to as A', B', and C'.

$$\beta = \cos^{-1}[A^2+B^2-C^2)/2AB] \qquad \text{(Equation 1)}$$

Once β has been calculated, angles σ and γ can be calculated by applying the Law of Sines (Equation 2,3).

$$\sigma = \sin^{-1}[(A\sin\beta)/C] \qquad \text{(Equation 2)}$$

$$\gamma = \sin^{-1}[(B\sin\beta)/C] \qquad \text{(Equation 3)}$$

Each of the three cases outlined in Figure 67 can now be solved. These three cases; Oblique Rotation (Case I), Rotation around the C-axis (Case II), and Rotation through the C-axis (Case III), are the only three cases which preserve a concentrically-zoned view with parallel apices. The three cases can be distinguished by the measured values as listed in Table 8. In Case III, C equals C' and no correction is required. For Case I and Case II, C' can be solved by comparison of the triangles created by; 1)

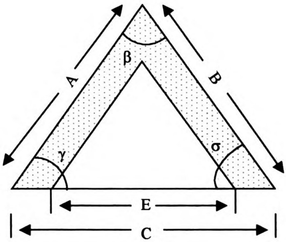

Figure 66. Slice Measurements

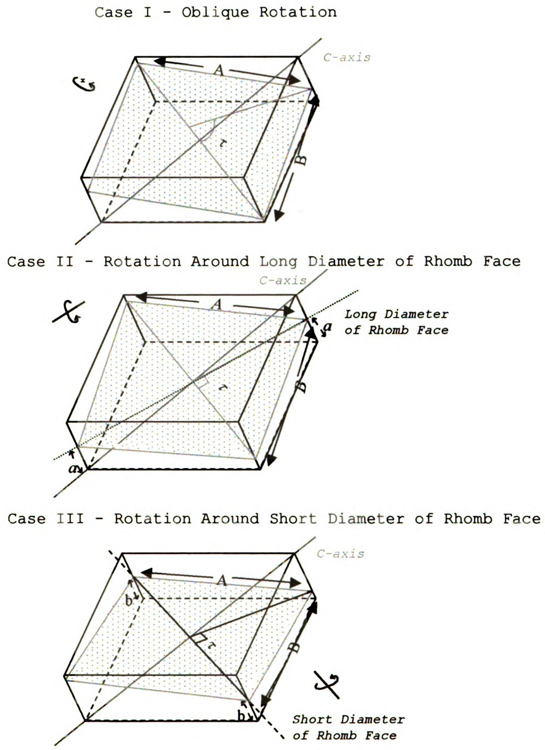

Figure 67. Three cases of rotation with corrections

Table 8. Parameters to distinguish Case I, II and III

	Case I	Case II	Case III
A	A>A'	A>A'	A>A'
B	B>B'	B>B'	B>B'
A=B?	A≠B	A=B	A=B
C	C>C'	C>C'	C=C'
β	$\beta>73.2^{o}$	$\beta>73.2^{o}$	$\beta<73.2^{o}$
γ	$\gamma<53.4^{o}$	$\gamma<53.4^{o}$	$\gamma>53.4^{o}$
σ	$\sigma<53.4^{o}$	$\sigma<53.4^{o}$	$\sigma>53.4^{o}$
$\gamma=\sigma$?	$\gamma\neq\sigma$	$\gamma=\sigma$	$\gamma=\sigma$
τ	variable	$\tau=90^{o}$	$\tau=90^{o}$

bisecting C and 2) the normal to C′, which cuts through the apex, labeled with the angle β.

In Case II, the line which is normal to length C' and the line which bisects C is the same line (Figure 68). In this case, length D' can be obtained by using the right triangle D'B(C/2).

$$D' = B \sin \sigma \qquad \text{(Equation 4)}$$

In Case I, the line that bisects C of the triangle ABC, is also the hypotenuse of the right triangle D'DX. The sides of D'DX are vectors (vector D' + vector X = vector D) which describe the orientation of the slice ABC relative to the triangle A'B'C' of the true rhomb face (Figure 69). The line that bisects C of the triangle ABC, or D, can be calculated from the Law of Cosines using triangle DB(C/2).

$$D = [B^2 + (C/2)^2 - 2B(C/2)\cos\sigma]^{1/2} \qquad \text{(Equation 5)}$$

Once D is known, the angle τ of the triangle DB(C/2) can be calculated from the Law of Sines.

$$\tau = \sin^{-1}[(B\sin\sigma)/D] \qquad \text{(Equation 6)}$$

The angle λ of the triangle D'DX is a complementary angle to τ.

$$\lambda = 180 - \tau \qquad \text{(Equation 7)}$$

The length D' can be calculated from the right triangle D'DX.

$$D' = D \sin \lambda \qquad \text{(Equation 8)}$$

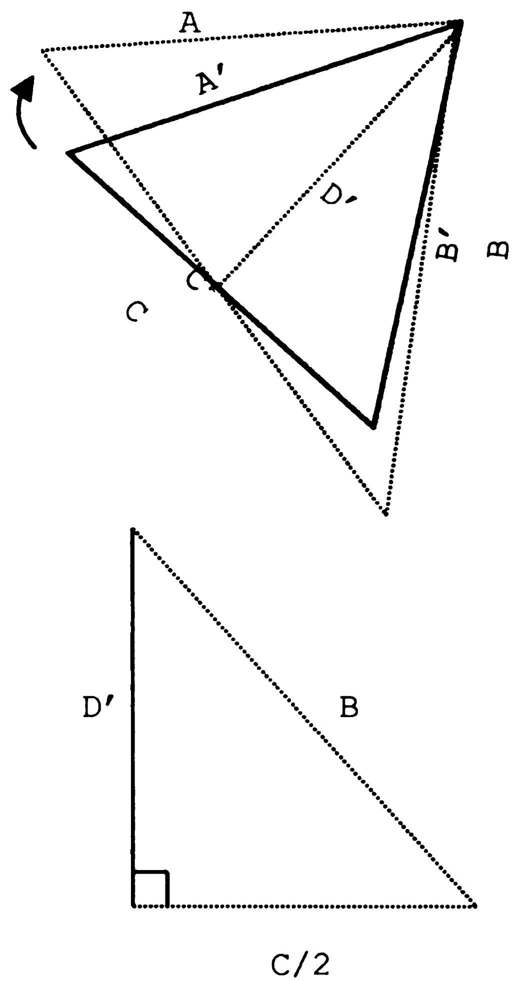

Figure 68. Case II Solution

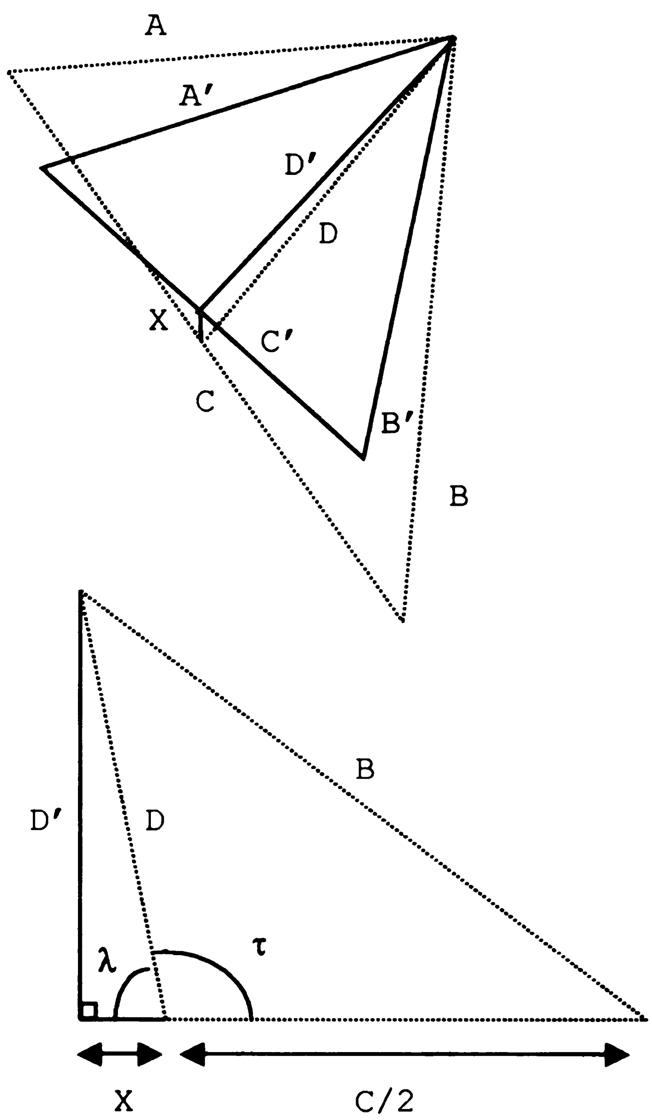

Figure 69. Case I Solution

For Cases I and II, B' and C'/2 can be calculated from the right triangle D'B'(C'/2) (Figure 70). In the triangle A'B'C', A' is equal to B' due to the symmetry of the rhomb face and σ is equal to γ. From crystal symmetry, the angle β equals 73.2 degrees and σ equals 53.4 degrees in the true rhomb face. Since the line D' equally bisects β, the angle θ of the triangle D'B'(C'/2) equals 36.6 degrees.

$$B' = D'/(\sin 53.4°) \qquad \text{(Equation 9)}$$

$$C' = (B' \sin 73.2°)/\sin 53.4° \qquad \text{(Equation 10)}$$

Since E (Figure 66), the inner zone width, changes proportionately to C, E' can be calculated by scaling E by the amount C is shortened.

$$E' = (C'E)/C \qquad \text{(Equation 11)}$$

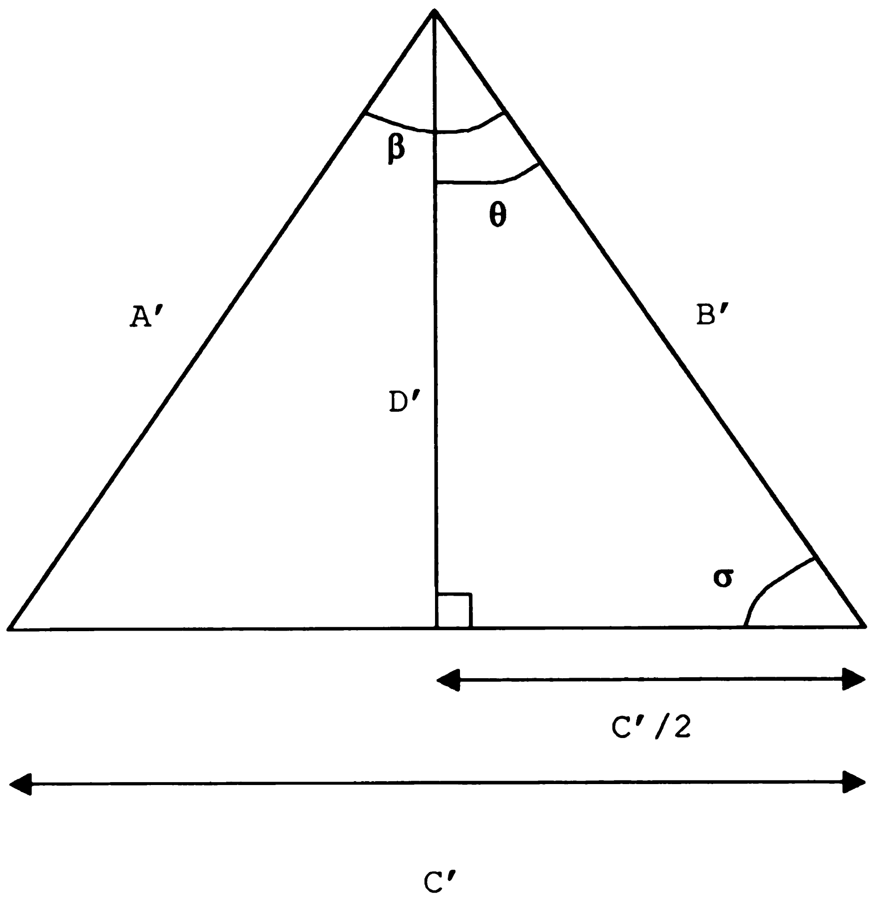

Figure 70. Triangle A′B′C′

APPENDIX B

APPENDIX B

Data Tables

Table 9. Sample List for Saluda Formation Hwy 421 Outcrop

Sample Number	Sample ID	Number of Crystals	Sample Number	Sample ID	Number of Crystals
1	m1	30	25	sd7	38
2	m2	33	26	sd11	31
3	m4	30	27	sd13	36
4	m8	30	28	sd15	30
5	m11	31	29	sd23	30
6	m20	35	30	p2	31
7	m21	30	31	p5	30
8	m26	30	32	p17	31
9	m28	33	33	p19	30
10	m30	31	34	p27	30
11	m34	30	35	p31	30
12	m42	30	36	p34	30
13	g1	33	37	p36	39
14	g3	31	38	p37	37
15	g4	43	39	p40	34
16	g5	32	40	p41	36
17	g6	30	41	p45	33
18	g7	34			
19	g8	37			
20	d6	44			
21	d8	31			
22	d10	31			
23	d12	30			
24	sd3	36			

Table 10. Sample M1 Measurements

A	B	C	E	crystal size	zone width
25	28	32.5	27	12.9	2.6
14	19	21	17	7.4	1.7
29.5	32.5	38	32	15.3	2.9
42	41.5	51	42	20.2	4.3
45.5	39.5	56	45	19.0	4.6
23.5	25	29	25.5	12.7	1.7
24	22	28	23	11.1	2.4
26.5	25.5	33.5	29	12.8	2.0
24.5	24	29	27.5	13.7	0.7
35	35	43.5	33.5	15.7	4.7
17	17	17.5	16	8.0	0.8
21.5	20	27	23	10.0	1.7
40	39.5	47.5	39.5	19.7	4.0
12	11	13.5	11.5	5.8	1.0
11	11	12	10	5.0	1.0
43	45.5	57	49	21.6	3.5
18.5	18.5	25.5	23	9.0	1.0
18.5	20.5	20	16	8.0	4.4
30	40	38	33	16.5	4.6
28	25.5	32	29	14.4	1.5
45.5	49	57.5	50	24.2	3.6
26	28.5	33	28.5	13.9	2.2
45.5	48	58	50	23.5	3.8
22.5	21	26	21	10.4	2.5
25.5	21.5	29	26	12.2	1.4
25.5	28.5	32	29.5	14.8	1.3
46	48.5	58.5	51	24.0	3.5
19	22	22	18	9.0	3.7
30.5	35	38	33	16.5	3.2
16	14.5	18	16	8.0	1.0

Table 11. Sample M2 Measurements

A	B	C	E	crystal size	zone width
20	19.5	22.5	18.5	9.3	2.0
9	9.5	12.5	7.5	3.0	2.0
28	31	35.5	28.5	14.0	3.4
23	26	31.5	24.5	10.8	3.1
26	25	27	23	11.5	2.0
20.5	20	24	19.5	9.8	2.3
21	21	21	18	9.0	1.5
23	22	25	19	9.5	3.0
18	19.5	22	19	9.5	1.5
26	28	32.5	27.5	13.5	2.5
40	39	48	40	19.4	3.9
17	17.5	20.5	16.5	8.3	2.0
46	44.5	57	44.5	20.4	5.7
32	31	41	31.5	13.6	4.1
32	31	40	32	14.5	3.6
10.5	19	20	17	6.2	1.1
22	27.5	33	27	11.1	2.5
37.5	35	44	36.5	17.7	3.6
22	24	26	23	11.5	2.5
20.5	22	26	22	10.5	1.9
17	20.5	25	20.5	8.4	1.8
14.5	15	17	15	7.5	1.0
18	17	19	17	8.5	1.0
14	14.5	16.5	14.5	7.3	1.0
25	25	30	24.5	12.1	2.7
30	29	31	27	13.5	2.0
21.5	21.5	28	24	10.4	1.7
23	22.5	25	21	10.5	2.0
27	27	33	28.5	13.7	2.2
16	14	18.5	16.5	7.8	0.9
20.5	21	24	20.5	10.3	1.8
25	21.5	33	24	8.8	3.3
15	15.5	18	13	6.5	2.5

Table 12. Sample M4 Measurements

A	B	C	E	crystal size	zone width
28	35	38.5	29	13.7	4.5
18.5	23	27.5	22.5	9.3	2.1
39	39	42.5	33	16.5	4.8
30.5	28	36.5	30	13.9	3.0
22.5	25	28.5	24	11.8	2.2
21.5	19.5	23.5	20.5	10.3	2.2
18.5	17	22	18.5	8.7	1.6
42.5	42	48	38	19.0	5.0
34	32.5	34.5	27.5	13.8	3.5
17	20	23.5	17.5	7.8	2.7
23	23	26.5	22	11.0	2.3
22	23	25.5	20.5	10.3	2.5
26.5	21.5	30.5	25.5	11.4	2.2
20.5	21.5	24	19.5	9.8	2.3
16	13.5	19	15.5	6.8	1.5
14	13	16	14	7.0	1.0
9.5	10	10.5	6.5	3.3	2.0
15	12	16.5	12.5	5.9	1.9
21	17.5	23.5	18	8.6	2.6
36	34	43	36	17.2	3.3
18	19.5	19.5	17.5	8.8	1.0
24.5	24	28	24	12.0	2.0
24.5	31.5	35	26.5	12.0	3.9
29	26.5	38	29.5	11.6	3.4
15.5	15	16	13	6.5	1.5
30.5	29	37.5	30.5	13.9	3.2
18.5	18.5	22	17	8.5	2.5
21.5	21	24	18.5	9.3	2.8
38	40	48	42	20.0	2.9
50	43	56.5	50.5	24.3	2.9

Table 13. Sample M8 Measurements

A	B	C	E	crystal size	zone width
30	27	34.5	29	14.1	2.7
22	27	30	28.8	13.6	0.6
15	19	22	16.5	7.1	2.4
22	29	31	24	11.3	3.3
30.5	26	35	28	13.1	3.3
18	18	22	18.5	8.9	1.7
19.5	16.5	22	19	9.1	1.4
17	22	24.5	20.5	9.2	1.8
16	18	20.5	16	7.8	2.2
34	32	41.5	36	16.5	2.5
15	15	19	16	7.3	1.4
20	20	24	20	9.9	2.0
19	22.5	26	22.5	10.3	1.6
12	10	13.5	10.5	5.0	1.4
23	22	26	21.5	10.8	2.3
32	25.5	37.5	30.5	13.0	3.0
19	18.5	22	20	10.0	1.0
26	32	35.5	29.5	13.9	2.8
17	15.5	22.5	18.5	7.1	1.5
22	20.5	23.5	19	9.5	2.3
25.5	27	32.5	28.5	13.4	1.9
28	22	30.5	23.5	11.1	3.3
27	30	35.5	28	13.0	3.5
29.5	35	43	33.5	13.8	3.9
21.5	21	26	20.5	9.8	2.6
25.5	32	36	30	13.6	2.7
34.5	35.5	41	36	18.0	2.5
17.5	15	20	17	8.0	1.4
38.5	35	45	40	19.1	2.4
34	34	41	35	17.2	2.9

Table 14. Sample M11 Measurements

A	B	C	E	crystal size	zone width
19	17.5	22	19.5	9.6	1.2
26.5	24.5	29	23.5	11.8	3.8
26	24.5	27	24	12.0	1.5
13.5	14	16.5	13	6.4	1.7
19.5	23	28	23.5	9.9	1.9
20	22.5	27	23	10.3	1.8
24	21.5	28	23	10.9	2.4
24.5	25	28	25.5	12.8	1.3
29.5	27	34	29.5	14.5	2.2
20	15.5	22.5	19.5	8.7	1.3
27	29	31.5	30	15.0	2.2
13	15.5	18.5	15.5	6.7	1.3
16.5	17	17	16.5	8.3	0.3
26	29	34	29	13.6	2.4
16.5	14	19	16.5	7.6	1.2
19.5	18.5	22.5	21	10.5	0.8
18	20	22.5	20.5	10.3	1.1
20	18	23	22	10.7	0.5
17.5	19.5	21	19	9.5	1.8
14.5	14	19	16	6.6	1.2
25	26	26.5	22	11.0	2.3
13	12	14.5	11.5	5.8	1.5
24	27	32.5	27	12.1	2.5
17.5	15	19.5	16	7.9	1.7
15.5	14.5	17	15	7.5	1.0
26	27.5	32	26	12.9	3.0
28	23.5	31.5	28	13.3	1.7
23	23.5	25	23.5	11.8	0.8
24.5	28.5	32.5	27	12.8	2.6
44.5	45.5	53	47.5	23.8	2.8
29	23	31.5	29	13.9	1.2

Table 15. Sample M20 Measurements

A	B	C	E	crystal size	zone width
41	37.5	49	38.5	17.8	4.9
28	28.5	34	28.5	14.0	2.7
26.5	26	38.5	28	9.6	3.6
25	26.5	34.5	22	9.0	5.1
19.5	19.5	22	18	9.0	2.0
26.5	22.5	30	25	11.9	2.4
30	33.5	41	34	14.9	3.1
22.5	20	26	21	10.0	2.4
22	22	26	21	10.5	2.5
32	26	44	37.5	11.8	2.1
27	25	40	31.5	9.7	2.6
25	36	38	31.5	14.1	2.9
24	23	28.5	23.5	11.4	2.4
25	29	33.5	26	12.1	3.5
26.5	22.5	32.5	27	11.2	2.3
27	26	30.5	23	11.5	3.8
47	40	54.5	49	22.5	2.5
27.5	30.5	35	30	14.7	2.4
35.5	32.5	41	34	16.7	3.4
13.5	15	18.5	16.5	7.2	0.9
22	26	30	24.5	11.3	2.5
19	21	23.5	20.5	10.3	1.7
40	35	49	37	15.8	5.1
21	20	22	17.5	8.8	2.3
21	20	21.5	19	9.5	1.3
13.5	14.5	18	14.5	6.4	1.5
31	25	35	24.5	11.2	4.8
25.5	20	29.5	23.5	10.1	2.6
31.5	30.5	36.5	29	14.5	3.8
31.5	26	36	25.5	11.7	4.8
24	22	26	19.5	9.8	4.3
20.5	18.5	21.5	18	9.0	3.0
13.5	19.5	26	22.5	6.4	1.0
20	18	21	18	9.0	2.7
27	27	34	29	13.3	2.3

Table 16. Sample M21 Measurements

A	B	C	E	crystal size	zone width
19	21.5	25	21	9.9	1.9
42.5	47	56	48	22.1	3.7
24	22.5	29	24	11.2	2.3
20.5	22.5	30	27	10.3	1.1
32	31	37	25	12.5	6.0
21	19.5	25	22	10.4	1.4
19	20	24	20	9.5	1.9
22	20	25	21	10.5	2.0
12.5	13	14	12	6.0	1.0
15.5	16.5	19.5	18	8.7	0.7
22	27	31	28	12.6	1.3
21	15	22	19.5	9.0	1.2
43.5	37.5	50	43.5	20.4	3.1
13.5	14	16	13	6.5	1.5
14.5	12	16.5	12	5.5	2.1
17	31	39	32	8.0	1.7
27.5	28	32.5	26	13.0	3.3
39.5	43	50	41	19.9	4.4
19.5	19.5	24.5	20	9.2	2.1
33	33.5	35.5	31	15.5	2.3
27	25	30	24.5	12.3	3.5
22	19.5	26	22	10.1	1.8
20	13.5	21	17.5	7.7	1.5
19.5	19	22	19	9.5	1.5
21	22.5	26	23	11.4	1.5
34.5	31	39.5	32.5	15.9	3.4
28	26.5	34	28.5	13.2	2.6
18.5	16.5	20.5	18	9.0	1.5
19	17	24	23	9.5	0.4
19.5	22.5	25.5	21	10.1	2.2

Table 17. Sample M26 Measurements

A	B	C	E	crystal size	zone width
14	15	19	14	6.0	2.1
18.5	14	20.5	19	8.5	0.7
13.5	12	16	14.5	6.7	0.7
29.5	29	29	25	12.5	2.0
22.5	22	26	22	11.0	2.0
22	17	26	23	9.4	1.2
12.5	19	20	18	7.7	0.9
21	20	26	23	10.4	1.4
20.5	26	29	23	10.5	2.7
30	33.5	38	33.5	16.6	2.2
20.5	26.5	29	23	10.7	2.8
15.5	15	18	15.5	7.8	1.3
22.5	18.5	25	22	10.5	1.4
27.5	28	34	30	14.4	1.9
21.5	18.5	25	23	10.6	0.9
19.5	16	22	19	8.8	1.4
8	8	10.5	8.5	3.6	0.9
32	33.5	44.5	37.5	15.0	2.8
10	15.5	16	14.5	6.3	0.6
28.5	28	33	28.5	14.3	2.3
19.5	24	27	24	11.1	1.4
16	18	19	17	8.5	1.9
17.5	19	23	19	8.7	1.8
18.5	20	22	19	9.5	1.5
28	28	35	30	13.9	2.3
32	26	35	32.5	15.7	1.2
16	14	17.5	15	7.5	1.5
29	30	35	31	15.5	2.0
15	15	18	16	7.9	1.0
24	22	25	22	11.0	3.3

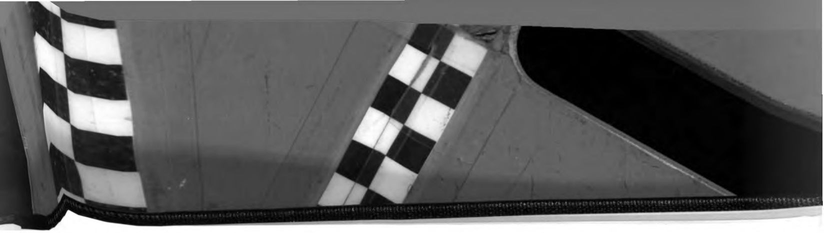

Table 18. Sample M28 Measurements

A	B	C	E	crystal size	zone width
28	23.5	32	26.5	12.3	2.5
29.5	25.5	34	31	14.5	1.4
41	46	52.5	44	21.5	4.2
18	17.5	21	18.5	9.3	1.3
25	25	29.5	24	12.0	2.8
19	21	25	22	10.2	1.4
19	18.5	23.5	21	9.7	1.2
18.5	18	20	18.5	9.3	0.8
20.5	22.5	23.5	21	10.5	2.8
23.5	23.5	26.5	24.5	12.3	1.0
35.5	35.5	41.5	36	18.0	2.8
41	35	47	40.5	19.0	3.0
42	47.5	55.5	51	23.8	2.1
18.5	18.5	23	20.5	9.6	1.2
39	40.5	48.5	44.5	21.5	1.9
19.5	23	25.5	23.5	11.5	1.0
22.5	26.5	30.5	27	12.5	1.6
21.5	23.5	25	22.5	11.3	2.6
28	23	32	29	13.2	1.4
25	27	29.5	28	14.0	1.9
17	18	19	16.5	8.3	1.3
26.5	21.5	34	29	10.6	1.8
19.5	23.5	26.5	23.5	11.0	1.4
28.5	28	32	26	13.0	3.0
42	37	48	42	20.3	2.9
21	24	27	24.5	12.1	1.2
41	31	45	37.5	17.0	3.4
49	38.5	58	52	21.5	2.5
21.5	20	22.5	19	9.5	1.8
28.5	34.5	38	32.5	15.8	2.7
17	19	22	18.5	8.9	1.7
20.5	19	24	21.5	10.4	1.2
27.5	28.5	34	31	15.1	1.5

Table 19. Sample M30 Measurements

A	B	C	E	crystal size	zone width
27.5	25.5	34.0	27.0	12.0	3.1
31.0	21.0	37.0	32.0	11.3	1.8
31.0	31.5	36.5	27.5	13.8	4.5
36.0	38.0	44.0	37.0	18.5	3.6
39.5	42.0	51.0	42.0	19.4	4.2
37.0	37.5	43.0	35.5	17.8	3.8
32.0	27.0	37.0	30.0	13.7	3.2
39.0	36.0	49.0	39.5	17.0	4.1
23.0	29.0	33.0	27.5	12.2	2.4
37.0	37.5	45.0	39.5	19.4	2.7
36.0	39.0	47.0	39.5	18.2	3.5
14.0	12.0	17.5	15.0	6.1	1.0
37.5	32.0	44.0	36.5	16.4	3.4
23.0	23.5	27.0	22.5	11.3	2.3
15.0	18.0	20.0	16.0	7.7	1.9
19.5	18.0	22.0	20.5	10.3	0.8
20.5	21.0	25.0	22.0	10.8	1.5
42.0	39.0	48.5	43.5	21.6	2.5
36.5	34.5	41.0	35.0	17.5	4.0
25.0	23.5	32.0	29.0	12.3	1.3
12.5	14.0	15.5	13.5	6.8	1.0
18.0	18.0	21.0	19.0	9.5	1.0
15.0	14.5	18.0	16.5	8.0	0.7
27.0	28.0	35.5	31.5	13.8	1.8
16.0	16.5	19.5	17.5	8.7	1.0
19.0	16.0	22.0	20.0	9.1	0.9
24.0	26.0	28.5	25.0	12.5	2.7
28.0	28.5	35.5	33.0	15.2	1.1
16.0	16.0	16.5	13.5	6.8	1.5
50.0	42.0	56.5	50.0	23.6	3.1
14.0	19.0	21.0	18.5	8.1	1.1

Table 20. Sample M34 Measurements

A	B	C	E	crystal size	zone width
29.0	27.5	38.0	33.5	13.7	1.8
40.0	43.0	54.5	49.0	20.9	2.3
22.0	24.0	29.0	24.5	11.2	2.1
38.5	43.5	49.5	41.5	20.2	3.9
40.5	31.0	47.5	39.0	16.0	3.5
28.5	27.0	34.0	27.5	13.2	3.1
39.0	33.5	46.0	39.5	17.7	2.9
14.0	17.5	22.0	18.0	6.8	1.5
28.0	30.0	34.5	27.0	13.5	3.8
19.5	21.5	27.5	22.5	9.2	2.0
28.5	30.5	34.0	27.0	13.5	4.4
25.5	24.0	27.5	21.5	10.8	3.0
27.0	27.5	39.0	32.5	11.8	2.4
29.0	25.0	32.5	27.0	13.2	2.7
29.0	36.0	42.5	36.0	15.3	2.8
16.0	14.0	18.5	16.0	7.5	1.2
26.5	26.0	36.0	31.5	12.4	1.8
28.5	25.5	34.5	30.0	13.4	2.0
28.5	28.0	36.0	30.0	13.5	2.7
30.0	35.5	40.5	36.0	16.8	2.1
28.0	29.5	36.5	31.5	14.2	2.3
35.5	32.0	40.5	36.0	17.8	2.2
25.5	24.5	32.0	26.5	11.8	2.5
24.0	22.0	28.5	23.5	11.0	2.3
19.0	20.5	20.0	15.5	7.8	2.3
27.5	25.5	32.5	29.5	14.1	1.4
35.0	27.0	39.0	30.5	13.7	3.8
25.5	16.5	28.0	26.0	10.2	0.8
20.0	20.5	25.0	19.5	9.2	2.6
12.0	13.0	15.0	13.5	6.7	0.7

Table 21. Sample M42 Measurements

A	B	C	E	crystal size	zone width
17.0	13.5	19.0	17.5	8.0	0.7
26.0	25.0	28.0	24.0	12.0	2.0
19.0	18.5	21.0	20.0	10.0	0.5
46.0	40.0	53.0	46.0	21.7	3.3
27.0	24.0	33.0	29.0	12.6	1.7
20.0	22.0	24.5	22.5	11.3	1.4
24.0	25.0	26.5	23.5	11.8	1.5
19.0	24.0	27.0	23.0	10.4	1.8
15.0	15.0	18.5	16.0	7.6	1.2
34.5	28.5	40.0	32.0	14.3	3.6
30.0	27.0	38.0	31.0	12.8	2.9
26.5	26.0	27.0	24.0	12.0	1.5
26.0	21.0	29.0	27.0	12.6	0.9
21.0	21.5	26.0	22.5	10.8	1.7
32.0	33.5	37.0	32.0	16.0	2.5
30.5	33.5	41.0	33.5	14.9	3.3
26.0	25.0	29.0	27.0	13.5	1.0
18.0	20.0	20.0	17.0	8.5	3.4
19.5	19.0	26.0	21.0	8.5	2.0
19.0	20.5	26.0	21.5	9.1	1.9
32.0	27.0	37.0	31.0	14.2	2.7
37.0	39.0	48.0	45.0	20.5	1.4
24.0	30.5	35.0	28.5	12.4	2.8
38.0	32.0	51.0	46.0	15.9	1.7
23.0	25.0	28.0	25.5	12.8	1.7
22.0	28.0	30.5	26.5	12.5	1.9
14.0	14.5	17.0	15.0	7.5	1.0
30.5	21.5	33.0	29.0	12.6	1.7
17.0	18.5	21.0	17.5	8.8	1.8
56.0	56.0	72.0	66.0	29.2	2.7

Table 22. Sample G1 Measurements

A	B	C	E	crystal size	zone width
21.0	29.5	36.5	31.0	10.7	1.9
58.0	52.0	69.0	57.0	26.2	5.5
17.5	23.5	25.0	22.0	10.3	1.4
26.0	21.5	30.0	27.0	12.2	1.4
20.0	21.0	24.0	20.5	10.3	1.8
29.0	24.0	32.0	28.5	13.8	1.7
17.5	16.5	20.0	18.0	9.0	1.0
13.0	16.0	17.5	14.0	6.8	1.7
17.0	22.0	26.0	21.0	8.6	2.0
26.0	24.0	28.0	26.5	13.3	2.1
48.0	51.0	59.5	52.5	25.9	3.5
28.0	18.5	29.0	22.5	9.9	2.9
26.0	36.0	41.0	36.5	14.9	1.8
21.5	20.0	23.0	18.0	9.0	2.5
14.5	16.0	19.5	16.0	7.1	1.6
26.5	35.0	46.0	41.5	13.4	1.5
31.0	32.0	41.5	34.5	14.6	3.0
21.5	21.0	26.0	22.5	10.8	1.7
16.5	16.5	18.0	16.5	8.3	0.8
19.5	18.0	23.0	20.5	9.8	1.2
16.5	15.0	18.0	14.0	7.0	2.0
31.5	32.5	38.5	33.0	16.3	2.7
17.0	13.0	18.5	14.5	6.7	1.9
38.0	33.0	45.0	37.5	16.9	3.4
19.0	24.0	27.0	22.0	10.0	2.3
24.5	23.0	29.5	24.5	11.5	2.3
17.5	16.5	20.0	17.0	8.5	1.5
14.5	17.0	19.0	16.0	7.8	1.5
20.5	24.5	27.5	22.5	10.7	2.4
13.0	18.0	20.0	17.0	7.2	1.3
15.0	16.5	22.5	19.5	7.1	1.1
14.0	16.0	17.0	16.0	8.0	1.1
16.5	18.5	22.0	19.0	8.7	1.4

Table 23. Sample G3 Measurements

A	B	C	E	crystal size	zone width
26.0	26.0	32.0	27.0	12.8	2.4
40.0	47.0	56.0	48.0	21.0	3.5
15.0	16.0	17.0	14.5	7.3	1.3
17.5	16.0	23.0	20.0	7.8	1.2
19.5	21.0	21.5	20.5	10.3	0.5
34.5	24.0	38.5	30.5	12.5	3.3
22.0	26.0	29.0	24.5	11.9	2.2
15.0	21.5	22.5	21.5	9.8	0.5
27.5	27.5	33.0	29.0	14.4	2.0
20.0	21.5	27.0	24.5	10.6	1.1
15.0	14.0	16.5	15.5	7.8	0.5
32.0	32.0	38.5	34.5	17.0	2.0
25.0	23.0	24.5	22.5	11.3	4.0
19.5	20.5	24.0	19.5	9.6	2.2
14.5	16.5	18.0	17.0	8.5	0.8
29.0	26.5	40.5	33.0	11.5	2.6
21.0	22.0	25.0	23.0	11.5	1.0
23.5	24.0	26.0	23.5	11.8	1.3
16.5	17.5	20.0	17.5	8.8	1.3
26.0	22.0	30.0	27.0	12.4	1.4
14.0	14.0	16.0	14.0	7.0	1.0
15.0	14.0	17.0	16.0	8.0	0.5
38.0	55.0	63.0	49.0	19.0	5.4
23.0	23.0	27.0	22.0	11.0	2.5
25.0	28.0	32.0	30.0	14.6	1.0
20.0	23.0	27.0	24.5	11.2	1.1
27.0	27.5	38.0	29.0	11.1	3.4
28.0	25.0	33.0	27.5	12.8	2.6
20.5	21.0	25.0	22.0	10.8	1.5
19.0	29.0	30.5	27.0	11.5	1.5
18.5	23.0	26.0	24.5	11.1	0.7

Table 24. Sample G4 Measurements

A	B	C	E	crystal size	zone width
17.0	23.0	27.0	22.5	8.9	1.8
30.5	28.0	38.0	27.5	11.9	4.6
18.0	19.0	23.5	17.5	7.9	2.7
17.0	26.0	27.0	21.5	9.3	2.4
32.0	27.0	37.0	27.0	12.3	4.6
23.0	24.0	28.0	24.0	12.0	2.0
34.5	37.0	46.0	35.5	15.7	4.6
29.0	25.0	32.5	24.0	11.7	4.2
29.5	28.5	35.5	26.0	12.5	4.6
28.0	23.0	33.0	26.5	11.5	2.8
13.0	17.5	19.0	14.0	6.3	2.3
17.5	23.0	26.0	19.5	8.5	2.8
19.0	26.5	29.0	24.5	10.6	2.0
18.0	21.5	25.0	20.0	9.0	2.2
26.5	21.0	31.5	28.5	11.8	1.2
63.0	62.0	80.0	69.0	30.8	4.9
21.5	39.0	41.0	31.5	11.5	3.5
17.5	15.5	21.0	16.0	7.2	2.2
25.0	39.5	45.0	35.0	12.6	3.6
34.0	33.0	44.5	36.5	15.3	3.3
39.0	37.0	48.0	40.0	18.2	3.6
42.0	42.0	44.0	33.0	16.5	5.5
42.5	43.0	47.5	42.0	21.0	2.8
27.0	27.5	33.0	25.5	12.4	3.7
16.0	17.0	19.0	15.0	7.5	2.0
42.0	42.5	49.0	42.0	21.0	3.5
27.0	28.0	33.0	30.5	15.1	1.2
15.5	17.0	20.0	15.5	7.4	2.1
31.5	28.0	36.0	29.5	14.3	3.2
22.0	27.0	30.0	26.0	12.3	1.9
26.0	27.5	32.0	25.0	12.4	3.5
30.5	27.5	35.0	30.0	14.7	2.4
21.0	26.5	31.0	26.0	11.0	2.1
16.0	15.0	18.0	15.0	7.5	1.5
23.0	16.0	24.5	19.5	8.6	2.2
29.0	31.0	40.0	33.5	13.9	2.7
38.0	38.0	47.5	41.0	19.0	3.0

Table 24 (cont'd).

A	B	C	E	crystal size	zone width
26.0	22.5	29.5	23.5	11.3	2.9
24.0	22.0	22.5	20.5	10.3	4.6
29.5	32.0	37.0	30.5	15.0	3.2
20.0	17.5	23.5	20.5	9.4	1.4
25.5	26.0	31.0	25.0	12.3	3.0
29.5	27.5	35.5	29.0	13.5	3.0

Table 25. Sample G5 Measurements

A	B	C	E	crystal size	zone width
22.5	23.0	27.0	23.5	11.8	1.8
18.5	20.5	26.5	22.0	8.8	1.8
24.0	28.0	32.5	26.0	12.0	3.0
25.0	28.5	33.5	28.0	12.9	2.5
20.0	18.5	24.0	21.0	9.8	1.4
12.0	16.5	18.0	15.5	6.8	1.1
21.5	19.0	24.5	23.5	11.4	0.5
37.0	37.0	43.0	39.0	19.5	2.0
14.0	15.0	15.0	11.5	5.8	1.8
12.5	11.5	15.0	13.0	6.0	0.9
20.0	20.5	23.0	20.0	10.0	1.5
13.0	11.0	15.0	13.0	6.0	0.9
13.5	15.0	17.5	16.0	7.6	0.7
8.5	8.5	10.0	8.0	4.0	1.0
31.5	32.5	32.0	27.0	13.5	2.5
20.5	21.0	26.0	22.0	10.2	1.8
25.5	27.0	32.0	28.5	13.7	1.7
23.0	24.5	30.0	26.5	12.1	1.6
20.5	22.0	24.0	17.0	8.5	3.5
14.0	13.5	17.5	16.5	7.4	0.4
15.5	17.0	20.0	18.0	8.5	0.9
9.5	11.0	12.0	10.0	5.0	1.0
12.0	14.0	15.0	14.0	7.0	0.8
33.0	25.5	37.0	31.0	13.8	2.7
20.0	20.0	23.0	19.5	9.8	1.8
33.5	26.0	36.0	31.0	14.8	2.4
15.5	16.5	20.0	17.5	8.1	1.2
23.0	23.0	28.0	26.5	12.8	0.7
21.5	21.0	28.0	25.0	10.6	1.3
26.0	21.0	29.0	25.5	11.9	1.6
21.0	22.5	25.0	20.5	10.3	2.3
22.0	28.0	30.5	27.0	12.8	1.7

Table 26. Sample G6 Measurements

A	B	C	E	crystal size	zone width
37.0	27.5	45.0	37.0	13.8	3.0
25.0	27.0	30.0	26.5	13.3	2.5
19.0	18.0	22.0	19.5	9.8	1.3
33.0	30.5	43.0	38.5	15.5	1.8
18.0	18.5	21.5	19.0	9.5	1.3
28.5	21.0	33.0	28.5	11.5	1.8
22.0	23.5	27.0	22.0	11.0	2.5
28.5	34.5	39.0	35.5	16.5	1.6
34.5	34.0	41.0	37.0	18.4	2.0
19.5	19.0	24.0	21.5	10.0	1.2
20.5	22.5	26.0	23.5	11.5	1.2
38.6	35.0	45.0	38.0	18.2	3.4
20.5	22.5	26.0	23.0	11.2	1.5
31.0	39.0	43.0	37.0	17.3	2.8
11.5	11.0	13.0	11.5	5.8	0.8
23.5	22.5	26.0	22.5	11.3	1.8
21.0	24.0	29.0	26.5	11.6	1.1
17.0	17.5	17.5	16.0	8.0	0.8
32.0	38.5	44.0	36.0	16.6	3.7
12.0	11.5	13.5	11.0	5.5	1.3
32.0	36.0	44.0	38.0	16.6	2.6
20.5	21.0	25.0	22.5	11.1	1.2
16.5	17.0	20.0	17.0	8.5	1.5
30.0	31.0	35.5	33.5	16.8	1.0
50.0	40.5	55.0	46.5	22.2	4.1
20.5	20.0	24.0	21.5	10.8	1.3
13.5	17.0	18.5	15.5	7.4	1.4
29.0	28.0	33.0	29.0	14.5	2.0
23.0	25.0	28.0	24.5	12.3	2.2
41.0	32.5	47.0	43.0	18.9	1.8

Table 27. Sample G7 Measurements

A	B	C	E	crystal size	zone width
17.0	19.0	19.5	17.0	8.5	2.7
17.0	19.0	21.0	19.0	9.5	1.3
37.5	38.0	42.0	36.0	18.0	3.0
20.5	28.0	32.5	27.0	10.8	2.2
36.0	35.0	41.0	36.0	18.0	2.5
24.0	22.0	26.5	25.0	12.5	1.4
27.5	27.0	32.5	27.0	13.5	2.7
34.5	41.5	46.0	39.0	18.8	3.4
26.0	31.0	36.0	33.0	14.9	1.4
30.5	34.0	47.0	38.0	13.2	3.1
33.0	28.0	38.0	29.0	13.4	4.2
21.0	20.5	25.0	20.0	9.8	2.5
17.0	15.0	19.5	17.0	8.2	1.2
32.0	32.0	36.0	31.0	15.5	2.5
29.0	35.0	42.0	35.0	14.8	3.0
14.5	10.5	17.0	15.0	5.8	0.8
20.0	22.0	25.0	23.0	11.5	1.0
33.5	37.5	43.0	38.0	18.5	2.4
19.5	21.0	23.0	20.0	10.0	1.5
36.0	37.0	44.0	37.0	18.2	3.4
37.0	36.0	44.5	35.0	16.9	4.6
20.0	26.0	30.0	26.0	11.0	1.7
15.0	13.0	15.5	13.5	6.8	1.8
21.0	24.0	27.0	22.0	10.8	2.5
18.0	26.0	28.0	23.0	9.9	2.2
40.0	40.0	48.0	42.0	20.8	3.0
14.0	13.0	15.0	14.0	7.0	0.5
22.0	23.0	27.0	23.0	11.4	2.0
17.0	17.0	24.0	21.0	7.8	1.1
42.0	40.0	52.0	46.0	20.8	2.7
22.0	17.5	24.0	22.0	10.5	1.0
27.0	27.5	30.0	27.0	13.5	1.5
25.0	26.0	29.0	24.0	12.0	2.5
18.0	17.0	20.0	18.0	9.0	1.0

Table 28. Sample G8 Measurements

A	B	C	E	crystal size	zone width
22.0	24.0	27.0	23.0	11.5	2.3
36.0	35.0	39.5	32.0	16.0	3.8
18.0	18.5	18.0	17.0	8.5	0.5
28.0	26.0	35.0	29.0	12.6	2.6
34.0	32.0	40.0	31.0	15.1	4.4
30.0	31.5	36.0	32.0	16.0	2.0
31.0	32.0	37.0	32.0	16.0	2.5
31.0	31.5	37.0	31.0	15.5	3.0
37.0	41.0	47.0	34.0	16.7	6.4
31.0	31.0	37.0	31.0	15.5	3.0
48.0	54.0	62.0	54.0	26.1	3.9
30.0	32.0	40.0	35.0	15.4	2.2
31.0	32.5	40.0	35.0	16.0	2.3
31.0	29.0	36.0	31.0	15.3	2.5
23.0	25.0	27.0	23.5	11.8	2.9
16.0	18.0	20.0	17.0	8.5	1.7
20.0	18.0	22.0	20.0	10.0	1.5
45.0	40.0	52.0	42.0	20.1	4.8
22.0	20.0	26.0	21.0	9.9	2.3
27.0	27.0	28.0	23.0	11.5	2.5
36.0	46.0	52.0	44.0	19.5	3.6
34.0	35.5	37.0	32.0	16.0	2.5
15.0	16.5	18.0	15.0	7.5	1.5
30.0	34.0	40.0	34.0	15.7	2.8
36.0	30.0	42.0	37.0	16.5	2.2
44.0	43.0	50.0	44.0	22.0	3.0
36.0	31.5	44.0	37.0	15.9	3.0
42.5	43.0	51.0	43.0	21.5	4.0
20.0	26.5	29.0	26.0	11.8	1.4
22.0	20.0	22.0	20.0	10.0	3.2
24.0	24.0	27.0	25.0	12.5	1.0
17.0	14.0	22.0	18.0	6.6	1.5
16.0	18.0	20.5	18.0	8.8	1.2
32.0	29.0	37.0	25.0	12.1	5.8
19.5	20.0	22.0	19.0	9.5	1.5
32.0	28.0	36.0	30.0	14.8	3.0
46.0	46.0	56.0	42.0	20.3	6.8

Table 29. Sample D6 Measurements

A	B	C	E	crystal size	zone width
38.0	35.0	47.0	41.0	18.1	2.6
31.0	37.5	44.5	35.5	15.3	3.9
33.5	28.0	39.0	32.0	14.3	3.1
28.0	19.5	30.5	24.5	10.4	2.6
34.0	37.0	68.5	57.5	5.8	1.1
26.5	31.0	34.5	27.5	13.5	3.4
31.0	32.0	34.5	28.0	14.0	3.3
31.0	33.0	38.0	29.0	14.5	4.6
12.0	13.0	15.0	12.5	6.2	1.2
19.5	15.0	21.5	18.5	8.4	1.4
11.5	11.0	14.5	11.0	4.8	1.5
27.0	26.0	31.5	26.0	13.0	2.8
27.0	30.5	35.0	28.0	13.5	3.4
49.0	40.0	54.0	45.5	21.8	4.1
33.5	28.5	43.5	38.0	14.2	2.1
29.0	20.0	32.5	29.0	11.7	1.4
22.0	16.0	24.5	20.5	8.8	1.7
44.0	35.5	51.5	43.0	18.5	3.7
13.5	13.5	16.0	12.5	6.3	1.8
21.0	19.0	24.0	20.0	9.9	2.0
16.0	20.0	22.0	18.5	8.7	1.7
20.5	27.0	30.0	25.0	11.1	2.2
18.0	16.0	21.0	18.0	8.5	1.4
22.5	21.0	26.5	22.5	10.9	1.9
23.5	24.0	25.0	19.0	9.5	3.0
20.5	20.5	24.5	20.5	10.2	2.0
42.0	27.0	44.0	36.0	15.2	3.4
24.0	19.5	27.5	23.0	10.3	2.0
31.0	32.5	38.0	30.5	15.2	3.7
17.5	18.0	21.0	16.5	8.3	2.3
24.0	23.0	28.5	23.0	11.2	2.7
18.0	18.0	21.0	18.0	9.0	1.5
42.5	35.5	50.0	38.5	16.9	5.1
23.5	22.5	25.5	23.0	11.5	1.3
35.0	30.0	39.0	31.0	15.2	3.9
32.5	29.0	41.0	33.0	13.7	3.3
46.0	43.5	57.5	44.0	19.5	6.0

Table 29 (cont'd).

A	B	C	E	crystal size	zone width
47.0	50.5	59.0	44.5	21.7	7.1
20.5	22.0	25.0	21.0	10.5	2.0
22.5	20.0	28.0	21.5	9.1	2.7
27.0	32.0	37.0	30.0	13.7	3.2
20.5	22.0	25.5	21.0	10.4	2.2
18.0	19.0	23.0	18.5	8.6	2.1
30.5	30.0	33.0	29.5	14.8	1.8

Table 30. Sample D8 Measurements

A	B	C	E	crystal size	zone width
39.0	37.0	47.0	40.0	18.9	3.3
31.5	35.0	41.0	36.5	17.2	2.1
26.0	27.5	29.0	26.0	13.0	1.5
29.0	31.0	35.0	30.5	15.3	2.8
29.5	27.5	35.0	30.5	14.5	2.1
33.0	33.0	40.0	36.0	17.5	1.9
26.0	36.0	40.0	36.0	15.3	1.7
29.5	27.0	34.0	30.5	15.0	1.7
32.5	32.0	40.0	35.5	16.7	2.1
25.0	23.0	28.5	24.0	12.0	2.3
26.5	24.5	32.0	29.0	13.3	1.4
15.0	17.0	19.0	16.0	8.0	1.5
18.0	23.5	27.0	23.5	10.0	1.5
21.0	21.5	26.5	22.0	10.2	2.1
25.0	24.5	32.0	28.0	12.3	1.8
18.0	19.0	21.0	19.0	9.5	1.0
23.0	19.5	26.0	23.5	11.2	1.2
29.5	35.5	40.0	36.0	16.9	1.9
35.0	34.5	42.0	37.5	18.4	2.2
23.0	18.0	26.5	22.0	9.5	1.9
24.5	25.5	29.0	25.5	12.8	1.8
38.5	35.0	48.5	38.0	16.0	4.4
28.5	27.0	31.0	25.0	12.5	3.0
14.0	13.5	14.5	11.5	5.8	1.5
24.5	23.5	31.5	27.5	11.7	1.7
27.0	28.0	35.0	28.0	12.6	3.1
19.5	22.0	25.0	20.0	9.8	2.4
17.0	16.5	20.5	17.5	8.4	1.4
21.0	34.0	34.5	28.0	12.0	2.8
21.0	27.0	30.0	24.0	10.9	2.7
25.0	21.5	33.0	26.0	9.5	2.6

Table 31. Sample D10 Measurements

A	B	C	E	crystal size	zone width
34.0	33.5	42.5	35.5	16.3	3.2
21.0	19.0	23.0	18.5	9.3	2.9
38.5	40.5	52.0	44.5	18.9	3.2
30.5	34.0	40.0	36.5	17.1	1.6
39.0	40.5	53.0	43.0	17.8	4.1
42.0	52.0	59.5	49.0	21.9	4.7
23.5	21.0	27.5	25.5	12.0	0.9
28.0	28.0	33.5	29.5	14.7	2.0
31.0	35.5	43.5	39.0	16.7	1.9
22.0	22.0	26.0	23.0	11.5	1.5
33.5	34.5	37.0	31.0	15.5	3.0
19.0	21.0	27.0	22.0	8.9	2.0
32.0	27.0	40.5	34.0	13.3	2.5
28.0	34.0	41.5	36.5	14.9	2.0
25.5	27.0	31.5	23.5	11.6	4.0
28.0	34.5	40.5	37.0	15.9	1.5
26.0	26.5	32.5	21.5	10.1	5.2
25.5	24.0	26.5	22.5	11.3	2.0
21.0	27.0	29.5	24.5	11.4	2.3
21.5	19.5	25.0	22.0	10.6	1.4
20.0	18.0	24.5	21.0	9.2	1.5
34.0	35.0	43.0	35.5	16.5	3.5
32.5	32.0	40.0	35.0	16.4	2.3
22.0	23.0	27.0	22.0	10.9	2.5
13.0	11.5	15.0	13.0	6.2	1.0
17.5	18.5	23.0	20.5	9.2	1.1
24.5	20.5	30.0	27.0	11.1	1.2
21.0	15.5	22.5	17.5	8.0	2.3
16.0	18.5	21.0	18.5	8.9	1.2
24.0	22.5	28.5	24.5	11.7	1.9
36.5	35.5	42.0	37.0	18.5	2.5

Table 32. Sample D12 Measurements

A	B	C	E	crystal size	zone width
16.5	15.0	20.0	18.0	8.1	0.9
22.0	24.0	27.0	24.0	12.0	1.8
18.5	20.5	24.0	21.0	10.0	1.4
24.0	24.5	28.0	26.0	13.0	1.0
24.0	23.0	29.0	25.0	11.8	1.9
30.0	36.0	41.0	37.0	17.1	1.9
17.0	21.5	24.0	22.0	10.1	0.9
23.0	22.5	27.0	23.0	11.5	2.0
35.0	45.0	52.0	47.0	20.0	2.1
31.0	32.0	38.0	36.0	17.7	1.0
14.0	14.0	16.0	14.0	7.0	1.0
21.5	20.0	24.0	20.0	10.0	2.0
22.0	22.0	24.5	21.0	10.5	1.8
20.0	24.0	27.0	24.5	11.6	1.2
29.5	28.5	37.0	32.0	14.3	2.2
21.0	23.5	28.0	25.5	11.6	1.1
38.0	40.5	47.5	41.5	20.2	2.9
24.0	27.5	32.0	27.5	12.8	2.1
23.0	20.0	27.0	25.0	11.4	0.9
19.5	19.0	22.0	19.5	9.8	1.3
39.0	38.5	47.0	41.5	20.2	2.7
20.5	20.0	24.5	22.0	10.8	1.2
39.0	37.5	47.0	42.0	20.0	2.4
30.5	24.0	38.0	33.0	12.4	1.9
19.0	20.5	26.0	23.5	10.0	1.1
24.5	24.0	28.0	25.0	12.5	1.5
20.0	21.5	24.0	21.0	10.5	1.5
13.5	13.5	17.5	16.0	7.0	0.7
28.0	29.5	35.0	28.5	13.8	3.1
28.5	27.0	36.0	30.5	13.3	2.4

Table 33. Sample SD3 Measurements

A	B	C	E	crystal size	zone width
29.5	27.0	37.0	32.0	13.7	2.1
35.0	36.0	43.0	36.5	17.8	3.2
46.0	57.0	66.5	56.0	24.3	4.5
36.0	37.0	41.5	35.5	17.8	3.0
57.0	45.0	63.0	55.0	25.5	3.7
40.0	35.5	50.0	42.5	17.8	3.1
38.5	38.5	50.0	42.5	18.5	3.3
16.0	19.5	22.0	17.0	7.9	2.3
34.0	35.0	38.5	33.5	16.8	2.5
24.5	23.5	29.5	24.0	11.4	2.6
38.5	52.5	57.0	46.5	20.8	4.7
21.0	22.5	26.5	22.5	10.9	1.9
18.0	19.0	22.0	17.5	8.8	2.3
17.0	17.5	19.5	14.0	7.0	2.8
21.0	20.0	23.0	19.5	9.8	1.8
14.0	15.5	17.5	13.0	6.5	2.3
12.5	12.5	15.0	12.0	5.9	1.5
19.0	19.0	23.0	18.0	8.8	2.4
36.0	33.5	42.5	35.5	17.0	3.4
25.5	25.0	29.5	25.0	12.5	2.3
28.5	27.5	31.0	26.0	13.0	2.5
24.5	25.0	27.5	22.5	11.3	2.5
26.5	20.0	31.0	28.0	11.4	1.2
24.0	22.0	27.5	22.5	11.2	2.5
31.0	30.0	35.5	31.5	15.8	2.0
19.5	18.0	23.0	16.5	7.9	3.1
36.0	39.0	46.5	41.0	19.2	2.6
52.5	42.5	64.0	53.0	21.3	4.4
35.5	36.5	41.0	35.0	17.5	3.0
28.0	22.5	33.5	24.0	9.9	3.9
35.5	35.0	41.5	36.0	18.0	2.8
19.0	14.5	21.0	17.0	7.7	1.8
43.0	45.0	53.0	42.5	20.9	5.2
26.0	25.5	28.0	21.5	10.8	3.3
12.5	14.0	15.5	12.0	6.0	1.8
31.0	30.0	32.0	24.5	12.3	3.8

Table 34. Sample SD7 Measurements

A	B	C	E	crystal size	zone width
35.5	32.0	46.0	31.0	12.3	6.0
35.5	30.5	41.0	34.5	16.0	3.0
17.5	17.0	18.0	14.5	7.3	1.8
14.5	14.5	17.0	14.5	7.3	1.3
20.0	24.0	29.5	26.0	10.6	1.4
27.5	37.0	41.0	35.0	15.4	2.6
39.5	39.5	47.0	39.5	19.8	3.8
50.0	44.0	57.0	47.5	23.0	4.6
14.5	14.0	15.0	13.0	6.5	1.0
19.0	17.5	19.5	18.0	9.0	0.8
19.0	19.0	22.0	19.5	9.8	1.3
18.0	17.0	21.0	17.5	8.7	1.7
17.0	18.0	20.0	18.0	9.0	1.0
29.0	29.0	29.0	26.5	13.3	1.3
35.0	27.5	39.0	33.5	15.3	2.5
49.0	44.0	59.0	50.0	22.5	4.1
34.0	36.0	40.0	35.5	17.8	3.6
34.0	28.0	37.5	33.5	16.2	1.9
33.5	32.5	42.0	36.0	16.2	2.7
48.0	44.0	58.0	48.0	21.9	4.6
28.0	30.0	35.0	30.0	14.7	2.4
41.0	31.0	45.5	39.5	17.5	2.7
27.5	30.0	35.0	31.0	15.0	1.9
42.0	31.0	46.0	39.0	17.3	3.1
43.0	33.0	49.0	43.0	18.5	2.6
14.0	16.0	17.0	15.0	7.5	1.6
11.5	12.0	13.0	11.0	5.5	1.0
13.5	13.0	15.5	12.0	6.0	1.8
17.5	20.0	23.0	19.0	9.0	1.9
18.0	18.0	21.0	17.5	8.8	1.8
27.0	30.5	35.0	29.0	14.0	2.9
26.0	29.5	36.0	28.0	12.1	3.5
18.0	18.0	21.0	18.5	9.3	1.3
18.0	18.5	21.5	17.0	8.5	2.3
30.0	35.0	42.0	36.0	15.7	2.6
18.5	24.0	26.0	21.0	9.9	2.3
23.0	14.5	23.5	19.0	8.2	1.9

Table 34 (cont'd).

A	B	C	E	crystal size	zone width
30.0	33.5	38.0	32.0	15.8	3.0

Table 35. Sample SD11 Measurements

A	B	C	E	crystal size	zone width
33.0	20.0	35.0	28.0	11.0	2.7
29.0	29.0	34.0	29.0	14.5	2.5
34.0	49.0	53.0	43.5	18.7	4.1
32.0	32.0	47.0	33.0	11.3	4.8
32.0	32.0	34.5	25.0	12.5	4.8
35.5	41.0	53.0	46.5	17.9	2.5
48.0	37.0	51.5	43.5	20.7	3.8
14.5	13.0	17.0	13.5	6.3	1.6
15.5	16.0	18.0	15.5	7.8	1.3
19.0	21.0	23.5	18.5	9.3	2.7
17.0	16.5	20.0	18.0	9.0	1.0
28.5	27.0	31.5	26.0	13.0	2.8
26.5	24.0	31.0	25.0	11.9	2.9
17.5	10.0	18.5	15.5	5.8	1.1
27.5	20.0	30.0	25.5	11.3	2.0
26.5	23.0	31.0	26.0	11.9	2.3
16.5	11.5	18.0	16.0	6.8	0.9
18.5	26.5	29.0	25.0	10.6	1.7
24.0	26.0	33.5	28.5	11.7	2.1
29.5	28.0	33.5	28.0	14.0	2.8
40.5	33.0	47.0	39.0	17.2	3.5
14.5	14.0	15.5	13.0	6.5	1.3
29.5	29.5	35.0	27.5	13.8	3.8
13.0	13.0	15.5	12.5	6.3	1.5
32.0	31.0	40.5	34.5	15.3	2.7
17.5	16.0	19.5	17.0	8.5	1.3
18.0	20.0	23.5	18.5	8.7	2.4
21.5	21.0	23.0	19.0	9.5	2.0
24.0	25.5	29.0	22.5	11.3	3.3
17.5	16.0	20.5	16.5	7.9	1.9
12.5	11.0	14.5	11.5	5.4	1.4

Table 36. Sample SD13 Measurements

A	B	C	E	crystal size	zone width
18.0	18.0	20.5	19.0	9.5	0.8
36.0	35.0	44.0	38.0	17.9	2.8
27.5	27.5	33.0	31.0	15.3	1.0
25.0	28.0	33.0	29.0	13.5	1.9
27.0	25.0	35.0	26.5	10.8	3.5
19.5	21.0	24.0	20.0	10.0	2.0
20.0	21.5	26.0	20.0	9.2	2.8
25.0	23.0	31.0	26.0	11.4	2.2
18.0	19.0	21.0	20.0	10.0	0.5
26.0	23.0	31.5	27.0	11.9	2.0
31.0	35.0	40.0	35.5	17.2	2.2
26.0	28.0	34.0	29.0	13.3	2.3
17.0	16.0	19.0	16.0	8.0	1.5
23.0	24.0	27.0	21.0	10.5	3.0
27.5	21.0	30.0	25.0	11.5	2.3
19.5	18.0	22.0	20.0	10.0	1.0
23.5	28.0	31.0	26.5	12.9	2.2
20.0	18.5	23.0	20.5	10.2	1.2
22.5	20.0	27.5	23.0	10.0	2.0
27.0	25.0	31.0	25.0	12.5	3.0
18.0	16.0	17.0	16.5	8.3	2.6
21.0	21.0	25.5	21.5	10.4	1.9
13.0	20.0	21.0	17.0	7.2	1.7
20.5	15.5	22.0	20.0	9.4	0.9
25.0	25.0	28.0	22.0	11.0	3.0
16.0	14.5	20.0	15.0	6.4	2.1
21.5	19.5	24.5	20.0	9.9	2.2
25.0	26.5	28.0	22.0	11.0	3.0
20.5	21.0	23.5	20.0	10.0	1.8
29.0	22.5	33.0	29.5	12.9	1.5
29.0	29.5	36.0	26.0	12.4	4.8
22.0	23.0	27.5	22.0	10.6	2.6
29.5	30.0	38.0	30.5	13.6	3.4
32.0	30.0	34.0	28.0	14.0	5.2
19.5	19.0	21.5	16.5	8.3	2.5
18.0	17.5	22.0	17.5	8.2	2.1

Table 37. Sample SD15 Measurements

A	B	C	E	crystal size	zone width
33.0	32.0	41.0	34.5	15.8	3.0
18.0	19.0	22.0	19.0	9.5	1.5
19.0	20.0	24.0	18.5	8.8	2.6
22.0	19.0	25.0	16.5	7.9	4.1
21.0	20.0	25.0	21.5	10.4	1.7
16.5	15.0	22.5	15.5	5.6	2.5
20.0	20.5	23.5	17.0	8.5	3.3
42.5	49.0	64.0	52.5	19.8	4.3
29.0	28.0	32.5	26.5	13.3	3.0
22.5	25.0	30.5	24.0	10.6	2.9
19.5	23.0	25.5	19.5	9.6	2.9
35.5	35.0	39.0	30.0	15.0	4.5
19.5	22.0	26.5	18.5	8.2	3.6
32.5	34.0	36.5	27.5	13.8	4.5
36.5	37.0	50.5	39.0	15.3	4.5
24.0	24.0	31.0	24.0	10.5	3.1
19.5	24.0	26.5	19.5	9.3	3.3
19.5	25.0	31.0	23.5	8.8	2.8
20.0	24.5	27.0	20.0	9.6	3.4
35.0	29.0	41.0	31.5	13.9	4.2
26.0	26.5	32.0	27.0	13.0	2.4
24.0	24.0	30.5	23.5	10.6	3.2
27.5	28.5	29.5	24.5	12.3	2.5
31.0	32.0	30.5	25.5	12.8	2.5
13.0	11.0	18.0	13.5	4.4	1.5
23.5	28.0	36.0	29.0	10.9	2.6
20.5	18.5	23.5	18.5	9.1	2.5
41.0	31.0	44.0	37.0	17.3	3.3
25.5	23.5	32.0	29.0	12.5	1.3
21.0	17.0	23.0	21.0	10.1	1.0

Table 38. Sample SD23 Measurements

A	B	C	E	crystal size	zone width
44.0	39.0	54.0	44.5	19.2	4.1
34.0	33.0	37.0	35.0	17.5	1.0
23.0	22.5	25.5	24.0	12.0	0.8
20.0	17.0	24.0	20.5	8.9	1.5
14.5	13.0	17.5	15.0	6.7	1.1
11.0	11.0	13.5	12.0	5.7	0.7
20.0	17.0	23.5	19.0	8.5	2.0
33.0	25.0	36.5	33.0	14.8	1.6
15.0	11.0	16.0	14.5	6.7	0.7
25.0	24.0	26.0	24.5	12.3	0.8
14.5	18.0	20.5	19.0	8.6	0.7
39.0	40.0	46.0	41.0	20.5	2.5
15.5	14.0	17.0	13.0	6.5	2.0
25.0	24.0	29.0	27.5	13.8	0.8
15.0	16.0	18.5	17.5	8.8	0.5
25.5	28.5	32.5	29.5	14.5	1.5
20.0	18.0	21.0	18.0	9.0	2.7
20.0	24.5	27.5	25.5	11.9	0.9
13.0	15.0	16.0	13.5	6.8	1.7
17.5	17.0	21.0	19.5	9.4	0.7
21.0	22.0	23.0	22.0	11.0	0.5
20.0	17.5	22.5	20.0	9.8	1.2
36.0	41.5	47.5	42.5	20.2	2.4
17.0	16.0	18.0	16.0	8.0	1.0
34.5	34.0	39.0	35.0	17.5	2.0
18.0	20.0	23.0	21.5	10.5	0.7
9.5	10.0	11.5	10.5	5.3	0.5
26.0	27.5	37.5	31.0	11.7	2.5
16.5	16.0	17.0	15.0	7.5	1.0
25.0	26.0	30.0	24.0	12.0	3.0

Table 39. Sample P2 Measurements

A	B	C	E	crystal size	zone width
38.0	33.5	43.0	38.0	18.6	2.5
12.0	14.0	16.0	12.5	5.9	1.7
14.5	15.0	17.0	14.5	7.3	1.3
20.5	14.0	21.5	18.5	8.2	1.3
13.0	14.5	16.0	14.5	7.3	0.8
29.0	23.0	32.5	27.0	12.3	2.5
19.0	31.5	33.5	28.0	10.9	2.1
13.0	12.0	16.0	12.5	5.6	1.6
27.5	28.0	27.0	23.0	11.5	2.0
11.5	16.0	17.0	14.0	6.4	1.4
14.0	15.0	18.0	14.0	6.6	1.9
16.0	21.0	23.0	18.0	8.2	2.3
24.0	17.0	26.0	21.5	9.4	2.0
17.5	22.0	24.0	21.0	10.0	1.4
26.0	23.0	30.0	24.0	11.5	2.9
45.0	33.0	50.0	47.0	20.3	1.3
19.5	18.5	23.5	17.5	8.3	2.8
15.0	14.0	18.0	15.0	7.0	1.4
20.5	20.5	20.5	18.0	9.0	1.3
24.0	30.0	33.0	29.0	13.7	1.9
29.5	32.5	38.0	32.0	15.3	2.9
28.0	22.5	32.0	27.0	12.1	2.2
31.0	31.0	39.0	33.5	15.4	2.5
21.0	24.0	30.0	26.5	10.9	1.4
16.5	22.0	25.5	21.0	8.6	1.8
10.5	13.5	16.0	13.0	5.3	1.2
35.5	35.0	39.5	35.5	17.8	2.0
14.5	18.0	20.5	17.5	7.9	1.4
23.5	26.0	31.0	25.5	11.7	2.5
16.0	15.0	19.5	17.5	8.0	0.9
18.0	15.0	20.0	15.5	7.5	2.2

Table 40. Sample P5 Measurements

A	B	C	E	crystal size	zone width
44.0	42.5	51.0	44.5	22.3	3.3
37.0	34.0	43.0	35.5	17.3	3.7
24.0	22.0	27.5	22.0	10.9	2.7
20.0	19.5	23.5	21.5	10.8	1.0
30.0	31.5	37.0	29.0	14.3	3.9
32.0	33.5	36.5	32.0	16.0	2.3
11.0	11.0	12.5	7.5	3.8	2.5
34.0	38.0	43.5	38.5	18.8	2.4
17.0	22.5	24.0	19.0	9.0	2.4
23.5	24.5	27.5	21.0	10.5	3.3
29.0	28.0	34.5	28.0	13.7	3.2
30.0	29.0	36.0	29.0	14.0	3.4
30.5	29.0	35.0	32.0	16.0	1.5
16.5	20.5	23.0	19.0	8.8	1.8
44.0	47.0	54.5	48.5	24.0	3.0
32.0	27.0	36.0	31.0	14.8	2.4
30.0	32.5	38.5	34.0	16.1	2.1
27.5	21.0	31.0	26.0	11.4	2.2
11.0	12.5	14.0	13.0	6.5	0.5
29.5	27.5	34.0	31.0	15.5	1.5
18.5	15.0	22.0	18.5	7.8	1.5
27.0	27.0	33.0	28.5	13.7	2.2
34.0	32.5	36.0	30.5	15.3	2.8
11.5	9.5	11.0	10.0	5.0	1.5
14.0	17.0	19.0	17.0	8.0	0.9
21.0	26.0	30.0	25.5	11.3	2.0
29.5	29.0	34.0	31.0	15.5	1.5
21.0	27.0	33.0	28.0	10.8	1.9
25.5	24.0	29.5	27.0	13.5	1.3
21.0	27.5	32.0	28.0	11.6	1.7

Table 41. Sample P17 Measurements

A	B	C	E	crystal size	zone width
20.0	20.0	22.5	18.0	9.0	2.3
17.0	22.5	25.5	22.0	9.4	1.5
27.0	34.0	37.0	28.0	13.4	4.3
41.5	42.0	50.0	41.0	20.4	4.5
25.5	25.0	29.5	22.0	11.0	3.8
32.5	32.5	39.0	32.5	16.1	3.2
35.0	29.0	41.5	33.5	14.5	3.5
29.5	27.5	33.0	27.5	13.8	3.5
27.5	24.0	31.0	25.0	12.2	2.9
39.0	37.5	44.0	37.0	18.5	3.5
20.0	13.0	21.5	18.5	7.6	1.2
22.5	20.5	22.5	19.0	9.5	4.1
21.0	15.0	22.5	15.5	6.9	3.1
28.0	19.0	29.0	26.0	11.7	1.4
33.0	29.0	39.5	36.0	16.1	1.6
21.0	22.0	28.5	23.5	9.9	2.1
26.5	28.0	33.5	28.5	13.6	2.4
17.0	13.0	19.5	16.5	7.0	1.3
34.5	22.0	35.5	30.0	12.9	2.4
21.0	16.0	24.0	17.5	7.5	2.8
17.0	12.0	19.0	14.5	6.0	1.9
42.5	55.0	60.5	52.0	23.9	3.9
19.5	17.5	21.5	17.5	8.8	2.4
23.5	21.5	27.0	22.0	10.9	2.5
25.5	27.0	29.0	24.0	12.0	2.5
19.0	23.0	26.0	20.5	9.5	2.6
25.5	21.0	35.0	28.5	9.2	2.1
22.0	24.0	27.0	21.5	10.8	3.0
16.0	15.5	18.0	15.0	7.5	1.5
15.5	14.5	17.5	15.0	7.5	1.3
41.0	45.0	61.0	50.0	18.4	4.1

Table 42. Sample P19 Measurements

A	B	C	E	crystal size	zone width
19.5	17.5	24.0	19.0	8.2	2.2
18.0	22.0	25.0	20.0	9.2	2.3
39.0	43.0	50.0	42.0	20.2	3.8
18.0	18.5	21.0	18.5	9.3	1.3
15.0	16.5	18.0	16.0	8.0	1.0
15.0	14.0	17.0	14.0	7.0	1.5
27.0	26.0	30.0	23.5	11.8	3.3
15.5	18.5	25.0	20.0	6.8	1.7
18.0	16.5	23.0	19.0	7.9	1.7
16.0	16.0	20.0	16.0	7.4	1.9
17.0	21.0	23.5	19.0	8.8	2.1
28.0	22.5	31.5	26.0	11.9	2.5
22.0	20.0	25.0	22.0	11.0	1.5
22.5	22.5	27.0	21.0	10.4	3.0
23.5	22.5	28.5	22.0	10.3	3.1
13.5	11.0	16.0	14.5	6.2	0.6
22.0	23.0	24.5	22.0	11.0	1.3
37.0	37.5	41.0	36.0	18.0	2.5
12.0	11.5	14.0	10.0	5.0	2.0
34.5	33.0	39.0	33.0	16.5	3.0
31.5	30.0	32.5	29.0	14.5	1.8
23.0	23.0	25.5	21.5	10.8	2.0
21.5	18.0	26.0	22.5	9.5	1.5
19.5	20.0	22.0	20.0	10.0	1.0
29.5	23.0	32.5	27.5	12.7	2.3
12.0	15.0	17.5	13.5	5.8	1.7
13.0	15.0	19.0	16.0	6.4	1.2
21.0	23.0	24.5	21.0	10.5	3.0
34.0	30.0	39.5	31.0	14.6	4.0
17.0	17.5	18.0	17.0	8.5	0.5

Table 43. Sample P27 Measurements

A	B	C	E	crystal size	zone width
33.0	24.0	36.0	31.0	13.7	2.2
42.0	43.0	44.5	40.0	20.0	2.3
42.0	43.0	45.0	40.0	20.0	2.5
22.0	24.0	24.0	19.5	9.8	4.8
26.0	23.5	30.0	25.0	12.1	2.4
26.0	25.0	31.0	26.0	12.6	2.4
27.0	21.0	30.0	25.0	11.4	2.3
21.5	21.0	24.8	19.0	9.5	2.9
24.0	18.5	28.0	20.5	8.5	3.1
27.0	34.0	39.5	32.0	13.8	3.2
27.0	31.0	39.0	31.5	12.8	3.0
24.5	30.0	33.5	29.5	13.9	1.9
15.0	16.5	18.0	13.0	6.5	2.5
27.5	28.5	34.0	30.0	14.6	1.9
28.5	30.5	40.0	33.0	13.3	2.8
28.0	24.0	33.0	27.5	12.3	2.5
25.0	27.0	31.5	28.0	13.6	1.7
34.5	33.5	42.5	38.0	17.6	2.1
24.5	24.5	24.0	19.5	9.8	2.3
23.5	16.5	25.5	23.0	9.9	1.1
35.5	37.5	42.5	37.5	18.8	3.3
27.5	26.0	33.0	27.5	13.0	2.6
22.5	20.5	25.5	21.0	10.5	2.3
10.5	11.5	14.5	11.0	4.6	1.5
13.5	11.5	16.0	13.0	5.8	1.3
40.0	38.5	47.5	41.0	20.0	3.2
9.0	11.5	13.5	10.0	4.2	1.5
38.0	40.0	45.0	40.0	20.0	3.6
14.5	16.0	19.0	16.0	7.4	1.4
10.5	12.0	12.0	9.0	4.5	1.5

Table 44. Sample P31 Measurements

A	B	C	E	crystal size	zone width
21.0	21.5	25.5	19.0	9.4	3.2
27.5	24.0	32.0	25.5	11.9	3.0
23.0	23.0	27.5	25.0	12.4	1.2
24.5	25.5	30.5	26.0	12.5	2.2
10.0	11.0	12.5	11.5	5.8	0.5
25.5	25.5	28.0	25.5	12.8	1.3
16.0	14.5	16.0	12.5	6.3	1.8
25.0	24.5	28.0	23.5	11.8	2.3
25.0	25.0	27.5	25.0	12.5	1.3
16.0	20.0	22.0	20.0	9.5	0.9
20.0	19.0	23.0	21.0	10.5	1.0
15.0	15.0	18.0	16.0	7.9	1.0
27.5	33.5	40.0	36.0	15.2	1.7
37.0	35.0	41.5	34.5	17.3	4.6
27.5	33.0	40.0	35.0	14.6	2.1
17.5	16.5	19.5	17.0	8.5	1.3
26.5	22.0	30.5	28.5	12.9	0.9
26.0	26.5	33.5	27.5	12.3	2.7
27.5	26.0	29.5	25.5	12.8	2.0
13.5	10.0	14.5	13.0	6.0	0.7
22.0	26.0	29.5	25.0	11.8	2.1
19.0	21.0	25.0	23.0	10.6	0.9
23.0	23.5	29.5	25.5	11.5	1.8
12.5	14.0	15.0	13.0	6.5	1.0
18.0	17.0	20.5	18.5	9.3	1.0
21.0	20.5	24.5	21.0	10.5	1.8
28.0	32.0	38.5	35.0	15.5	1.5
27.0	30.0	35.0	32.5	15.5	1.2
18.5	17.5	20.0	19.5	9.8	0.3
22.5	25.0	29.0	26.0	12.5	1.4
24.0	23.0	25.0	23.0	11.5	1.0

Table 45. Sample P34 Measurements

A	B	C	E	crystal size	zone width
30.0	22.0	32.0	26.0	12.0	2.8
31.0	25.0	35.0	31.5	14.4	1.6
31.0	30.0	35.0	29.0	14.5	3.0
27.0	23.0	31.5	25.0	11.4	3.0
27.0	23.0	30.0	24.0	11.8	2.9
30.0	24.5	38.5	31.0	11.4	2.8
18.0	20.0	24.5	19.0	8.3	2.4
27.0	31.0	43.0	39.0	13.1	1.3
13.5	14.5	15.5	12.5	6.3	1.5
20.5	19.0	24.0	22.0	10.7	1.0
43.0	34.0	60.0	54.5	16.1	1.6
19.5	27.0	32.0	24.5	9.3	2.9
21.0	25.5	29.0	25.0	11.5	1.8
20.0	24.0	27.5	21.5	9.9	2.8
13.5	13.0	15.5	13.5	6.8	1.0
13.0	16.5	18.5	12.0	5.4	2.9
19.5	20.0	24.0	17.0	8.3	3.4
20.0	20.0	24.0	16.5	8.2	3.7
13.5	17.0	19.5	16.5	7.2	1.3
42.0	43.5	53.0	42.5	20.0	4.9
17.5	23.0	25.0	22.0	10.2	1.4
26.0	23.5	31.0	23.5	10.8	3.5
29.5	22.0	32.0	25.0	11.4	3.2
21.5	23.5	26.0	23.0	11.5	2.1
17.5	19.5	21.5	18.0	9.0	2.1
35.5	35.0	34.0	28.5	14.3	2.8
21.0	20.5	22.0	19.0	9.5	1.5
25.5	34.5	43.0	30.0	10.6	4.6
18.0	18.5	21.0	17.5	8.8	1.8
12.5	11.0	12.0	8.5	4.3	1.8

Table 46. Sample P36 Measurements

A	B	C	E	crystal size	zone width
30.5	25.5	36.0	30.0	13.1	2.6
22.0	24.0	25.5	20.0	10.0	4.2
33.5	38.5	44.5	37.5	17.6	3.3
22.0	23.0	26.5	20.5	10.3	3.0
39.5	41.0	47.0	39.0	19.5	4.0
29.0	22.0	32.0	26.0	11.7	2.7
18.0	19.0	24.0	19.0	8.3	2.2
14.0	14.0	16.5	13.0	6.5	1.8
15.0	13.0	16.0	13.5	6.8	1.7
22.5	23.5	26.0	22.5	11.3	1.8
37.0	42.0	51.0	43.0	18.8	3.5
26.5	25.0	29.0	21.5	10.8	3.8
38.0	30.5	46.5	36.0	14.3	4.2
19.5	13.0	23.0	17.0	6.0	2.1
14.0	12.0	13.5	11.0	5.5	2.7
16.5	20.0	24.5	21.5	8.7	1.2
35.0	30.0	39.0	31.0	15.2	3.9
14.0	14.0	15.0	12.0	6.0	1.5
18.5	17.0	26.5	15.5	5.1	3.6
34.0	30.5	41.0	34.5	15.5	2.9
25.0	20.0	27.5	23.0	10.9	2.1
13.0	19.5	21.0	17.0	7.1	1.7
40.0	37.0	48.0	40.5	18.8	3.5
26.5	23.0	31.0	25.0	11.5	2.8
14.0	13.5	16.0	12.5	6.3	1.8
13.0	12.0	15.5	14.0	6.6	0.7
16.0	20.0	24.0	19.5	8.0	1.8
21.5	20.5	25.0	23.5	11.8	0.8
14.5	12.5	16.5	13.5	6.4	1.4
21.5	21.0	23.0	19.5	9.8	1.8
24.0	23.0	26.5	21.0	10.5	2.8
8.0	7.5	9.0	7.0	3.5	1.0
17.0	17.0	18.5	16.0	8.0	1.3
15.0	16.0	18.0	15.0	7.5	1.5
36.5	36.0	44.0	35.5	17.3	4.1
26.5	29.5	35.0	28.0	12.9	3.2
23.0	20.5	27.0	21.5	10.0	2.6

Table 46 (cont'd).

A	B	C	E	crystal size	zone width
28.5	27.5	34.5	26.0	12.3	4.0
20.0	22.0	26.5	20.0	9.1	3.0

Table 47. Sample P37 Measurements

A	B	C	E	crystal size	zone width
33.0	35.0	39.0	34.0	17.0	3.7
49.0	48.5	59.5	51.0	24.6	4.1
28.5	26.0	35.0	26.0	11.5	4.0
12.0	14.0	15.0	12.0	6.0	1.8
29.0	27.0	31.0	22.0	11.0	6.3
35.0	34.0	39.5	33.0	16.5	3.3
37.0	35.0	41.0	30.0	15.0	7.0
36.0	41.0	48.0	35.0	16.2	6.0
15.5	16.5	19.5	16.0	7.7	1.7
49.0	51.0	69.0	52.0	20.2	6.6
22.5	22.0	28.5	21.5	9.6	3.1
38.0	47.0	56.0	40.0	16.7	6.7
11.0	10.5	14.0	6.0	2.6	3.5
52.0	35.0	55.0	39.0	16.9	6.9
28.0	28.0	32.5	23.0	11.5	4.8
27.0	23.0	31.5	26.0	11.8	2.5
48.5	42.0	55.0	40.0	19.3	7.2
28.0	26.0	32.0	25.0	12.5	3.6
28.5	27.5	33.0	26.0	13.0	3.5
54.0	52.0	57.0	52.0	26.0	7.2
40.0	44.0	52.0	44.0	20.7	3.8
15.0	13.5	16.5	14.0	7.0	1.3
24.0	24.0	25.0	21.0	10.5	2.0
27.0	24.0	32.0	20.0	9.2	5.5
25.5	22.0	31.0	24.0	10.3	3.0
13.0	15.0	18.0	14.0	6.2	1.8
8.0	8.0	10.5	7.5	3.2	1.3
8.0	9.5	10.0	6.0	3.0	2.0
12.0	10.0	12.5	8.0	4.0	2.6
18.0	20.5	24.0	17.5	8.1	3.0
22.0	21.5	22.0	16.0	8.0	3.0
18.0	18.5	20.0	13.0	6.5	3.5
17.0	16.0	20.5	14.0	6.6	3.0
35.5	43.0	49.0	34.5	15.8	6.7
21.0	22.0	22.0	15.5	7.8	3.3
14.0	14.5	18.0	13.0	5.9	2.3
24.5	24.0	28.5	17.5	8.8	5.5

Table 48. Sample P40 Measurements

A	B	C	E	crystal size	zone width
18.5	13.5	20.0	15.5	7.0	2.0
11.0	10.5	10.0	9.0	4.5	0.5
15.5	13.5	18.0	15.0	7.0	1.4
18.0	17.0	19.0	14.5	7.3	2.3
18.5	20.0	24.0	18.5	8.6	2.6
15.5	16.0	18.0	14.5	7.3	1.8
18.0	15.0	20.0	17.0	8.2	1.4
25.0	30.0	33.5	28.5	13.6	2.4
13.0	15.0	18.5	15.5	6.5	1.3
17.5	23.5	25.5	20.0	9.1	2.5
16.0	14.5	17.5	15.5	7.8	1.0
24.0	30.5	35.5	29.0	12.3	2.8
22.0	27.5	30.0	22.0	10.5	3.8
26.0	25.5	27.0	22.0	11.0	2.5
25.5	25.5	30.0	25.0	12.5	2.5
19.0	18.0	23.0	16.0	7.5	3.3
17.5	11.5	19.5	15.0	5.8	1.8
21.5	21.0	24.5	21.0	10.5	1.8
14.5	14.0	16.5	12.5	6.3	2.0
12.5	13.0	15.0	10.0	5.0	2.5
10.0	12.0	12.5	8.5	4.3	2.4
15.5	18.5	20.5	13.5	6.6	3.4
16.5	12.0	19.0	15.0	6.1	1.6
19.2	19.5	23.5	17.5	8.5	2.9
15.5	15.5	18.5	14.0	7.0	2.2
14.5	13.0	17.5	14.0	6.3	1.6
14.5	13.5	17.5	14.5	6.7	1.4
9.0	14.0	15.0	10.0	4.1	2.0
23.0	21.0	24.0	18.0	9.0	4.6
24.0	17.5	26.0	19.5	8.7	2.9
33.0	27.5	38.5	30.0	13.4	3.8
16.5	18.5	20.0	15.5	7.8	2.9
29.0	34.0	38.5	32.0	15.3	3.1
22.5	23.5	24.5	20.5	10.3	2.0

Table 49. Sample P41 Measurements

A	B	C	E	crystal size	zone width
15.5	15.0	18.5	14.0	6.8	2.2
10.0	11.0	13.0	11.5	5.4	0.7
25.0	23.0	28.5	23.0	11.5	2.8
25.0	29.5	38.0	31.0	11.8	2.7
21.0	26.0	29.0	22.5	10.5	3.0
32.5	40.0	55.5	42.5	13.1	4.0
25.5	21.5	28.5	20.5	9.9	3.9
34.0	38.5	43.5	36.5	18.0	3.4
12.0	11.0	13.0	10.0	5.0	1.5
16.5	16.5	20.5	14.5	6.8	2.8
17.0	20.5	23.5	20.0	9.1	1.6
19.5	19.5	23.5	19.5	9.6	2.0
24.5	22.5	27.0	20.0	10.0	4.2
12.0	20.0	20.5	16.0	6.6	1.8
16.5	16.5	19.5	16.5	8.3	1.5
11.5	12.0	13.5	11.0	5.5	1.3
12.5	20.0	20.5	17.0	7.2	1.5
28.0	31.0	36.5	30.5	14.3	2.8
24.0	25.5	29.5	22.0	11.0	3.8
22.5	24.0	28.0	22.0	10.8	2.9
29.5	26.5	35.5	28.0	12.6	3.4
25.0	28.5	33.0	24.5	11.5	4.0
15.5	14.0	15.5	10.5	5.3	2.5
29.0	28.0	35.0	25.0	11.9	4.8
29.0	32.0	40.5	31.0	12.9	4.0
16.5	14.5	18.5	15.0	7.5	1.7
15.0	14.0	16.0	11.0	5.5	2.5
11.0	11.5	13.5	8.0	4.0	2.7
20.5	22.0	24.5	20.0	10.0	2.3
28.0	29.0	32.5	23.5	11.8	4.5
13.5	13.5	16.5	11.0	5.3	2.6
17.5	17.5	19.0	13.0	6.5	3.0
33.0	28.5	37.0	28.5	13.9	4.2
22.5	20.5	26.5	23.5	11.1	1.4
19.0	20.5	23.0	18.0	9.0	2.5
25.5	23.5	26.0	18.0	9.0	6.4

Table 50. Sample P45 Measurements

A	B	C	E	crystal size	zone width
16.5	16.5	20.0	15.0	7.3	2.4
24.0	23.0	24.0	18.0	9.0	3.0
26.5	23.0	34.5	27.0	10.3	2.9
20.5	18.5	23.5	19.0	9.3	2.2
16.0	15.0	16.5	13.5	6.8	1.5
13.5	11.5	14.5	11.5	5.8	1.7
35.5	35.5	41.5	36.0	18.0	2.8
33.0	34.0	47.0	40.0	15.1	2.6
14.0	16.0	19.0	14.5	6.5	2.0
22.0	19.0	26.0	20.0	9.0	2.7
24.8	23.5	29.0	24.0	11.9	2.5
28.5	23.5	33.0	26.5	11.8	2.9
20.5	21.5	24.5	20.0	10.0	2.3
24.0	22.0	27.5	23.0	11.4	2.2
28.0	26.0	35.0	22.0	9.6	5.7
41.5	34.0	47.0	39.0	18.0	3.7
16.0	14.0	17.5	15.5	7.8	1.2
26.5	28.0	35.0	27.0	12.0	3.5
12.5	14.0	18.0	13.0	5.2	2.0
27.0	28.0	35.0	28.0	12.6	3.1
7.5	8.0	9.5	7.5	3.6	1.0
21.0	19.5	25.5	18.5	8.5	3.2
22.0	24.0	28.0	23.0	11.1	2.4
29.0	24.0	32.5	24.0	11.3	4.0
27.0	26.0	35.0	24.0	10.1	4.6
41.0	35.0	47.0	38.0	17.8	4.2
21.0	20.5	22.5	19.0	9.5	1.8
13.5	19.0	20.5	10.0	4.4	4.6
12.0	9.5	13.0	10.5	5.0	1.2
24.0	22.5	28.0	21.5	10.6	3.2
27.5	26.5	32.5	22.0	10.8	5.2
13.5	15.5	17.0	12.0	6.0	2.7
23.5	27.0	33.5	27.5	11.5	2.5

Table 51. Sample List for Saluda Formation Hwy 7 and Hwy 56 Outcrops

Sample Number	Sample ID	Number of Crystals
1	Sal R-1	37
2	Sal R-5	33
3	Sal R-10	30
4	Sal D-25	30
5	Sal D-34	30
6	Sal A-1d	32
7	Sal A-5d	30
8	Sal A-7d	45
9	Sal A-5g	30
10	Sal A-7g	30
11	Sal 56-1	31
12	Sal 56-5	30
13	Sal Pay-1	30
14	Sal Pay-5	34
15	Sal Pay-11	30
16	Sal Ton-11	54
17	Sal How-1	33
18	Sal How-6	30
19	Sal 7-8	30

Table 52. Sample Sal R-1 Measurements

A	B	C	E	crystal size	zone width
17.0	16.0	19.0	15.0	7.5	2.0
25.5	32.0	36.0	30.0	13.6	2.7
28.0	28.0	30.5	25.0	12.5	2.8
32.0	24.5	36.0	33.0	14.5	1.3
31.0	25.0	34.5	29.5	13.8	2.3
13.0	16.0	18.0	16.5	7.6	0.7
8.0	8.0	9.5	8.0	4.0	0.8
10.5	11.0	13.0	12.0	5.9	0.5
17.5	19.5	23.0	18.0	8.4	2.3
26.0	23.0	30.0	23.0	11.0	3.3
9.5	10.5	13.0	10.5	4.5	1.1
21.0	21.0	25.0	21.0	10.5	2.0
28.0	25.5	33.0	22.5	10.6	5.0
35.0	32.0	40.5	33.0	16.1	3.7
32.0	34.0	39.0	29.0	14.5	5.2
23.0	19.5	26.5	20.0	9.2	3.0
25.5	25.5	31.0	23.5	11.4	3.6
34.0	35.0	40.5	33.5	16.8	3.5
27.5	19.5	29.0	24.0	10.9	2.3
22.0	22.5	26.0	22.0	11.0	2.0
11.5	9.5	12.5	9.0	4.5	1.7
22.5	21.0	26.0	15.5	7.7	5.2
39.0	39.5	53.5	45.5	18.1	3.2
27.0	19.5	29.0	20.5	9.2	3.8
27.0	24.0	32.0	27.0	12.4	2.3
25.0	18.5	29.0	21.5	8.7	3.0
22.5	21.5	26.0	19.5	9.8	3.3
34.0	32.0	36.5	31.0	15.5	4.9
21.0	15.0	23.0	16.0	6.9	3.0
25.5	24.5	30.5	22.0	10.6	4.1
11.5	16.5	20.0	15.0	5.3	1.8
33.5	34.5	39.5	30.0	15.0	4.8
22.5	19.5	26.0	21.5	10.1	2.1
24.0	24.5	29.5	23.0	11.1	3.1
26.0	19.5	29.5	23.5	10.0	2.6
21.5	22.5	25.5	21.0	10.5	2.3
18.5	20.5	21.5	15.5	7.8	4.3

Table 53. Sample Sal R-5 Measurements

A	B	C	E	crystal size	zone width
16.0	19.0	22.0	17.0	7.7	2.3
18.0	16.0	23.0	18.0	7.2	2.0
19.0	18.0	21.0	16.5	8.3	2.3
28.0	31.0	40.5	27.0	10.6	5.3
28.0	43.0	45.5	35.5	14.9	4.2
14.5	15.5	18.0	13.0	6.4	2.5
21.0	20.0	22.0	16.5	8.3	2.8
17.5	18.0	20.0	18.0	9.0	1.0
16.0	16.0	18.0	14.0	7.0	2.0
18.0	17.5	19.0	15.0	7.5	2.0
8.5	10.0	11.5	9.0	4.2	1.2
17.0	18.0	19.0	15.0	7.5	2.0
21.0	24.0	28.0	24.5	11.4	1.6
13.0	15.0	16.0	14.0	7.0	1.5
16.0	17.5	21.0	16.0	7.4	2.3
27.0	27.5	29.0	26.0	13.0	1.5
21.0	20.5	25.0	20.5	10.1	2.2
21.5	21.5	24.5	19.0	9.5	2.8
21.5	20.5	23.5	16.0	8.0	3.8
16.5	19.0	22.0	20.0	9.3	0.9
27.0	27.5	31.0	26.5	13.3	2.3
24.5	18.0	26.0	21.5	10.0	2.1
30.0	26.0	34.5	29.0	13.7	2.6
16.5	15.0	17.5	15.0	7.5	1.3
25.0	23.5	32.5	24.5	10.1	3.3
14.5	14.5	16.0	11.5	5.8	2.3
23.0	31.0	35.0	24.5	10.4	4.5
21.0	19.5	27.0	17.0	7.0	4.1
28.0	27.5	36.0	28.0	12.2	3.5
26.5	24.0	31.0	25.5	12.1	2.6
36.0	34.0	38.0	30.5	15.3	6.5
19.0	16.5	23.0	21.0	9.1	0.9
30.0	26.0	37.0	29.5	12.4	3.1

Table 54. Sample Sal R-10 Measurements

A	B	C	E	crystal size	zone width
16.0	17.0	21.0	18.0	8.1	1.3
17.0	18.0	18.5	16.0	8.0	1.3
20.5	22.0	25.0	21.0	10.5	2.0
22.0	16.0	25.5	21.0	8.4	1.8
23.0	19.5	26.5	23.0	10.6	1.6
10.0	11.0	12.0	10.0	5.0	1.0
36.0	34.0	41.0	37.0	18.5	2.5
16.5	19.0	22.0	19.0	8.9	1.4
30.5	33.0	41.0	33.0	14.5	3.5
28.5	28.0	35.5	26.0	12.0	4.4
35.0	36.0	44.0	41.0	19.3	1.4
33.5	33.5	41.0	37.0	17.8	1.9
10.0	9.5	10.5	7.5	3.8	1.5
31.0	33.5	39.0	33.5	16.4	2.7
28.5	29.0	32.0	27.5	13.8	2.3
15.0	19.0	21.0	13.5	6.3	3.5
32.5	35.0	41.5	36.0	17.1	2.6
28.5	30.0	31.0	25.0	12.5	3.0
31.5	26.0	35.0	27.5	13.1	3.6
21.0	25.5	28.0	23.0	11.2	2.4
21.0	21.0	24.0	17.5	8.8	3.3
40.0	41.5	49.0	42.0	20.7	3.5
17.0	17.5	21.0	16.0	7.7	2.4
32.0	21.5	34.5	30.0	12.6	1.9
27.0	27.0	33.5	27.0	12.7	3.1
40.5	42.0	51.0	40.0	18.9	5.2
25.5	22.0	29.5	26.5	12.3	1.4
45.0	47.0	52.5	44.0	22.0	6.0
28.5	30.5	29.0	26.0	13.0	6.0
40.0	38.0	39.0	32.0	16.0	9.1

Table 55. Sample Sal D-25 Measurements

A	B	C	E	crystal size	zone width
26.5	18.0	27.5	22.5	10.1	2.2
24.0	29.5	34.0	28.5	12.7	2.4
17.0	16.5	19.0	17.0	8.5	1.0
41.0	38.0	47.5	38.0	18.7	4.7
26.5	24.5	31.0	24.5	11.9	3.1
18.0	16.0	20.0	16.5	8.3	1.9
41.5	48.0	54.0	45.0	21.9	4.4
21.0	19.0	24.5	20.0	9.6	2.1
21.0	22.5	25.0	22.5	11.3	1.3
27.5	28.0	29.0	25.5	12.8	1.8
12.5	14.0	16.0	13.5	6.6	1.2
21.5	21.0	28.5	25.0	10.3	1.4
26.0	24.0	30.0	25.5	12.6	2.2
13.0	14.5	16.5	14.0	6.9	1.2
28.0	29.0	33.0	30.0	15.0	1.5
25.5	22.5	30.0	23.0	10.6	3.2
25.5	16.5	27.0	21.0	8.8	2.5
19.5	22.0	25.0	20.5	10.0	2.2
22.0	22.0	25.5	21.5	10.8	2.0
15.5	14.0	19.0	16.5	7.3	1.1
31.5	30.0	41.0	33.5	13.9	3.1
39.5	37.5	44.0	39.0	19.5	3.9
34.0	28.5	38.0	31.5	15.1	3.1
19.5	24.5	27.0	20.5	9.6	3.1
24.0	23.5	32.0	28.5	11.6	1.4
21.0	22.0	25.0	20.5	10.3	2.3
16.5	18.5	19.0	14.0	7.0	3.9
9.0	8.5	11.5	7.0	3.0	1.9
26.0	18.0	27.5	21.5	9.5	2.7
24.0	23.5	28.0	26.5	13.3	0.8

Table 56. Sample Sal D-34 Measurements

A	B	C	E	crystal size	zone width
16.0	19.5	22.0	17.5	8.1	2.1
33.5	36.0	43.0	34.5	16.2	4.0
34.0	35.5	48.0	38.0	14.8	3.9
20.5	20.0	27.0	21.5	8.9	2.3
22.5	22.0	26.0	22.0	11.0	2.0
53.0	49.0	68.5	51.0	20.9	7.2
34.0	35.0	39.5	29.0	14.5	5.3
26.0	17.0	27.5	22.5	9.5	2.1
29.5	26.0	37.0	34.0	14.1	1.2
13.0	11.5	14.5	9.0	4.5	2.8
14.5	13.0	16.0	11.5	5.8	2.3
25.5	24.0	29.0	24.0	12.0	2.5
25.5	35.5	38.5	33.0	14.5	2.4
14.0	14.5	18.5	18.0	7.8	0.2
25.5	35.0	40.5	33.0	13.2	3.0
33.0	23.0	37.5	29.5	11.7	3.2
20.0	20.0	23.0	14.5	7.3	4.3
44.5	42.0	56.5	45.5	19.6	4.7
21.0	32.0	34.0	23.5	9.9	4.4
39.0	40.0	48.0	37.5	18.2	5.1
21.0	15.5	25.0	19.0	7.3	2.3
39.0	42.5	49.5	43.0	20.8	3.1
20.0	18.0	32.0	26.0	6.2	1.4
21.5	23.0	31.0	23.0	8.8	3.1
32.5	32.0	36.5	32.5	16.3	2.0
35.0	34.0	41.0	32.0	16.0	4.5
47.0	49.0	58.5	50.0	24.1	4.1
39.0	39.0	46.0	38.5	19.3	3.8
16.0	16.0	19.0	15.5	7.8	1.8
15.5	13.5	17.0	12.5	6.3	2.4

Table 57. Sample Sal A-1d Measurements

A	B	C	E	crystal size	zone width
19.5	20.0	21.0	17.5	8.8	1.8
28.5	23.5	32.5	26.0	11.9	3.0
21.5	22.0	24.0	18.5	9.3	2.8
48.5	41.0	56.0	46.0	21.1	4.6
31.5	30.5	37.5	30.0	14.7	3.7
29.5	22.0	32.0	27.0	12.3	2.3
36.0	23.0	45.0	30.5	9.2	4.4
24.5	19.0	29.0	22.0	9.0	2.9
21.5	20.0	25.0	19.0	9.3	2.9
27.0	25.0	31.0	24.0	12.0	3.5
30.5	32.0	37.0	25.0	12.5	6.0
19.5	24.0	29.5	24.0	9.5	2.2
28.0	17.0	29.0	25.0	10.2	1.6
22.0	14.0	24.5	18.0	6.8	2.5
15.0	14.0	16.5	11.0	5.5	2.8
15.0	19.0	22.0	15.5	6.7	2.8
22.0	28.0	35.0	25.5	9.5	3.5
25.5	23.0	33.5	26.0	10.1	2.9
49.5	33.0	53.0	40.0	16.8	5.5
18.0	16.5	20.0	17.0	8.5	1.5
24.5	16.5	28.0	20.0	7.6	3.0
20.0	24.5	31.5	26.0	9.5	2.0
20.5	24.5	32.0	27.0	9.8	1.8
19.0	17.0	20.0	16.5	8.3	2.8
12.5	11.0	13.5	11.0	5.5	1.3
19.5	21.0	20.0	15.5	7.8	2.3
16.0	16.0	22.0	18.0	7.1	1.6
20.5	20.5	24.0	20.5	10.3	1.8
22.0	28.0	33.5	24.0	9.7	3.8
19.5	15.5	24.5	21.5	8.0	1.1
31.0	24.5	36.0	30.0	12.9	2.6
8.0	12.0	14.5	10.0	3.4	1.5

Table 58. Sample Sal A-5d Measurements

A	B	C	E	crystal size	zone width
32.0	31.5	32.0	31.0	15.5	0.5
11.0	11.0	12.0	9.5	4.8	1.3
11.5	10.5	12.5	11.0	5.5	0.8
17.0	19.0	20.0	17.0	8.5	2.6
12.0	12.5	15.5	12.5	5.7	1.4
26.5	25.0	32.5	26.5	12.1	2.7
20.0	20.0	23.0	19.0	9.5	2.0
17.0	15.0	20.0	16.5	7.6	1.6
37.5	33.5	42.5	40.0	19.8	1.2
16.0	15.0	19.0	15.5	7.4	1.7
10.5	14.5	16.0	13.5	5.8	1.1
25.0	23.5	28.0	25.5	12.8	1.3
15.5	16.0	18.0	16.5	8.3	0.8
23.0	25.0	27.0	22.5	11.3	3.4
34.0	38.0	44.5	41.0	19.3	1.6
17.5	18.0	24.0	20.0	8.1	1.6
20.0	18.0	23.0	19.5	9.5	1.7
51.0	49.0	64.0	50.0	22.3	6.2
31.0	34.0	41.0	33.5	15.3	3.4
18.0	16.0	24.5	18.0	6.4	2.3
31.0	34.5	42.0	34.0	15.1	3.5
19.5	20.0	25.5	19.5	8.6	2.6
16.5	17.0	21.5	16.0	7.1	2.4
17.0	23.0	28.0	23.5	8.7	1.7
19.5	19.0	26.0	20.5	8.3	2.2
31.0	34.5	41.0	34.0	15.7	3.2
29.5	36.0	43.0	34.0	14.3	3.8
24.5	19.5	28.5	19.5	8.4	3.9
18.5	18.5	20.5	16.0	8.0	2.3
16.0	17.0	22.5	16.5	6.6	2.4

Table 59. Sample Sal A-7d Measurements

A	B	C	E	crystal size	zone width
29.0	24.0	32.5	28.0	13.2	2.1
16.5	21.5	24.5	18.5	8.0	2.6
26.0	22.0	29.0	22.5	10.9	3.2
32.0	28.0	36.0	27.5	13.5	4.2
23.5	16.0	26.0	20.0	8.1	2.4
29.0	28.0	32.0	26.5	13.3	2.8
16.0	16.5	19.0	14.0	7.0	2.5
15.5	20.5	22.0	18.5	8.7	1.6
23.5	23.0	28.0	23.0	11.3	2.5
38.0	38.0	44.0	35.5	17.8	4.3
28.5	28.5	31.5	26.0	13.0	2.8
19.5	18.0	22.0	18.0	9.0	2.0
28.0	32.0	37.0	29.0	13.7	3.8
20.5	13.5	22.0	16.5	6.8	2.3
16.0	15.5	18.5	15.0	7.5	1.8
26.0	25.5	32.0	25.5	11.9	3.0
26.0	23.0	31.5	23.0	10.1	3.7
12.5	14.0	15.5	12.5	6.3	1.5
25.0	21.5	28.0	23.5	11.5	2.2
16.0	18.0	18.5	13.5	6.8	3.8
15.5	17.5	19.5	16.5	8.3	1.6
30.0	29.5	33.0	24.5	12.3	4.3
20.0	21.0	25.0	18.0	8.7	3.4
22.5	21.5	23.5	18.5	9.3	2.5
30.0	32.0	37.0	29.0	14.5	3.9
11.5	14.5	16.0	11.0	5.1	2.3
32.5	36.0	41.0	33.0	16.3	4.0
16.5	16.0	20.5	17.0	7.8	1.6
17.5	19.0	21.5	17.0	8.5	2.3
20.5	30.0	37.5	29.0	9.4	2.8
24.5	24.0	28.5	25.0	12.5	1.8
36.5	35.0	39.0	32.5	16.3	3.3
30.0	22.0	32.0	26.0	12.0	2.8
17.0	20.0	24.0	16.5	7.1	3.2
19.5	18.0	23.0	17.5	8.4	2.6
36.5	37.5	40.5	31.5	15.8	4.5
17.0	16.0	20.0	16.5	8.0	1.7

Table 59 (cont'd).

A	B	C	E	crystal size	zone width
25.0	20.0	27.5	22.0	10.4	2.6
28.0	25.0	32.0	24.0	11.7	3.9
28.5	28.0	34.0	28.5	14.0	2.7
28.0	27.0	32.0	26.0	13.0	3.0
31.0	25.0	36.0	30.0	13.1	2.6
36.0	35.0	42.5	33.5	16.6	4.5
31.0	32.0	41.0	33.0	14.3	3.5
36.0	31.0	43.0	33.5	14.8	4.2

Table 60. Sample Sal A-5g Measurements

A	B	C	E	crystal size	zone width
9.5	11.5	13.5	12.5	5.5	0.4
37.5	34.5	45.5	37.5	17.0	3.6
24.0	26.0	28.5	20.5	10.3	5.0
39.0	35.0	46.0	36.0	16.8	4.7
13.5	8.5	14.5	9.5	3.8	2.0
43.5	42.0	53.0	43.0	20.2	4.7
14.5	16.5	17.0	12.5	6.3	3.3
13.0	15.0	15.5	11.0	5.5	3.1
32.5	35.5	41.0	35.0	17.2	2.9
29.0	30.5	35.0	29.0	14.5	3.0
49.0	50.0	61.0	49.0	23.3	5.7
15.0	15.0	15.5	11.5	5.8	2.0
30.5	29.5	27.5	22.0	11.0	2.8
49.5	50.5	62.0	49.0	23.0	6.1
17.5	17.0	20.0	14.5	7.3	2.8
44.0	45.5	45.5	38.5	19.3	3.5
17.5	17.5	19.0	15.0	7.5	2.0
27.0	26.5	33.0	23.0	10.9	4.7
10.5	12.5	13.0	9.5	4.8	2.2
25.5	22.5	32.0	24.0	9.9	3.3
18.0	22.5	26.0	22.0	9.6	1.7
34.5	39.0	47.0	33.0	14.7	6.2
33.0	35.0	41.0	35.0	17.2	2.9
29.0	39.0	47.5	31.5	11.7	5.9
19.0	16.5	22.0	16.0	7.5	2.8
15.5	17.0	21.0	15.5	6.8	2.4
10.0	16.5	17.0	13.5	5.5	1.4
18.0	19.5	22.5	20.0	9.9	1.2
27.0	27.0	36.0	28.0	11.6	3.3
28.0	27.5	35.0	30.0	13.7	2.3

Table 61. Sample Sal A-7g Measurements

A	B	C	E	crystal size	zone width
19.5	17.0	22.0	19.5	9.5	1.2
33.0	32.0	44.0	29.5	11.9	5.9
18.5	17.0	21.5	18.0	8.8	1.7
10.0	12.0	12.0	9.5	4.8	2.0
9.5	9.0	12.0	9.5	4.1	1.1
15.0	17.0	20.0	19.0	8.8	0.5
17.5	18.5	19.5	16.5	8.3	1.5
11.5	13.5	12.5	11.0	5.5	2.4
28.0	28.5	33.0	28.5	14.3	2.3
11.0	10.5	13.0	11.5	5.6	0.7
17.0	17.5	19.0	14.0	7.0	2.5
30.5	30.5	35.0	28.5	14.3	3.3
20.5	21.0	24.0	20.5	10.3	1.8
17.5	16.5	20.0	17.5	8.8	1.3
12.0	10.0	12.5	11.0	5.5	1.1
24.0	19.0	29.0	24.5	9.8	1.8
14.5	15.5	17.0	15.5	7.8	0.8
13.0	12.0	14.0	13.0	6.5	0.5
29.5	23.5	32.0	28.5	13.7	1.7
21.0	21.0	24.5	18.5	9.3	3.0
18.5	19.0	23.0	18.5	8.8	2.2
11.5	12.5	16.5	12.5	4.9	1.6
21.5	21.0	24.5	19.5	9.8	2.5
26.0	25.0	30.5	27.0	13.4	1.7
21.0	24.0	28.0	23.0	10.7	2.3
25.5	22.5	29.5	23.5	11.1	2.8
28.5	32.0	39.0	36.5	16.0	1.1
12.0	12.0	14.5	12.5	6.1	1.0
20.0	21.0	23.0	19.0	9.5	2.0
21.0	19.0	23.0	20.5	10.3	1.9

Table 62. Sample Sal 56-1 Measurements

A	B	C	E	crystal size	zone width
27.5	29.0	31.0	24.5	12.3	3.3
26.5	24.5	31.0	26.0	12.6	2.4
26.0	22.5	30.0	25.0	11.7	2.3
37.5	30.5	46.5	40.5	15.9	2.4
14.5	16.5	20.5	15.0	6.3	2.3
16.0	17.5	19.5	15.0	7.5	2.3
44.0	49.0	59.0	48.5	21.9	4.7
19.0	18.5	21.0	15.0	7.5	3.0
24.5	17.0	26.0	21.5	9.5	2.0
10.0	11.0	12.0	9.5	4.8	1.3
20.5	22.5	26.0	21.5	10.5	2.2
26.5	30.5	35.0	28.0	13.3	3.3
23.5	27.0	30.5	22.5	11.0	3.9
13.5	13.0	16.0	12.0	5.9	2.0
9.5	10.0	13.0	9.5	3.9	1.5
13.5	16.5	22.0	16.5	5.6	1.9
17.5	17.0	22.5	17.5	7.6	2.2
23.0	27.5	31.5	25.0	11.5	3.0
38.5	40.0	52.0	41.0	17.2	4.6
48.0	37.5	56.0	45.0	18.9	4.6
27.0	27.0	32.0	27.0	13.5	2.5
13.5	15.0	17.5	13.5	6.4	1.9
19.0	18.5	21.5	18.5	9.3	1.5
31.0	35.5	40.0	34.5	16.9	2.7
12.0	10.5	13.0	10.5	5.3	1.3
27.5	28.0	34.0	23.5	11.3	5.0
13.5	15.0	15.5	12.0	6.0	1.8
28.0	28.0	34.5	29.5	14.0	2.4
32.0	29.0	37.0	33.0	16.0	1.9
9.0	11.0	12.0	11.0	5.5	0.4
22.5	25.0	33.0	26.0	10.0	2.7

Table 63. Sample Sal 56-5 Measurements

A	B	C	E	crystal size	zone width
22.5	15.0	28.0	14.0	4.5	4.5
40.0	38.0	46.0	40.0	20.0	3.4
14.5	15.0	19.0	12.0	5.3	3.1
19.0	18.5	22.5	13.0	6.4	4.7
40.0	40.0	48.0	30.0	14.9	8.9
22.0	16.0	27.0	14.0	5.0	4.7
30.0	31.0	39.0	28.5	12.7	4.7
16.5	17.0	20.0	10.0	5.0	5.0
25.5	29.0	34.5	23.0	10.4	5.2
29.5	27.5	38.5	21.0	8.5	7.1
8.5	10.0	12.0	8.0	3.5	1.7
12.0	12.0	15.5	8.5	3.7	3.1
30.0	26.0	38.5	31.0	12.1	2.9
22.5	20.0	27.5	22.0	9.6	2.4
23.5	27.0	34.5	26.0	10.3	3.4
14.5	15.0	17.0	13.5	6.8	1.8
29.0	25.5	34.5	20.0	9.0	6.6
11.0	10.5	13.5	8.5	3.9	2.3
10.5	10.0	12.0	8.5	4.3	1.8
31.0	38.0	42.0	32.0	15.3	4.8
7.5	6.5	8.5	5.0	2.4	1.7
24.0	24.5	34.0	27.0	10.2	2.6
24.0	23.0	26.5	20.0	10.0	3.3
16.5	19.0	23.0	12.0	5.2	4.8
25.0	28.0	32.0	24.0	11.7	3.9
23.0	20.5	26.5	21.5	10.3	2.4
25.0	18.5	32.5	23.5	7.6	2.9
24.5	26.5	31.5	26.5	12.5	2.4
23.0	22.0	28.5	23.0	10.4	2.5
17.5	16.0	20.0	11.0	5.5	4.5

Table 64. Sample Pay-1 Measurements

A	B	C	E	crystal size	zone width
11.5	9.0	14.0	12.0	4.7	0.8
12.5	15.0	17.0	15.5	7.2	0.7
18.0	17.0	22.0	19.0	8.7	1.4
26.0	32.5	36.0	30.5	14.3	2.6
19.5	19.0	22.5	20.5	10.3	1.0
10.5	11.0	12.5	10.0	5.0	1.3
28.0	26.0	32.0	28.0	14.0	2.1
15.0	15.5	20.0	18.0	7.7	0.9
26.5	20.5	28.5	25.0	11.9	1.7
30.5	26.5	35.0	31.0	14.7	1.9
29.5	21.0	34.0	28.0	11.1	2.4
18.5	17.5	21.5	18.5	9.2	1.5
15.5	15.5	18.0	15.5	7.8	1.3
45.0	37.0	52.0	46.0	20.6	2.7
13.0	14.5	15.5	13.0	6.5	1.3
15.5	15.5	18.5	15.5	7.7	1.5
28.0	27.5	30.0	26.0	13.0	2.0
21.5	30.5	32.0	27.5	12.6	2.1
10.0	9.0	12.0	9.5	4.3	1.1
19.0	19.0	20.0	17.5	8.8	1.3
18.5	18.5	24.5	21.5	9.0	1.3
17.5	17.5	21.5	18.0	8.6	1.7
15.5	18.0	22.0	19.5	8.3	1.1
19.0	19.0	23.0	20.0	9.8	1.5
24.0	18.0	27.5	24.5	10.2	1.3
17.5	18.0	21.5	17.5	8.5	2.0
18.0	21.5	24.0	22.5	10.8	0.7
22.5	24.5	25.5	22.0	11.0	3.6
14.5	12.5	15.5	14.0	7.0	1.1
24.0	23.5	29.0	24.5	11.8	2.2

Table 65. Sample Pay-5 Measurements

A	B	C	E	crystal size	zone width
31.0	34.0	42.0	34.5	15.1	3.3
12.0	13.0	15.0	11.0	5.4	2.0
19.5	20.0	23.5	20.5	10.3	1.5
37.0	36.0	44.0	33.5	16.5	5.2
22.0	18.0	24.5	22.0	10.4	1.2
14.0	12.5	15.0	11.5	5.8	1.8
21.0	21.0	24.5	20.0	10.0	2.3
18.0	19.0	23.0	18.5	8.6	2.1
25.0	22.0	33.5	27.0	9.8	2.4
14.0	10.5	15.5	13.0	5.8	1.1
18.0	21.5	27.0	22.5	8.8	1.8
18.5	21.5	25.5	23.0	10.3	1.1
10.0	12.5	14.0	12.5	5.7	0.7
11.5	12.5	14.5	13.0	6.4	0.7
35.0	34.0	44.5	37.0	16.3	3.3
10.0	12.0	14.0	11.5	5.1	1.1
17.0	16.5	17.5	16.5	8.3	0.5
13.0	11.0	14.5	13.0	6.3	0.7
15.5	15.5	18.5	17.5	8.7	0.5
20.5	19.0	23.0	20.0	10.0	1.5
29.0	37.5	47.0	37.0	13.5	3.7
26.0	25.0	26.0	21.0	10.5	2.5
22.0	23.0	27.0	25.0	12.4	1.0
27.0	24.0	31.0	26.0	12.6	2.4
17.0	19.0	22.0	20.0	9.6	1.0
20.0	19.0	21.5	18.0	9.0	1.8
46.0	42.0	56.0	50.0	22.4	2.7
13.5	15.5	17.5	14.0	6.8	1.7
15.0	14.0	18.5	16.0	7.2	1.1
18.0	15.0	21.5	18.5	7.9	1.3
20.5	22.0	26.0	22.0	10.5	1.9
26.0	26.5	31.5	29.0	14.4	1.2
24.5	26.0	30.0	27.0	13.5	1.5
16.0	14.0	18.5	14.5	6.8	1.9

Table 66. Sample Pay-11 Measurements

A	B	C	E	crystal size	zone width
15.0	13.0	19.0	16.0	6.4	1.2
19.0	20.0	24.5	23.0	10.6	0.7
8.5	6.5	9.0	8.0	4.0	0.3
20.5	18.5	24.0	21.5	10.2	1.2
31.5	33.0	36.5	30.0	15.0	3.3
17.5	17.5	21.0	19.5	9.7	0.7
8.0	7.5	8.5	7.5	3.8	0.5
10.0	10.0	11.5	10.0	5.0	0.8
36.5	33.0	45.0	36.0	15.7	3.9
24.0	23.5	30.0	26.0	11.9	1.8
20.0	19.0	25.5	19.5	8.4	2.6
25.0	25.0	27.5	23.5	11.8	2.0
18.0	16.0	21.5	19.0	8.6	1.1
13.0	13.0	15.5	13.0	6.5	1.3
13.0	13.0	15.0	12.5	6.3	1.3
15.0	13.5	16.5	15.0	7.5	0.8
23.5	21.5	24.0	21.0	10.5	3.6
22.5	23.0	24.5	21.0	10.5	1.8
30.5	41.0	48.0	39.5	15.8	3.4
22.0	24.0	30.0	25.0	10.8	2.2
32.5	24.0	35.0	30.0	13.7	2.3
31.5	31.0	35.0	31.5	15.8	1.8
20.0	20.0	25.0	22.5	10.4	1.2
19.0	19.0	21.0	17.5	8.8	1.8
20.0	20.5	23.5	22.5	11.3	0.5
27.0	29.5	36.0	31.5	14.1	2.0
12.0	11.0	13.0	12.0	6.0	0.5
20.0	15.5	23.5	19.5	8.0	1.7
20.0	18.5	24.0	22.0	10.2	0.9
40.0	43.5	53.0	44.0	19.8	4.1

Table 67. Sample Ton-11 Measurements

A	B	C	E	crystal size	zone width
22.5	21.0	24.0	21.5	10.8	1.3
12.5	14.0	15.5	13.0	6.5	1.3
17.0	18.0	20.5	17.0	8.5	1.8
19.5	17.5	21.0	17.5	8.8	2.5
23.0	18.5	27.0	20.5	8.8	2.8
42.0	40.0	52.0	41.0	18.5	5.0
15.5	15.5	19.5	16.5	7.6	1.4
16.0	22.5	26.0	20.5	8.0	2.2
39.0	34.0	49.0	39.0	15.9	4.1
20.5	20.5	24.5	19.5	9.7	2.5
20.0	22.0	24.0	20.0	10.0	2.8
19.0	16.0	21.5	17.5	8.3	1.9
46.0	44.0	53.0	43.5	21.8	5.2
21.0	19.0	22.0	20.0	10.0	2.4
25.0	30.0	33.5	26.5	12.7	3.3
25.5	25.0	31.0	28.0	13.4	1.4
29.5	28.0	35.0	26.0	12.6	4.4
21.0	23.0	28.0	20.5	9.2	3.4
18.5	14.0	20.0	15.5	7.2	2.1
31.0	27.0	41.0	31.5	11.6	3.5
19.0	21.0	26.0	22.0	9.5	1.7
24.0	26.0	27.0	23.5	11.8	3.8
26.0	25.5	30.5	24.0	12.0	3.3
24.0	22.0	28.0	23.0	11.1	2.4
31.0	33.0	33.0	27.0	13.5	6.8
24.0	24.0	30.0	23.5	10.9	3.0
26.0	24.0	30.0	28.5	14.1	0.7
20.0	14.0	21.0	18.0	8.2	1.4
20.5	21.5	23.5	18.0	9.0	2.8
27.0	32.0	37.5	28.0	12.5	4.2
30.5	30.0	36.0	30.0	15.0	3.0
30.0	43.5	48.0	39.0	16.1	3.7
21.0	23.0	25.0	19.0	9.5	3.9
23.0	21.5	27.5	23.0	10.8	2.1
14.0	12.0	16.5	12.0	5.4	2.0
15.5	15.5	17.5	15.0	7.5	1.3
22.0	16.0	24.0	19.5	8.6	2.0

Table 67 (cont'd).

A	B	C	E	crystal size	zone width
16.5	15.0	18.5	16.0	8.0	1.3
17.0	15.5	19.0	15.0	7.5	2.0
18.0	19.5	23.0	19.0	9.1	1.9
38.0	28.0	46.0	38.5	14.4	2.8
25.5	21.0	33.0	26.0	9.5	2.6
16.0	21.0	23.5	17.5	7.7	2.6
23.0	21.0	26.5	23.0	11.3	1.7
34.0	30.0	41.5	32.5	14.1	3.9
19.5	18.0	21.5	17.0	8.5	2.3
20.5	23.0	26.5	21.5	10.3	2.4
39.5	39.5	48.5	41.0	19.6	3.6
29.0	16.0	29.5	26.5	10.2	1.2
40.0	30.5	43.0	35.0	16.5	3.8
24.0	18.0	27.0	21.5	9.3	2.4
20.5	20.0	23.0	20.0	10.0	1.5
19.0	18.0	20.5	16.5	8.3	2.0
16.0	16.0	18.0	16.0	8.0	1.0

Table 68. Sample Sal How-1 Measurements

A	B	C	E	crystal size	zone width
33.0	36.0	44.5	36.5	16.0	3.5
15.0	14.5	18.0	13.0	6.3	2.4
10.5	15.5	17.5	14.0	5.5	1.4
20.5	23.0	28.5	22.0	9.4	2.8
20.0	18.5	22.0	17.5	8.8	2.3
21.0	20.0	25.5	19.5	9.1	2.8
19.5	11.0	19.5	14.0	5.6	2.2
15.5	15.5	18.0	13.5	6.8	2.3
17.5	21.0	26.0	20.5	8.2	2.2
12.0	14.5	17.5	14.5	6.1	1.3
15.5	15.0	22.5	19.5	6.6	1.0
16.5	11.5	18.5	16.0	6.5	1.0
24.5	24.5	26.5	24.0	12.0	1.3
17.5	16.5	21.0	15.5	7.3	2.6
25.5	25.5	28.0	23.5	11.8	2.3
23.5	25.0	27.0	25.0	12.5	1.0
18.5	18.0	23.0	21.0	9.6	0.9
50.0	41.0	61.5	51.5	20.6	4.0
31.0	31.0	39.5	31.0	13.9	3.8
33.5	38.5	46.0	42.0	18.7	1.8
15.5	15.5	18.0	14.5	7.3	1.8
30.5	34.0	39.0	33.5	16.3	2.7
14.5	16.5	18.0	15.5	7.8	1.6
37.0	35.5	42.0	36.5	18.3	2.8
14.0	15.0	15.0	12.5	6.3	1.3
34.0	40.0	51.0	40.5	15.7	4.1
34.0	30.0	38.5	30.5	15.0	3.9
27.5	28.5	38.5	30.5	12.0	3.1
24.0	22.0	26.5	22.5	11.3	2.7
36.0	25.5	40.0	32.5	13.6	3.1
19.0	17.0	21.5	19.0	9.5	1.2
18.5	18.5	21.5	19.0	9.5	1.3
34.5	33.0	40.0	31.0	15.5	4.5

Table 69. Sample Sal How-6 Measurements

A	B	C	E	crystal size	zone width
33.0	35.0	42.0	35.0	16.5	3.3
12.0	10.5	14.0	10.0	4.6	1.9
33.0	31.0	36.0	32.0	16.0	3.6
19.5	27.0	31.0	23.5	9.5	3.0
16.0	18.5	21.0	18.0	8.7	1.4
14.5	13.5	16.0	15.0	7.5	0.5
30.5	30.5	38.0	34.5	16.1	1.6
26.5	25.0	30.0	26.0	13.0	2.0
17.0	17.5	20.5	16.0	8.0	2.3
15.0	16.0	20.0	17.0	7.5	1.3
16.5	15.0	18.5	17.5	8.8	0.5
25.5	24.5	31.0	27.0	12.7	1.9
28.0	30.5	35.5	32.5	15.8	1.5
20.5	20.0	20.5	18.5	9.3	1.0
30.5	25.0	34.0	28.0	13.2	2.8
31.0	25.0	34.0	28.0	13.4	2.9
12.5	13.0	15.0	11.0	5.5	2.0
26.0	24.0	32.5	22.5	9.7	4.3
46.0	35.5	49.5	40.5	19.2	4.3
12.5	12.0	13.5	10.5	5.3	1.5
24.5	24.5	27.0	21.0	10.5	3.0
32.0	30.0	38.0	29.5	14.1	4.1
22.5	22.0	26.0	21.5	10.8	2.3
22.0	20.5	23.5	19.0	9.5	2.3
38.0	40.0	46.0	36.0	18.0	5.4
46.0	49.0	63.5	55.0	22.7	3.5
27.0	27.0	37.0	30.0	11.8	2.8
18.0	18.5	19.0	17.0	8.5	1.0
26.0	28.0	31.0	29.0	14.5	1.9
21.0	19.5	24.0	21.5	10.8	1.3

Table 70. Sample Sal 7-8 Measurements

A	B	C	E	crystal size	zone width
44.6	35.5	51.5	41.5	18.1	4.4
15.5	13.0	18.5	16.5	7.1	0.9
35.0	27.5	39.0	30.5	13.9	3.9
34.0	32.0	38.0	26.5	13.3	6.8
27.0	26.0	30.5	24.0	12.0	3.3
30.5	29.5	44.5	32.0	10.7	4.2
20.5	31.0	32.5	26.5	11.4	2.6
15.5	13.5	18.5	14.5	6.5	1.8
26.0	28.0	34.5	27.5	12.3	3.1
26.0	29.0	34.0	28.0	13.2	2.8
26.5	29.0	34.5	27.0	12.6	3.5
34.0	28.0	39.0	31.0	14.1	3.6
21.5	20.0	26.5	21.0	9.4	2.5
30.5	31.0	37.0	27.5	13.6	4.7
33.0	44.0	47.0	42.5	19.9	2.1
40.0	42.0	46.0	37.5	18.8	6.4
33.5	47.0	54.0	44.5	17.7	3.8
21.5	22.5	26.0	21.0	10.5	2.5
14.0	20.5	22.0	17.0	7.3	2.1
26.5	26.0	32.0	27.0	13.0	2.4
24.5	17.5	29.5	23.0	8.4	2.4
20.5	19.0	22.5	19.5	9.8	1.5
15.0	16.0	19.0	15.5	7.4	1.7
25.0	25.5	29.0	25.5	12.8	1.8
23.0	21.0	25.0	22.5	11.3	2.2
28.0	22.5	33.0	26.5	11.2	2.8
26.5	28.0	36.0	25.0	10.5	4.6
45.5	41.5	52.0	47.0	23.3	2.5
25.0	24.0	29.5	25.0	12.3	2.2
20.5	18.5	23.0	17.5	8.8	2.9

Table 71. Sample List for Burlington-Keokuk Formation Hwy 61 Outcrops

Sample Number	Sample ID	Number of Crystals
1	DFS-1	34
2	CAR-5	30
3	MIN-6	34
4	LAK-10	31
5	MIN-16	33
6	DFS-15	32
7	DFS-24	30
8	LAK-22	30
9	MIN-29	30
10	LAK-31	30
11	DFS-32	30
12	LAK-36	31
13	DFS-37	30
14	LAK-40	30
15	DUNC-56	30

Table 72. Sample DFS-1 Measurements

A	B	C	E	crystal size	zone width
34.0	32.0	37.5	31.5	15.8	4.4
18.0	15.0	20.0	17.5	8.4	1.2
14.5	13.0	16.0	13.5	6.8	1.3
19.5	19.0	23.0	21.5	10.7	0.7
13.0	13.0	15.0	13.5	6.8	0.8
9.5	12.0	13.0	11.5	5.5	0.7
21.5	24.5	30.0	28.5	12.2	0.6
13.0	17.5	19.0	16.0	7.2	1.4
18.0	17.5	18.0	15.5	7.8	1.3
15.0	13.0	16.0	12.0	6.0	2.5
16.0	17.0	18.0	13.0	6.5	2.5
27.5	27.0	34.0	28.0	13.0	2.8
26.0	25.0	29.0	25.5	12.8	1.8
25.5	26.0	29.0	22.0	11.0	3.5
20.0	20.0	24.0	20.5	10.1	1.7
17.5	17.5	19.0	14.5	7.3	2.3
14.0	15.0	15.5	14.0	7.0	0.8
14.5	15.0	16.0	13.0	6.5	1.5
17.0	19.0	23.0	18.0	8.0	2.2
37.0	34.0	43.0	32.5	15.8	5.1
20.0	18.0	21.0	16.0	8.0	3.7
19.0	18.0	20.5	14.5	7.3	3.0
18.5	18.0	19.0	12.5	6.3	3.3
17.0	18.0	21.0	18.0	8.9	1.5
18.0	16.0	20.0	13.5	6.8	3.4
23.5	25.0	28.0	22.5	11.3	2.8
20.5	19.0	23.0	16.0	8.0	3.5
25.0	24.0	25.0	21.5	10.8	1.8
9.5	8.0	11.0	8.5	3.9	1.1
17.0	17.5	22.0	15.5	7.0	2.9
15.5	15.0	16.5	14.0	7.0	1.3
15.0	15.0	18.0	15.5	7.7	1.2
27.0	25.0	32.0	25.0	11.9	3.3
14.5	15.0	17.5	13.5	6.8	2.0

Table 73. Sample CAR-5 Measurements

A	B	C	E	crystal size	zone width
17.0	14.5	20.5	18.0	7.7	1.1
30.0	30.0	35.0	31.0	15.5	2.0
13.0	19.0	22.5	18.0	6.5	1.6
9.5	10.0	11.5	10.0	5.0	0.8
22.0	28.0	32.0	26.0	11.4	2.6
19.0	18.5	23.0	16.5	7.9	3.1
10.0	12.0	12.0	10.0	5.0	1.8
13.0	14.5	16.0	14.0	7.0	1.0
20.5	20.5	23.5	18.5	9.3	2.5
21.0	19.0	24.0	20.0	9.9	2.0
21.5	20.0	27.5	24.0	10.1	1.5
10.5	11.5	14.5	12.5	5.3	0.8
19.0	22.5	25.0	22.5	11.0	1.2
30.0	28.5	34.0	29.0	14.5	2.5
24.0	24.0	27.0	22.5	11.3	2.3
19.0	21.0	23.0	20.0	10.0	2.1
19.5	21.0	20.5	18.0	9.0	1.3
13.0	11.5	14.5	10.0	5.0	2.3
33.5	27.0	37.0	27.5	13.0	4.5
17.0	14.0	19.5	15.0	6.8	2.0
25.0	23.0	28.0	21.5	10.8	3.7
12.0	12.0	12.0	10.0	5.0	1.0
15.0	14.0	17.5	14.5	7.1	1.5
18.0	18.5	22.0	16.0	7.9	2.9
11.0	11.5	13.5	9.5	4.7	2.0
18.0	17.5	20.5	16.0	8.0	2.3
20.0	17.0	22.5	17.0	8.2	2.6
18.0	16.5	23.0	18.5	7.7	1.9
9.0	11.5	13.0	9.5	4.2	1.6
27.0	27.0	31.0	27.5	13.8	1.8

Table 74. Sample MIN-6 Measurements

A	B	C	E	crystal size	zone width
22.0	21.5	26.0	21.5	10.7	2.2
20.0	18.5	22.0	17.0	8.5	2.5
29.0	29.0	34.0	25.5	12.8	4.3
12.0	12.5	14.5	11.5	5.8	1.5
22.0	22.0	26.0	22.5	11.3	1.8
11.5	10.0	18.5	10.0	2.2	1.9
19.0	17.5	20.0	17.5	8.8	1.3
13.5	12.0	16.5	11.0	4.8	2.4
15.5	16.0	22.0	19.0	7.2	1.1
10.0	11.5	12.5	11.5	5.8	0.5
21.0	20.5	22.5	19.5	9.8	1.5
14.0	14.5	17.0	15.5	7.7	0.7
33.0	33.5	35.5	25.0	12.5	5.3
23.0	16.5	25.0	18.0	7.9	3.1
12.5	12.0	14.5	12.5	6.3	1.0
13.0	12.0	14.0	12.5	6.3	0.8
15.5	11.0	16.5	14.5	6.5	0.9
9.5	8.5	10.0	8.0	4.0	1.0
44.0	32.0	53.0	41.5	15.4	4.3
19.5	25.5	27.5	24.0	11.3	1.6
23.0	23.0	25.0	19.0	9.5	3.0
28.0	28.0	29.0	22.0	11.0	3.5
19.5	17.5	22.5	16.5	8.0	2.9
11.0	9.0	11.0	9.0	4.5	1.6
43.0	42.0	53.0	41.0	19.1	5.6
15.0	16.5	19.5	17.5	8.2	0.9
13.0	19.0	21.0	16.0	6.5	2.0
18.5	20.0	19.5	17.5	8.8	1.0
16.5	15.0	19.5	17.5	8.2	0.9
23.5	22.5	25.0	19.0	9.5	3.0
14.5	15.5	19.0	12.5	5.7	2.9
16.5	18.0	20.0	15.0	7.5	2.5
27.0	28.0	31.0	29.0	14.5	1.0
24.0	24.0	33.0	24.5	9.6	3.3

Table 75. Sample LAK-10 Measurements

A	B	C	E	crystal size	zone width
28.0	26.5	28.0	10.0	5.0	9.0
16.5	14.5	17.0	14.0	7.0	2.6
40.5	39.0	50.0	35.0	16.1	6.9
20.0	20.0	25.0	18.0	8.3	3.2
18.0	21.5	26.0	22.5	9.5	1.5
19.5	19.5	23.0	19.0	9.5	2.0
19.5	20.0	20.0	16.0	8.0	2.0
21.0	18.5	25.0	19.0	8.6	2.7
15.0	13.5	14.5	10.5	5.3	2.0
14.5	15.0	17.5	14.0	7.0	1.8
12.5	12.5	13.5	12.0	6.0	0.8
29.0	20.5	30.5	24.0	10.9	3.0
21.5	28.5	35.5	28.0	10.1	2.7
22.0	22.0	25.0	20.0	10.0	2.5
16.0	17.0	18.0	16.0	8.0	1.0
18.5	20.0	25.0	19.0	8.2	2.6
31.5	30.0	34.0	28.0	14.0	3.0
15.5	16.5	19.0	16.0	8.0	1.5
35.5	30.0	42.0	33.0	14.5	4.0
11.5	11.5	13.0	10.0	5.0	1.5
31.0	33.0	35.0	27.5	13.8	6.1
26.5	30.0	34.0	28.0	13.7	2.9
13.0	15.0	15.5	11.5	5.8	2.8
22.5	22.0	27.0	20.0	9.7	3.4
24.0	25.5	31.0	27.0	12.5	1.8
10.5	11.0	13.0	11.5	5.6	0.7
19.0	20.0	23.0	20.5	10.3	1.3
27.0	29.0	31.0	25.0	12.5	4.8
13.0	13.0	16.0	13.0	6.2	1.4
25.0	23.5	26.5	19.5	9.8	3.5

Table 76. Sample MIN-16 Measurements

A	B	C	E	crystal size	zone width
21.5	32.5	35.0	30.0	12.4	2.1
38.0	38.5	45.0	37.0	18.5	4.0
14.0	12.5	14.0	11.5	5.8	1.3
19.0	23.0	28.0	22.0	9.0	2.5
12.0	13.5	13.5	12.0	6.0	0.8
22.0	24.0	28.0	15.5	7.5	6.0
26.0	22.0	29.0	23.0	11.2	2.9
24.5	23.0	27.5	20.5	10.3	3.5
12.5	13.0	15.5	12.5	6.1	1.5
18.5	17.5	21.0	18.0	9.0	1.5
13.0	11.0	15.0	10.0	4.6	2.3
12.0	12.0	14.0	11.0	5.5	1.5
20.5	13.0	22.0	16.5	6.6	2.2
27.5	27.0	29.0	26.0	13.0	1.5
8.5	9.5	11.0	9.0	4.3	1.0
14.5	16.0	18.0	16.0	8.0	1.0
14.5	15.0	17.0	15.0	7.5	1.0
13.5	15.0	16.0	14.5	7.3	0.8
15.5	16.0	18.5	15.0	7.5	1.8
15.0	12.0	17.0	14.0	6.3	1.4
12.5	13.5	15.0	12.0	6.0	1.5
23.0	22.0	24.5	20.5	10.3	2.0
16.5	12.0	20.0	13.5	5.0	2.4
15.0	17.0	21.0	15.5	6.6	2.3
23.5	24.0	26.0	20.0	10.0	3.0
15.5	15.0	18.5	14.0	6.8	2.2
22.0	24.0	25.0	20.0	10.0	4.3
17.5	18.5	20.0	14.5	7.3	2.8
13.0	12.0	13.5	12.0	6.0	0.8
20.0	22.0	26.0	21.0	9.9	2.3
11.0	10.0	13.0	8.5	4.0	2.1
19.5	17.5	23.0	20.0	9.3	1.4
14.5	17.0	19.0	18.0	8.8	0.5

Table 77. Sample DFS-15 Measurements

A	B	C	E	crystal size	zone width
30.0	29.0	36.0	33.0	15.9	1.4
30.5	29.0	35.5	33.0	16.5	1.2
13.0	14.0	15.0	11.0	5.5	2.0
17.0	18.5	22.0	14.0	6.6	3.8
14.0	16.0	18.0	13.0	6.4	2.5
21.5	29.0	34.0	29.0	11.5	2.0
24.5	17.0	26.5	21.0	9.0	2.4
23.0	14.0	24.5	18.5	7.2	2.3
16.0	15.0	19.0	13.5	6.5	2.6
11.0	11.0	14.0	12.0	5.4	0.9
31.5	34.0	40.5	31.0	14.6	4.5
21.5	22.5	26.0	19.5	9.8	3.3
14.0	18.5	20.0	18.0	8.3	0.9
24.5	25.0	27.5	24.0	12.0	1.8
11.0	11.5	11.5	10.0	5.0	0.8
17.5	16.0	18.0	14.0	7.0	2.0
17.0	17.0	21.5	17.0	7.7	2.0
12.0	11.5	14.0	10.5	5.3	1.8
15.5	17.5	18.5	15.5	7.8	2.3
15.0	13.0	15.0	12.0	6.0	2.7
17.5	17.5	20.0	17.5	8.8	1.3
16.0	18.0	18.5	16.0	8.0	2.5
32.0	31.5	41.5	35.5	15.3	2.6
11.5	11.5	12.0	11.0	5.5	0.5
12.5	14.0	14.5	11.0	5.5	1.8
32.0	30.5	38.0	30.0	14.5	3.9
37.0	32.0	42.0	32.5	15.6	4.6
24.0	16.0	25.0	18.5	8.1	2.9
19.0	20.0	20.0	16.0	8.0	2.0
14.5	13.0	17.5	13.5	6.1	1.8
32.0	29.0	37.0	30.5	14.8	3.2
17.0	15.0	18.0	15.5	7.8	2.0

Table 78. Sample DFS-24 Measurements

A	B	C	E	crystal size	zone width
20.0	22.0	24.0	17.0	8.5	4.3
19.0	18.0	20.0	16.5	8.3	1.8
27.5	19.0	29.0	22.0	9.8	3.1
17.0	16.5	19.5	16.0	8.0	1.8
16.0	14.0	17.0	14.0	7.0	2.1
23.0	24.5	28.0	16.0	8.0	6.0
19.0	18.0	21.0	18.0	9.0	1.5
20.0	16.0	22.0	18.0	8.5	1.9
23.0	20.0	26.0	20.5	10.0	2.7
30.0	22.0	32.0	26.5	12.2	2.5
13.0	14.5	16.0	12.5	6.3	1.8
18.0	20.0	20.0	18.0	9.0	2.9
10.0	11.0	12.0	9.5	4.8	1.3
23.0	25.5	30.5	24.5	11.2	2.7
15.0	15.0	17.0	13.5	6.8	1.8
22.0	23.0	24.0	19.5	9.8	2.3
14.5	14.0	18.0	14.0	6.4	1.8
28.0	29.0	36.0	27.5	12.5	3.9
23.0	23.5	23.0	16.0	8.0	3.5
19.0	15.5	21.0	17.0	8.1	1.9
18.0	16.5	20.0	17.0	8.5	1.5
20.0	21.0	26.0	21.0	9.5	2.3
15.0	14.0	16.0	10.0	5.0	3.0
14.0	14.0	15.0	11.5	5.8	1.8
18.0	13.5	20.0	15.0	6.6	2.2
18.5	19.0	24.0	19.0	8.5	2.2
56.0	48.0	72.0	57.0	21.9	5.8
9.0	10.0	13.0	10.0	3.9	1.2
56.0	47.0	69.0	56.0	22.8	5.3
22.5	21.0	25.0	19.0	9.5	3.0

Table 79. Sample LAK-22 Measurements

A	B	C	E	crystal size	zone width
22.5	24.5	29.0	24.0	11.3	2.4
21.0	18.5	24.0	17.5	8.4	3.1
19.0	17.5	21.0	19.0	9.5	1.0
14.5	10.0	16.0	14.5	6.0	0.6
26.0	24.0	33.0	25.5	10.8	3.2
28.0	23.0	31.0	23.5	11.3	3.6
27.5	36.0	39.0	35.0	16.3	1.9
36.0	35.0	42.0	37.0	18.5	2.5
17.0	15.0	18.0	15.0	7.5	2.3
20.5	18.5	24.0	20.0	9.5	1.9
17.5	19.0	20.0	15.5	7.8	2.3
22.0	23.0	25.5	22.0	11.0	1.8
24.5	20.0	29.0	23.0	9.8	2.6
27.5	27.0	31.5	24.0	12.0	3.8
24.0	23.5	28.0	24.0	12.0	2.0
22.5	22.0	27.0	25.5	12.4	0.7
20.5	19.0	23.0	20.5	10.3	1.3
14.5	14.0	15.0	13.5	6.8	0.8
18.0	18.0	21.5	19.5	9.7	1.0
18.0	19.0	21.0	18.0	9.0	1.5
16.0	14.0	16.0	12.0	6.0	3.3
18.5	17.5	23.0	21.0	9.4	0.9
14.5	14.0	17.0	15.5	7.7	0.7
31.0	28.5	36.0	28.0	13.6	3.9
23.5	24.0	29.0	23.0	11.1	2.9
14.5	16.0	19.0	15.5	7.2	1.6
27.5	29.0	31.0	28.0	14.0	1.5
31.5	33.0	38.0	30.0	15.0	4.0
26.5	23.5	30.0	23.5	11.6	3.2
10.5	11.0	14.0	11.5	5.0	1.1

Table 80. Sample MIN-29 Measurements

A	B	C	E	crystal size	zone width
12.5	13.0	15.0	13.0	6.5	1.0
19.0	16.0	22.0	16.0	7.3	2.7
17.0	16.5	18.5	13.5	6.8	2.5
13.0	14.0	17.5	14.0	6.1	1.5
27.5	27.0	31.0	22.0	11.0	4.5
13.0	14.0	16.0	10.5	5.3	2.8
14.0	13.5	16.0	14.0	7.0	1.0
29.5	31.0	34.0	28.5	14.3	2.8
19.0	17.0	20.5	15.5	7.8	3.2
15.5	15.0	17.0	13.5	6.8	1.8
13.0	13.0	17.5	12.0	4.9	2.2
20.0	18.5	23.0	17.0	8.5	3.0
16.0	15.5	17.0	13.5	6.8	1.8
20.5	21.5	28.5	22.5	9.0	2.4
14.5	14.5	16.0	12.0	6.0	2.0
17.5	19.0	21.0	18.0	9.0	1.5
16.0	20.0	24.0	20.0	8.2	1.6
12.0	12.0	13.5	12.0	6.0	0.8
14.0	13.5	16.0	15.0	7.5	0.5
12.0	10.0	11.5	8.0	4.0	2.9
15.5	16.0	17.5	14.5	7.3	1.5
15.5	15.5	20.0	16.0	7.0	1.8
33.5	26.5	37.5	32.5	14.8	2.3
19.5	15.5	24.0	19.0	7.4	1.9
23.5	25.0	32.0	28.0	11.8	1.7
21.5	21.5	27.0	22.5	10.4	2.1
18.0	17.0	18.0	13.5	6.8	2.3
21.0	19.0	23.0	18.0	9.0	3.1
13.5	11.0	15.0	13.0	6.1	0.9
20.0	20.0	27.5	21.5	8.4	2.4

Table 81. Sample LAK-31 Measurements

A	B	C	E	crystal size	zone width
14.0	14.5	18.0	16.5	7.5	0.7
36.0	32.5	42.0	36.0	17.2	2.9
36.0	34.0	42.0	36.5	18.1	2.7
28.5	30.0	36.0	30.5	14.5	2.6
20.5	22.0	25.0	20.0	10.0	2.5
28.0	28.0	33.0	24.5	12.3	4.3
24.0	23.5	27.0	23.5	11.8	1.8
28.0	28.0	31.5	27.5	13.8	2.0
19.5	18.0	20.0	13.0	6.5	3.5
9.0	9.5	12.0	9.5	4.1	1.1
29.5	32.5	37.5	31.5	15.4	2.9
19.5	23.0	28.0	20.5	8.6	3.2
21.0	20.5	24.0	20.5	10.3	1.8
26.0	25.0	30.0	25.5	12.8	2.3
30.0	32.0	37.0	30.0	15.0	3.4
16.0	16.0	18.5	15.5	7.8	1.5
15.5	18.0	21.0	16.0	7.3	2.3
23.0	26.0	30.0	26.0	12.4	1.9
28.0	30.0	34.0	26.5	13.3	4.2
27.0	27.0	31.0	23.5	11.8	3.8
22.0	26.5	33.0	30.0	11.9	1.2
50.0	36.5	62.5	49.0	17.0	4.7
23.0	26.0	34.5	30.5	11.4	1.5
28.0	22.5	36.0	27.0	9.7	3.2
23.5	25.5	26.0	21.5	10.8	4.6
29.5	27.5	31.0	22.5	11.3	6.5
20.5	21.0	26.0	23.0	10.6	1.4
20.5	26.0	30.0	27.0	11.7	1.3
13.0	13.0	16.0	13.0	6.2	1.4
36.0	36.5	46.0	33.0	14.9	5.9

Table 82. Sample DFS-32 Measurements

A	B	C	E	crystal size	zone width
15.0	13.5	18.0	15.0	6.8	1.4
19.5	18.0	21.5	17.0	8.5	2.3
16.0	15.0	17.0	15.0	7.5	1.0
24.5	23.5	29.0	25.0	12.2	2.0
10.0	10.0	13.0	11.5	5.0	0.7
17.5	16.0	18.0	9.5	4.8	4.3
15.0	16.5	18.0	15.5	7.8	1.3
15.5	15.0	18.0	14.5	7.3	1.8
16.5	18.5	22.0	17.5	8.0	2.1
19.0	17.0	21.0	16.0	8.0	2.8
16.5	14.0	19.0	14.5	6.7	2.1
26.0	24.0	28.5	20.5	10.3	5.0
19.0	19.0	20.0	16.5	8.3	1.8
27.0	25.5	33.5	30.0	13.4	1.6
15.0	11.0	17.0	14.0	5.8	1.3
15.5	15.5	18.0	13.5	6.8	2.3
15.0	17.0	17.0	14.0	7.0	3.0
11.5	13.0	14.5	11.0	5.5	1.8
17.0	19.0	21.0	15.5	7.8	3.1
20.0	20.0	24.0	20.5	10.1	1.7
20.5	22.0	25.0	22.0	11.0	1.5
16.0	18.0	20.0	17.0	8.5	1.7
20.5	22.5	27.0	22.5	10.3	2.1
17.0	19.0	25.0	22.0	8.4	1.2
37.0	36.0	44.0	37.0	18.2	3.4
20.5	18.5	19.5	15.5	7.8	4.7
19.5	18.5	21.0	17.5	8.8	1.8
27.0	29.0	28.0	25.5	12.8	5.2
12.5	12.0	14.0	10.5	5.3	1.8
18.5	17.5	23.0	20.0	8.9	1.3

Table 83. Sample LAK-36 Measurements

A	B	C	E	crystal size	zone width
13.5	12.5	14.0	13.0	6.5	0.5
12.0	14.5	16.0	13.0	6.3	1.5
31.0	29.0	33.0	25.5	12.8	5.8
15.0	14.0	17.0	15.0	7.5	1.0
38.5	38.0	44.0	33.0	16.5	5.5
14.0	13.5	14.0	10.0	5.0	2.0
11.0	10.0	12.0	9.0	4.5	1.5
19.5	17.0	22.0	18.0	8.8	2.0
14.5	15.5	17.5	13.5	6.8	2.0
13.5	21.5	22.0	17.0	7.3	2.1
18.5	18.0	20.0	17.5	8.8	1.3
31.0	33.0	40.0	32.5	15.1	3.5
24.0	25.0	32.5	22.5	9.4	4.2
12.5	14.0	14.5	13.5	6.8	0.5
16.5	16.0	19.0	17.0	8.5	1.0
22.0	20.0	27.0	21.0	9.3	2.6
19.0	18.0	21.0	16.0	8.0	2.5
22.0	15.5	23.0	18.0	8.3	2.3
37.0	39.0	42.0	33.0	16.5	7.0
23.5	24.0	26.0	19.0	9.5	3.5
18.5	18.0	22.5	17.0	8.1	2.6
20.5	20.0	22.0	18.5	9.3	1.8
23.5	22.5	28.0	21.0	10.2	3.4
19.0	22.0	26.0	20.0	9.0	2.7
16.5	12.0	17.5	16.0	7.4	0.7
12.5	12.5	14.5	11.5	5.8	1.5
19.0	19.0	24.0	18.5	8.4	2.5
20.0	19.0	26.0	19.5	8.1	2.7
28.0	24.0	34.0	22.0	9.4	5.1
22.0	23.5	26.0	23.0	11.5	1.5
24.5	28.0	32.0	25.0	12.0	3.4

Table 84. Sample DFS-37 Measurements

A	B	C	E	crystal size	zone width
26.0	25.5	31.0	27.0	13.3	2.0
21.5	20.0	24.0	18.5	9.3	2.8
28.5	26.5	32.0	27.0	13.5	3.1
32.0	34.0	38.0	32.5	16.3	3.8
20.5	21.0	24.5	17.0	8.5	3.8
17.5	16.0	21.0	18.0	8.3	1.4
26.0	19.0	28.0	24.0	10.9	1.8
18.0	16.0	19.5	16.5	8.3	2.0
26.0	27.0	33.0	25.5	11.9	3.5
27.0	25.0	29.0	23.0	11.5	4.5
36.0	38.0	44.0	32.0	16.0	6.1
32.0	30.0	36.0	28.5	14.3	4.5
27.5	29.0	33.0	26.5	13.3	3.3
20.0	18.0	23.0	17.5	8.5	2.7
31.5	30.0	37.0	27.5	13.5	4.7
21.0	22.0	23.5	16.5	8.3	3.5
26.5	28.0	30.0	26.0	13.0	2.0
26.0	23.5	30.0	24.0	11.7	2.9
20.0	22.0	22.0	18.5	9.3	4.0
29.0	27.0	32.0	26.5	13.3	3.8
25.0	23.0	27.5	23.0	11.5	3.1
20.0	20.0	23.0	16.5	8.3	3.3
34.5	32.5	39.5	33.0	16.5	3.6
25.0	27.0	29.5	24.5	12.3	3.6
24.5	26.5	29.5	24.0	12.0	3.4
19.5	20.0	22.5	18.5	9.3	2.0
17.0	15.0	17.0	12.0	6.0	4.0
34.5	34.0	41.0	32.0	15.9	4.5
15.0	13.5	17.0	15.0	7.5	1.0
37.0	35.0	36.5	27.0	13.5	9.5

Table 85. Sample LAK-40 Measurements

A	B	C	E	crystal size	zone width
20.0	19.5	22.0	17.5	8.8	2.3
32.0	34.0	41.0	27.5	12.9	6.3
22.5	25.0	28.5	24.5	12.1	2.0
25.5	27.0	27.0	22.0	11.0	2.5
27.0	29.0	33.5	28.5	14.2	2.5
39.0	45.0	51.0	43.5	21.0	3.6
30.0	28.0	35.5	29.0	13.9	3.1
17.0	17.0	20.0	16.5	8.3	1.8
39.0	34.0	44.0	38.0	18.6	2.9
18.5	18.5	20.5	16.0	8.0	2.3
25.0	27.0	29.0	25.0	12.5	3.5
24.0	30.0	34.0	25.0	11.3	4.1
27.5	29.0	32.0	26.5	13.3	2.8
27.0	27.0	32.0	27.0	13.5	2.5
26.5	32.5	38.0	29.5	12.8	3.7
19.5	19.5	22.0	19.0	9.5	1.5
19.0	17.0	21.0	18.0	9.0	1.8
25.5	29.0	37.0	30.5	12.2	2.6
27.0	30.0	36.0	32.5	14.8	1.6
28.0	28.5	28.0	24.5	12.3	1.8
32.0	31.0	39.0	33.0	15.5	2.8
35.0	28.0	39.0	30.0	13.9	4.2
14.0	15.5	18.0	15.0	7.2	1.4
40.0	35.5	47.0	36.0	16.7	5.1
21.0	19.0	24.0	17.0	8.4	3.5
17.0	16.5	19.0	14.5	7.3	2.3
30.0	28.5	29.0	26.0	13.0	1.5
19.0	18.0	22.0	18.5	9.3	1.8
20.0	20.0	21.0	16.0	8.0	2.5
18.0	17.0	14.0	13.5	6.8	0.3

Table 86. Sample DUNC-56 Measurements

A	B	C	E	crystal size	zone width
18.0	14.5	20.5	14.0	6.3	2.9
16.0	18.0	17.5	15.5	7.8	3.0
25.0	23.0	24.0	21.0	10.5	4.9
17.0	20.0	24.0	20.0	8.6	1.7
17.0	17.0	22.0	19.0	8.3	1.3
27.0	26.0	36.0	30.0	12.0	2.4
36.0	35.0	44.0	41.0	19.3	1.4
42.0	43.0	46.0	40.5	20.3	2.8
25.0	23.5	29.5	24.0	11.6	2.7
18.0	18.5	24.0	19.0	8.1	2.1
27.0	27.0	32.0	26.0	13.0	3.0
33.5	28.0	37.0	31.0	15.1	2.9
15.5	14.0	17.5	14.5	7.3	1.5
10.5	11.0	15.0	12.0	4.6	1.1
22.0	19.0	25.0	23.0	11.0	1.0
19.0	18.0	19.5	15.0	7.5	2.3
25.0	23.5	28.0	26.0	13.0	1.0
30.0	31.0	41.0	37.0	15.1	1.6
17.0	21.0	23.5	19.0	8.8	2.1
42.0	46.0	57.0	46.0	20.0	4.8
23.0	21.0	24.5	21.5	10.8	2.8
29.5	29.0	36.0	30.0	14.3	2.9
15.5	14.5	18.5	14.5	6.9	1.9
15.5	17.5	18.0	14.0	7.0	3.2
14.5	16.0	18.0	14.5	7.3	1.8
19.5	23.0	26.0	23.0	10.9	1.4
17.0	19.0	22.0	15.5	7.4	3.1
26.0	26.5	29.0	24.5	12.3	2.3
16.0	18.0	21.0	16.0	7.5	2.4
24.0	22.5	28.0	24.0	11.8	2.0

Table 87. Sample List for Seroe Domi Formation, Seru Blandan and St. Michielsburg Outcrops

Sample Number	Sample ID	Number of Crystals
1	SB-1 Zone I	30
2	SB-2 Zone I	20
3	SM-1 Zone I	15
4	SB-1 Zone II	30
5	SB-2 Zone II	20
6	SM-1 Zone II	15

Table 88. Sample SB-1 Zone I Measurements

A	B	C	E	crystal size	zone width
38.5	38.0	45.0	35.0	17.5	5.0
37.5	35.5	41.0	34.0	17.0	5.4
29.5	29.5	36.5	25.5	12.0	5.2
41.0	41.5	47.0	36.5	18.3	5.3
45.5	44.0	59.0	46.5	19.7	5.3
40.0	38.0	40.5	36.0	18.0	6.7
27.0	26.0	31.0	26.0	13.0	2.5
33.5	30.0	38.0	31.5	15.6	3.2
40.0	40.5	45.5	38.5	19.3	3.5
21.5	25.0	29.0	25.0	11.6	1.8
24.0	27.0	31.0	25.5	12.3	2.7
33.0	23.0	35.0	28.5	12.7	2.9
27.5	29.0	34.0	28.5	14.0	2.7
46.0	33.0	51.0	46.0	19.5	2.1
44.0	42.0	46.0	42.0	21.0	6.0
28.0	30.0	36.0	28.0	13.1	3.7
39.0	37.0	45.0	41.0	20.5	2.2
29.0	26.0	33.0	27.0	13.3	3.0
40.0	37.0	48.0	38.0	17.7	4.6
36.0	34.0	41.0	36.0	18.0	3.0
36.5	35.0	10.0	34.0	17.0	3.0
37.0	29.0	41.0	35.0	16.1	2.8
34.0	32.0	39.0	34.0	17.0	2.7
38.0	36.0	39.0	35.0	17.5	5.8
50.0	52.0	57.5	49.0	24.5	6.8
42.5	44.0	48.0	39.0	19.5	4.5
28.0	30.0	33.0	29.0	14.5	3.2
49.0	48.0	52.0	46.0	23.0	3.0
32.0	32.5	39.0	35.0	17.1	2.0
43.0	41.0	47.0	41.0	20.5	5.3

Table 89. Sample SB-1 Zone II Measurements

A	B	C	E	crystal size	zone width
30.5	28.0	35.0	4.0	2.0	15.4
28.5	28.5	34.0	8.5	4.2	12.7
22.0	24.0	25.5	3.0	1.5	12.7
32.0	30.0	36.5	9.0	4.5	14.1
37.0	37.5	46.5	12.5	5.8	15.8
32.0	28.0	36.0	7.0	3.4	14.3
21.0	22.5	26.0	4.5	2.2	10.7
26.0	23.0	31.5	6.5	2.9	11.0
31.0	32.0	38.5	8.5	4.1	14.4
18.0	23.0	25.0	3.5	1.7	10.2
18.0	23.0	25.5	4.0	1.8	9.9
23.0	18.0	28.5	2.5	0.9	9.8
22.0	25.0	28.5	2.0	1.0	12.8
37.0	32.0	46.0	13.0	5.4	13.6
38.0	31.0	42.0	11.5	5.5	14.6
24.0	26.0	28.0	2.5	1.3	14.1
37.5	30.0	41.0	12.5	6.0	13.6
23.0	22.0	27.0	5.0	2.5	10.9
30.0	32.0	38.0	9.0	4.3	13.9
32.0	27.5	36.0	3.0	1.5	16.0
28.0	28.0	34.0	7.0	3.4	13.1
30.0	27.0	35.0	8.0	3.8	12.8
29.0	28.0	34.0	7.0	3.5	13.5
34.0	32.0	35.0	9.0	4.5	16.2
37.0	44.0	49.0	15.0	7.3	16.4
37.0	38.0	39.0	9.0	4.5	15.0
22.0	25.0	29.0	6.0	2.8	10.8
39.0	41.0	46.0	17.0	8.5	15.8
28.0	28.5	35.0	8.0	3.8	12.7
35.0	35.0	41.0	11.0	5.5	15.0

Table 90. Sample SB-2 Zone I Measurements

A	B	C	E	crystal size	zone width
45.0	41.0	52.0	44.5	21.7	3.7
17.0	17.0	21.0	17.5	8.3	1.7
10.0	10.0	10.0	9.5	4.8	0.3
40.5	46.0	52.0	43.5	21.4	4.2
11.0	10.5	12.0	9.5	4.8	1.3
19.5	19.5	23.0	20.0	10.0	1.5
40.0	38.0	47.0	42.0	20.6	2.5
26.0	28.0	31.0	26.5	13.3	3.1
33.0	34.0	39.0	34.0	17.0	2.5
39.0	36.0	48.0	41.0	18.2	3.1
54.0	54.0	62.0	55.0	27.5	3.5
42.0	38.0	48.0	40.5	20.0	3.7
30.0	33.0	43.0	35.0	13.9	3.2
31.0	31.0	33.0	29.5	14.8	1.8
31.0	31.0	42.5	35.0	13.8	3.0
19.0	17.0	21.0	17.0	8.5	2.3
24.0	25.5	30.0	26.0	12.7	1.9
22.0	22.5	25.0	21.0	10.5	2.0
26.0	25.0	29.0	23.0	11.5	3.0
31.0	30.0	32.0	26.5	13.3	2.8

Table 91. Sample SB-2 Zone II Measurements

A	B	C	E	crystal size	zone width
42.0	31.0	44.5	13.5	6.3	14.5
18.0	16.0	17.5	5.0	2.5	8.3
8.0	8.0	9.5	2.5	1.3	3.5
33.0	39.0	43.5	7.5	3.6	17.5
8.0	8.0	9.5	2.5	1.3	3.5
15.0	16.0	20.0	4.0	1.8	7.0
32.0	34.0	42.0	14.0	6.3	12.6
22.0	24.0	26.5	5.5	2.8	11.2
26.0	28.0	34.0	9.0	4.1	11.4
35.0	31.0	41.0	10.0	4.7	14.5
47.0	46.5	55.0	20.0	10.0	17.5
35.0	31.0	40.5	9.0	4.3	15.0
28.5	27.5	35.0	9.0	4.2	12.1
26.0	27.0	29.5	9.0	4.5	10.3
24.5	27.0	35.0	7.0	2.8	11.2
14.0	12.0	17.0	3.0	1.3	6.0
15.5	22.5	26.0	8.0	3.0	6.9
16.0	18.5	21.0	4.5	2.2	7.9
21.0	22.0	23.0	5.0	2.5	9.0
20.0	20.0	26.5	8.0	3.4	7.8

Table 92. Sample SM-1 Zone I Measurements

A	B	C	E	crystal size	zone width
48.0	48.0	54.0	48.0	24.0	3.0
48.0	46.0	55.0	46.0	23.0	5.3
42.0	37.0	49.0	43.0	20.1	2.8
44.5	43.0	55.0	50.0	23.0	2.3
49.0	40.0	54.0	46.0	22.1	3.8
49.0	39.0	58.0	46.0	19.2	5.0
69.0	60.0	80.0	73.0	34.1	3.3
59.0	49.0	65.0	57.0	27.8	3.9
45.0	47.0	57.0	48.0	22.6	4.2
55.0	57.0	69.0	62.0	29.4	3.3
37.0	37.0	36.0	32.0	16.0	2.0
36.0	38.0	43.0	36.0	18.0	4.3
34.0	40.0	45.0	38.0	18.3	3.4
51.5	55.0	64.0	52.0	25.6	5.9
28.0	28.0	33.0	29.0	14.5	2.0

Table 93. Sample SM-1 Zone II Measurements

A	B	C	E	crystal size	zone width
39.0	38.0	48.0	11.5	5.4	17.0
39.0	38.0	46.0	11.0	5.5	17.4
34.0	29.0	43.0	11.0	4.3	12.6
34.0	39.0	50.0	11.0	4.3	15.3
40.0	34.0	46.0	4.5	2.1	19.3
40.0	37.0	46.0	7.5	3.7	19.2
55.0	55.0	73.0	19.0	8.0	22.6
50.0	39.0	57.0	13.5	5.9	19.0
35.5	40.0	48.0	6.0	2.7	18.9
45.0	49.0	62.0	15.0	6.3	19.8
31.0	29.0	32.0	9.0	4.5	14.3
26.0	32.0	36.0	9.0	4.2	12.5
30.0	33.0	38.0	10.5	5.1	13.5
40.0	45.0	52.0	9.0	4.3	20.6
22.0	22.0	29.0	8.0	3.4	8.9

BIBLIOGRAPHY

BIBLIOGRAPHY

Badiozamani, Khosrow, 1973, *The Dorag Dolomitization Model - Application to the Middle Ordovician of Wisconsin,* Journal of Sedimentary Petrology, volume 43, p. 965-984.

Baker, Paul A. and Kastner, Miriam, 1981, *Constraints on the Formation of Sedimentary Dolomite,* Science, volume 213, p. 214-216.

Banner, Jay L., Hanson, G. N. and Meyers, W.J., 1988, *Water-Rock Interaction History of Regionally Extensive Dolomites of the Burlington-Keokuk Formation (Mississippian): Isotopic Evidence,* Sedimentology and Geochemistry of Dolostones, SEPM Special Publication No. 43, p. 97-113.

Bennema, P., 1984, *Spiral Growth and Surface Roughening: Developments since Burton, Cabrera and Frank,* Journal of Crystal Growth, volume 69, p. 182-197.

Berner, R. A., 1980, Early Diagenesis, A Theoretical Approach, Princeton University Press, 241 p.

Berner, R. A., 1982, *Chemistry of Biogenic Matter at the Deep-Seafloor,* in The Environment of the deep sea; Rubey Volume II, Ernst, W. Gary and Morin, J. H. (eds.) Prentice Hall Publishers, p. 154-176.

Berner, R.A. and Morse, J.W., 1974, *Dissolution of calcium carbonate in seawater: IV Theory of Calcite Dissolution,* American Journal of Science, volume 274, p. 108-134.

Brown, C. D. Jr. and Lineback, L. A., 1966, *Lithostratigraphy of Cincinnatian Series (Upper Ordovician) in Southwestern Indiana,* AAPG Bulletin, volume 50, p. 1018-1032.

Bullen, Susan B. and Sibley, Duncan F., 1984, *Dolomite Selectivity and Mimic Replacement,* Geology, volume 12, p. 655-658.

Burton, W. K., Cabrera, N. and Frank, F.C., 1951, *The Growth of Crystals and the Equilibrium Structure of their Surfaces,* Philosophical Transactions of the Royal

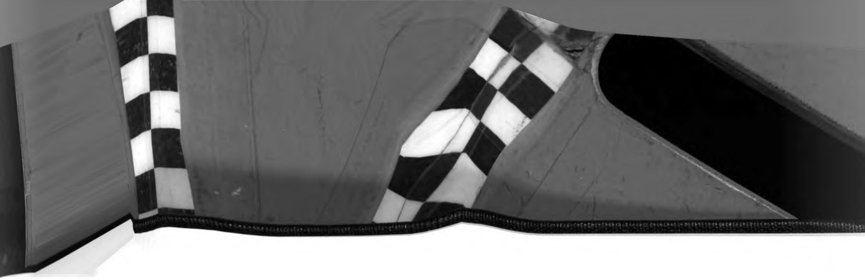

Society of London, Mathematical and Physical Sciences, Ser. A, volume 243, p. 299-358.

Cander, Harris S., Kaufman, Jonathan, Daniels, Lawrence D. and Meyers, William J., 1988, *Regional Dolomitization of Shelf Carbonates in the Burlington-Keokuk Formation (Mississippian), Illinois and Missouri: Constraints from Cathodoluminescent Zonal Stratigraphy,* Sedimentology and Geochemistry of Dolostones, SEPM Special Publication No. 43, p. 129-144.

Carpenter, Alden B., 1980, *The Chemistry of Dolomite Formation I: The Stability of Dolomite,* SEPM Special Publication No. 28, p. 111-121.

Carlson, William D., 1989, *The significance of intergranular diffusion to the mechanisms and kinetics of porphyroblast crystallization,* Contributions to Mineralogy and Petrology, volume 103, p. 1-24.

Carlson, William D., 1983, *Aragonite-Calcite Nucleation Kinetics: An Application and Extension of Avrami Transformation Theory,* Journal of Geology, volume 91, p. 57-71.

Carlson, William D. and Rosenfeld, John L., 1981, *Optical Determination of topotactic aragonite-calcite growth kinetics; metamorphic implications,* Journal of Geology, volume 89, no. 5, p. 615-638.

Choquette, Philip W. and Steinen, Randolph P., 1980, *Mississippian Non-Supratidal Dolomite, Ste. Genevieve Limestone, Illinois Basin: Evidence for Mixed-Water Dolomitization,* SEPM Special Publication No. 28, p. 163-196.

Christian, J. W., 1975, The Theory of Transformations in Metals and Alloys, Pergamon Press, 568 p.

Crow, Edwin L., Davis, Frances A. and Maxfield, Margaret W., 1960, Statistics Manual, Dover Publications, 288 p.

Domenico, P.A. and Schwartz, Franklin W., 1990, Physical and Chemical Hydrogeology, Wiley Publishers, New York, 824 p.

Eberl, D. D., Drits, V. A. and Srodon, J., 1998, *Deducing Growth Mechanisms for Minerals from the Shapes of*

Crystal Size Distributions, American Journal of Science, volume 298, p. 499-533.

Eberl, Dennis D., Srodon, Jan, Kralik, Martin, Taylor, Bruce E. and Petermen, Zell E., 1996, *Ostwald Ripening of Clays and Metamorphic Minerals,* Science, vol. 248, p. 474 - 477.

Ehlers, Ernest G. and Blatt, Harvey, 1982, Petrology: Igneous, Sedimentary and Metamorphic, W. H. Freeman and Company, p. 732.

Fairchild, Ian J., 1983, *Effects of Glacial Transport and Neomorphism on Precambrian Dolomite Crystal Sizes,* Nature, volume 304, p. 714-716.

Feazel, Charles T. and Schatzinger, Richard A., 1985, *Prevention of Carbonate Cementation in Petroleum Reservoirs,* Society of Economic Paleontologists and Mineralogists, p. 97-106.

Fouke, Bruce W., Beets, C. J., Meyers, William J., Hanson, Gilbert N. and Melillo, Allan J., 1996, *$^{87}Sr/^{86}Sr$ Chronostratigraphy and Dolomitization History of the Seroe Domi Formation, Curacao (Netherland Antilles),* Facies, volume 35, p. 293-320.

Fouke, Bruce W. and Reeder, Richard J., 1992, *Surface structural controls on dolomite composition: Evidence from sectoral zoning,* Geochimica et Cosmochimica Acta, volume 56, p. 4015-4024.

Frank, Tracy D., Lohmann, Kyger C. and Meyers, William J., 1995, *Chronostratigraphic significance of cathodoluminescence zoning in syntaxial cement: Mississippian Lake Valley Formation, New Mexico,* Sedimentary Geology, volume 105, p. 29- 50.

Gaines, Alan M., 1980, *Protodolomite Synthesis at 100°C and Atmospheric Pressure,* Science, volume 183, p. 518-520.

Gratz, A. J., Hillner, P. E. and Hansma, P. K., 1993, *Step Dynamics and Spiral Growth on Calcite,* Geochimica et Cosmochimica Acta, volume 57, p. 491-495.

Gregg, Jay M. and Sibley, Duncan F., 1984, *Epigenetic Dolomitization and the Origin of Xenotopic Dolomite Texture,* Journal of Sedimentary Petrology, volume 54, p. 908-931.

Harris, Paul M., Kendall, Christopher G. St. C. and Lerche, Ian, 1985, *Carbonate Cementation - A Brief Review,* SEPM Special Publication No. 36, Carbonate Cements, p. 79-95.

Harris, D.C., 1982, Carbonate Cement Stratigraphy and Diagenesis of the Burlington Limestone (Mississippian), southeast Iowa, western Illinois, M.S. thesis, University of New York at Stony Brook, 296 p.

Hatfield, C.B., 1968, *Stratigraphy and Paleoecology of the Saluda Formation (Cincinnatian) in Indiana, Ohio and Kentucky,* Geological Society of America Special Paper 95, 34 p.

Hillner, P. E., Gratz, A. J., Manne, S. and Hansma, P. K., 1992, *Atomic-scale imaging of calcite growth and dissolution in real time,* Geology, volume 20, p. 359-362.

Jancic, S. and Garside, J., 1975,*On the Determination of Crystallization Kinetics from Crystal Size Distribution Data,* Chem. Eng. Sci., volume 30, p. 1299-1301.

Kessels, Lisa A., 1995, The Dolomite Growth Mechanism in the Calcite to Dolomite Transformation, M. S. Thesis, Michigan State University, 90 p.

Katz, Amitai and Matthews, Alan, 1977, *The Dolomitization of $CaCO_3$: An experimental study at 252-295°C,* Geochimica et Cosmochimica Acta, volume 41, p. 297-308.

Kretz, Ralph, 1974, *Some Models for the Rate of Crystallization of Garnet in Metamorphic Rocks,* Lithos, volume 7, p. 123-131.

Kretz, Ralph, 1973, *Kinetics of the Crystallization of Garnet at Two Localities Near Yellowknife,* The Canadian Mineralogist, volume 12, p. 1-20.

Land, Lynton S., 1980, *The Isotopic and Trace Element Geochemistry of Dolomite: The State of the Art,* SEPM Special Publication No. 28, p. 87-110.

Lane, H.P. and DeKeyser, T. L., 1980, *Paleogeography of the late Early Mississippian (Tournaisian 3) in the central and southwestern United States,* in Paleozoic Paleography of the West-Central United States: West-

Central United States Paleography Symposium I: Rocky Mountain Section, Fouch, T. D. and Magathan, E.R.(eds.), SEPM, p. 149-162.

Larson, M. A. and Randolph, A. D., 1965, *Size Distribution Analysis in Continuous Crystallization,* Chemical Engineering Progress Symposium Series, vol. 65, no. 95, p. 1-13.

Lasaga, A.C., 1981, *Rate Laws of Geochemical Reactions,* Kinetics of Geochemical Processes, Reviews in Mineralogy, volume 8, p. 1-81.

Lu, Feng H. and Meyers, William J., 1998, *Massive Dolomitization of a Late Miocene Carbonate Platform: A Case of Mixed Evaporative Brines with Meteoric Water, Nijar, Spain,* Sedimentology, volume 45, p. 263-277.

Lucia, F. J. and Major, R. P., 1994, *Porosity Evolution Through Hypersaline Reflux Dolomitization,* Special Publication No. 21 of the International Association of Sedimentologists, p. 325-341.

Lumsden, David N. and Chimahusky, John S., 1980, *Relationship Between Dolomite Nonstoichiometry and Carbonate Facies Parameters,* SEPM Special Publication No. 28, p. 123-137.

Machel, H. G., 1989, *Relationships between sulphate reduction and oxidation of organic compounds to carbonate diagenesis, Hydrocarbon accumulation, salt domes and metal sulphide deposits,* in Carbonates and Evaporites, Mazzullo, S.J. and Gregg, Jay (eds.), p. 137-152.

Machel, H. G., 1983, *Cathodoluminescence in calcite and dolomite and its chemical interpretation,* Geoscience Canada, vol. 12, p. 139 - 147.

Machel, H.G. and Burton, Elizabeth, 1994, *Golden Grove Dolomite, Barbados; origin from modified seawater,* Journal of Sedimentary Research, vol. A64, p. 741-751.

Martin, Wayne D., 1975, *The Petrology of a Composite Vertical Section of Cincinnatian Series Limestones (Upper Ordovician) of Southwestern Ohio, Southeastern Indiana, and Northern Kentucky,* Journal of Sedimentary Petrology, volume 45, p. 907-925.

Mattes, Bret W. and Mountjoy, Eric W., 1980, *Burial Dolomitization of the Upper Devonian Miette Buildup, Jasper National Park, Alberta,* SEPM Special Publication No. 28, p. 259-297.

McKenzie, Judith A., 1981, *Holocene Dolomitization of Calcium Carbonate Sediments from the Coastal Sabkhas of Abu Dhabi, U.A.E.: A Stable Isotope Study,* Journal of Geology, volume 89, p. 185-198.

Meyers, William J., 1974, *Carbonate Cement Stratigraphy of the Lake Valley Formation (Mississippian) Sacramento Mountains, New Mexico,* Journal of Sedimentary Petrology, volume 44, p. 837-861.

Middleburg, Jack J., de Lange, Gert J. and Kreulen, Rob, 1990, *Dolomite Formation in Anoxic Sediments of Kau Bay, Indonesia,* Geology, volume 18, p. 399-402.

Morrow, D. W. and Abercrombie, H. J., 1994, *Rates of Dolomitization: the influence of dissolved sulphate,* Special Publication No. 21 of the International Association of Sedimentologists, p. 377-386.

Morse, John W., 1983, *The Kinetics of Calcium Carbonate Dissolution and Precipitation,* Carbonates, MSA Mineralogy and Chemistry Reviews, p. 227-264.

Muir, Marjorie, Lock, David and Von Der Borch, Chris, 1980, *The Coorong Model for Penecontemporaneous Dolomite Formation in the Middle Proterozoic McArthur Group, Northern Territory, Australia,* SEPM Special Publication No. 28, p. 51-67.

Negra, M. H., Purser, B. H. and M'Rabet A., 1994, *Permeability and Porosity Evolution in Dolomitized Upper Cretaceous Pelagic Limestones of Central Tunisia,* Special Publication No. 21 of the International Association of Sedimentologists, p. 309-323.

Nielson, Arne E., 1964, Kinetics of Precipitation, Pergamon Press, 271 p.

Nordeng, Stephan H. and Sibley, Duncan F., 1994, *Dolomite Stoichiometry and Ostwald's Step Rule,* Geochimica et Cosmochimica Acta, volume 58, p. 191-196.

Nordeng, Stephan H. and Sibley, Duncan, F., 1996, *A Crystal Growth Rate Equation for Ancient Dolomites: Evidence*

for Millimeter-Scale Flux-Limited Growth, Journal of Sedimentary Research, volume 66, p. 477-481.

Nyvlt, J., 1985, The Kinetics of Industrial Crystalllization, Chemical Engineering Monographs 19, 350 p.

Ohara, M. and Reid, R. C., 1973, Modeling Crystal Growth Rates from Solution, Englewood Cliffs, New Jersey, Prentice-Hall, 272 p.

Ottens, E.P.K., Janse, A.H., and de Jong, E.J., 1972, *Secondary Nucleation in a Stirred Vessel Cooling Crystallizer,* Journal of Crystal Growth, volume 13, p. 500-503.

Pierson, B. J, 1978, *Control of catho-luminescence of dolomite by Fe and Mn,* AAPG Bulletin, vol. 62, p. 553-554.

Pierson, B.J., 1981, *The Control of Cathodoluminescence in dolomite by Fe and Mn,* Sedimentology, vol. 28, no.5, p. 601-610.

Purser, B. H., Brown, A. and Aissaoui, D. M., 1994, *Nature, Origins and Evolution of Porosity in Dolomites,* Special Publication No. 21 of the International Association of Sedimentologists, p. 283-308.

Qing, Hairuo and Veizer, Jan, 1994, *Oxygen carbon isotopic composition of Ordovician brachiopods; implications for coeval seawater,* Geochimica et Cosmochimica Acta, vol. 58, p. 4429-4442

Rachlin, Alan L., Henderson, Grant S. and Goh, M. Cynthia, 1992, *An Atomic Force Microscope (AFM) study of the calcite cleavage plane, image averaging in Fourier space,* American Mineralogist, vol. 77, p. 904-910.

Reddy, M. M, Plummer, L. N. and Busenberg, E., 1981, *Crystal Growth of calcite from calcium bicarbonate solutions at constant* PCO_2 *and 25 degrees C; a test of a calcite dissolution model,* Geochimica et Cosmochimica Acta, vol. 45, p. 1281-1289.

Ristic, R. I., Sherwood, J.N. and Shripathi, T., 1991, *The Role of Dislocations and Mechanical Deformation in growth rate dispersion in Potash Alum Crystals,* for Millimeter-Scale Fine Laminar Growth, Journal of Sedimentary Research, v. [illegible] 6[illegible], p. 437-441.

, J., 1985, The Kinetics of Industrial Crystallization, Chemical Engineering [illegible], 10, 350 p.

, M. and Reid, R. C., 19[illegible], Modeling Crystal Growth Rates from Solution, [illegible], New Jersey, Prentice-Hall, 272 p.

, E.P.K., Janse, A.H., [illegible] 197[illegible], Secondary Nucleation in [illegible] Crystallizer, Journal of Crystal Growth, Volume [illegible] 500-503.

n, B. J, 1978, C[illegible] of Dolomite by Fe and Mn, [illegible] 54.

n, B.J., 1981, The C[illegible] Dolomite by Fe and Mn, Sediment[illegible], v. [illegible] 25, [illegible] 601-610.

, B. H., Brown, A. and A[illegible], 1971, [illegible] Origins and Evolution [illegible], Special Publication No. 21 [illegible] Association of Sedimentologists, p. [illegible]

Mattuo and Velzer, [illegible] Composition of Ordo[illegible] Seawater, Geoc[illegible] Acta, v. [illegible], p. 4429-4442

, Alan L., Henderson, [illegible], M. [illegible] 1992, An Atomic Force Microscope (AFM) study of the calcite cleavage plane, image averaging in Fourier space, American Mineralogist, vol. 77, p. 904-91[illegible]

, M. M, Plummer, L. N. and Busenberg, E., 1981, Crystal growth of calcite from calcium bicarbonate solutions at constant PCO2 and 25 degrees C; a test of a calcite dissolution model, Geochimica et Cosmochimica Acta, vol. 45, p. 1281-1289.

R. L., Sherwood, J.N. and Shripath, T., 1991, The Role of Dislocations and Mechanical Deformation in growth rate dispersion in Potash Alum Crystals, Advances in Industrial Crystallization, Garside, Davey and Jones (eds.), p. 77-91.

Roehl, Perry O. and Choquette, Philip W., 1985, Carbonate Petroleum Reservoirs, Springer Verlag, p. 1-18.

Saller, Arthur H., 1984, *Petrologic and Geochemical Constraints on the Origin of Subsurface Dolomite, Enewetak Atoll: An Example of Dolomitization by Normal Seawater,* Geology, volume 12, p. 217-220.

Sandberg, Philip, 1985, *Aragonite Cements and their Occurrence in Ancient Limestones,* in Carbonate Cements, SEPM Special Publication No. 36, Carbonate Cements, p. 33-57.

Sibley, Duncan F., 1990, *Unstable to Stable Transformations During Dolomitization,* Journal of Geology, volume 98, p. 739-748.

Sibley, Duncan F., 1982, *The Origin of Common Dolomite Fabrics: Clues from the Pliocene,* Journal of Sedimentary Petrology, volume 52, p. 1087-1100.

Sibley, Duncan F., 1980, *Climatic Control of Dolomitization, Seroe Domi Formation (Pliocene), Bonaire, N.A.,* SEPM Special Publication No. 28, p. 247-258.

Sibley, Duncan F. and Bartlett, T. R., 1987, *Nucleation as a Rate Limiting Step in Dolomitization,* in Geochemistry and Mineral Formation in the Earth Science, Proceedings of the International Meeting on Geochemistry of the Earth Surface and Processes of Mineral Formation, p. 733-741.

Sibley, Duncan F., Nordeng, Stephan H. and Borkowski, Michelle L., 1994, *Dolomitization Kinetics in Hydrothermal Bombs and Natural Settings,* Journal of Sedimentary Research, volume A64, p. 630-637.

Sibley, Duncan F., Gregg, Jay M., Brown, Robert G. and Laudon, Peter R., 1993, *Dolomite Crystal Size Distribution,* in Carbonate Microfacies, Rezak R. and Lavoie, D.(eds.), Springer-Verlag, New York, p. 195-208.

Sibley, Duncan F., Dedoes, Robert E. and Bartlett, Timothy R., 1987, *Kinetics of Dolomitization,* Geology, volume 15, p. 1112-1114.

Simo, J. A., Johnson, C. M., Vandrey, M. R., Brown, P. E., Castrogiovanni E., Drezewiecki, P. E., Valley, J. W. and Boyer, J., 1994, *Burial Dolomitization of the Middle Ordovician Glenwood Formation by Evaporitic Brines, Michigan Basin,* Special Publication No. 21 of the International Association of Sedimentologists, p. 169-186.

Steefel, Carl I. and Van Cappellen, Philippe, 1990, *A New Kinetic Approach to Modeling Water-Rock Interaction: The Role of Nucleation, Precursors, and Ostwald Ripening,* Geochimica et Cosmochimica Acta, volume 54, p. 2657-2677.

Stipp, S. L. S., Eggleston, C. M. and Nielsen, B. S., 1994, *Calcite Surface Structure observed at Microtopographic and Molecular Scales with Atomic Force Microscopy (AFM),* Geochimica et Cosmochimica Acta, volume 58, p. 3023-3033.

Sunagawa, Ichiro, 1982, *Morphology of crystals in relation to growth conditions,* in Proceedings of the First International Symposium on Crystal Growth Processes in Sedimentary Environments, Rodriguez, Clemente Rafael and Sunagawa I.(eds), Estudios Geologicos (Madrid), vol. 38, p. 127-134.

Sunagawa, Ichiro, 1984, *Growth of Crystals in Nature,* Materials Science of the Earth's Interior, Terra Scientific Publishing Company, p. 63-105.

Tucker, Maurice E. and Wright, V. Paul, 1990, Carbonate Sedimentology, Blackwell Scientific Publications, 482 p.

Usdowski, E., 1994, *Synthesis of Dolomite and Geochemical Implications,* Special Publication No. 21 of the International Association of Sedimentologists, p. 345-360.

Vahrenkamp, V. C. and Swart, P. K., 1994, *Late Cenozoic Dolomites of the Bahamas: Metastable Analogues for the Genesis of Ancient Platform Dolomites,* Special Publication No. 21 of the International Association of Sedimentologists, p. 13-153.

Walter, Lynn M., 1985, *Relative Reactivity of Skeletal Carbonates During Dissolution: Implications for*

Diagenesis, SEPM Special Publication, Carbonate Cements, no. 36, p. 3-16

Whitaker, F. F., Smart, P. L., Vahrenkamp, V. C., Nicholson, H. and Wogelius, R. A., 1994, *Dolomitization by Near-Normal Seawater? Field Evidence from the Bahamas,* Special Publication No. 21 of the International Association of Sedimentologists, p. 111-132.

White, E. T., Bendig, L.L., and Larson, M.A., 1974, *The Effect of Size on the Growth Rate of Potassium Sulfate Crystals,* A.I.Ch.E Symposium Series, vol. 72, no. 153, p. 41-47.

Wilkinson, Bruce H., Drummond, Carl N. and Diedrich, Nathaniel W., 1996, *Shoaling Cyclicity in Peritidal Carbonate Sequences,* Journal of Sedimentary Research, vol B66, p. 1065-1078.

Zenger, Donald H. and Dunham, John B., 1980, *Concepts and Models of Dolomitization-An Introduction,* SEPM Special Publication No. 28, p. 1-9.